Università degli studi di Cassino e
del Lazio meridionale

Dipartimento di Ingegneria Elettrica e
dell'Informazione

Corso di Dottorato in
Metodi, modelli e tecnologie per l'ingegneria

Control and management systems of distribution Smart Grids based on distributed and decentralized architectures

Relatore
Prof. Mario Russo

Candidata
Chiara Risi

Anno Accademico 2021/2022

Alla mia famiglia, quella di sangue e quella che ho scelto.
Per il sostegno e l'amore che mi danno da sempre.

Ai professori, indispensabili guide in questo percorso.
Per il metodo che mi hanno insegnato.

Ai colleghi, ottimi compagni di viaggio.
Per tutto quello che abbiamo condiviso e che non si apprende sui libri.

Abstract

The reference frame of this research is the radical transformation of electrical systems which are evolving toward smart grids.

The main motivations behind this development are political and technical in nature including the growth of energy demand, environmental problems, international climate agreements, the diffusion of distributed generation and the diffusion of new components and new technologies, including electric energy storage systems.

A contribution to this evolution is the increase of Distributed Generation (DG) from Renewable Energy Sources (RESs) as a form of energy production with zero emissions. In this new scenario, the distribution systems completely change their role and functions, gradually moving from "passive" networks, in which energy flows from the transmission system to the distribution nodes of consumption, to "active" networks", in which the consumer becomes also producer, with consequent bi-directional power flows along the distribution feeders.

As the grid has changed compared to traditional operation, new technical problems have emerged, and in particular the voltage control in this new type of grid has been tackled in recent years. In fact, the DGs mainly use "intermittent" RESs which can cause sudden and rapid variations of the power injections thus inducing over/under voltages.

Conventional voltage regulation relies on transformer on-load tap-changers in HV/MV substations, step voltage regulators and capacitor banks, which have slow response times. It is therefore necessary to identify new devices, management tools and control strategies in the evolving distribution systems.

At the same time, an important issue to consider is the need for economic solutions, which allow to improve the flexibility of existing networks, allowing for a large increase Distributed Energy Resources (DERs), but at

the same time require acceptable investments.

In this research, taking note of the imminent and necessary evolution of the electricity system, a solution is sought to the problem of optimizing the voltage, starting from a modeling of the system itself, and arriving at control via a decentralized approach with different methodologies. Summarizing, the three main topics treated in this Thesis are:

- PART I: the evolution of the traditional electrical systems toward Smart Grids;
- PART II: the Distribution System linear modelling, both exact and approximated with and without losses;
- PART III: the voltage optimization problem in Smart Distribution Grids using the distributed and decentralized approaches in three different ways.

In particular, after studying the characteristics of different control structures, the decentralized approach is preferred, where the distribution system is usually divided into voltage control zones. This approach ensures the optimal solution for each Voltage Control Zone (VCZ) and requires a light communication infrastructure.

To model the distribution system, in the presence of DER, after representing it through the equivalent circuit, we started from the branch, considering three different types of modeling. The exact one, the linearized one and the linearized one with losses. By merging more branches, it is obtained the feeder modeling, with and without losses. Finally, the modeling of the lateral is carried out, with and without losses,

Finally, a structural load flow algorithm is defined to calculate the Sensitivity Matrices of the Powers to the Injected Powers, Sensitivity Matrices of the Voltages to the Injected Powers and Sensitivity Matrices of the Voltages to the Voltage Regulators.

In the last part of this research, the problem of optimizing voltage in distribution networks is tackled adopting the decentralized approach with different methodologies: the alternate direction multiplier method (ADMM)

and the auxiliary problem principle (APP). Finally, the problem of optimizing voltage profiles in energy distribution networks has been tackled with a two-step procedure in which traditional and innovative controllers are integrated.

Therefore, after an analysis of the reasons that are leading the system to evolve, the problem of optimizing voltage in smart distribution networks is addressed. A method has been defined for modeling the system itself both in the presence and absence of losses, starting from the brach, to the feeder up to the lateral. The control and management of this new system is achieved with the decentralized approach with different methodologies. Concluding with numerical tests on distribution test networks to demonstrate the effectiveness of the proposed tools.

Contents

I Introduction to smart grids **1**

1 The Evolution of the Traditional Electrical System **2**
1.1 Differences Between the Traditional Electrical System and Smart Grids 4
1.2 The Problem of Voltage Regulation in Smart Grids 7

2 Control Strategies of Smart Grids **8**
2.1 Centralized control architecture 9
2.2 Distributed control architecture 9
2.3 Decentralized control architecture 10

II Distribution System Modeling **12**

3 Linear modelling of the distribution system **13**
3.1 Electric Equivalent Circuit of the Distribution System 13
3.2 Branch Model 17
3.2.1 Exact non-linear model 17
3.2.2 Linearized model 17
3.2.3 Structural linear model 18
3.2.4 Structural linear model with losses 19
3.3 Feeder Model 20
3.3.1 Structural linear model 20
3.3.2 Structural linear model with losses 24
3.4 Lateral Model 30
3.4.1 Structural linear model 30
3.5 Structural Load Flow Algorithm 35
3.5.1 Initializations 36

3.5.2 Description of the Network Topology 36
3.5.3 Evaluation of the Sensitivity Matrices of the Powers to the Injected Powers 37
3.5.4 Evaluation of the Sensitivity Matrices of the Voltages to the Injected Powers 38
3.5.5 Evaluation of the Sensitivity Matrix of the Voltages to the Voltage Regulators action 39
Appendix 40

III The voltage optimization problem in smart grids 42

4 Decentralized Voltage Optimization Problem 43
4.1 Decentralized VOP with ADMM 45
4.1.1 VOP Partitioning 46
4.1.2 Additional Variables 46
4.1.3 Method of Multipliers 46
4.1.4 Alternating Direction Method of Multipliers 47
4.1.5 Case Study with ADMM 49
4.1.6 Final considerations about ADMM 54
Appendix 55
4.2 Decentralized VOP with APP 58
4.2.1 VOP Partitioning 58
4.2.2 Method of Multipliers 59
4.2.3 Auxiliary Problem Principle 60
4.2.4 Case Study with APP 63
4.2.5 Final considerations about APP 69
Appendix 69
4.3 Decentralized VOP with two-levels algorithm 70
4.3.1 Voltage Optimitation Problem Formulation 71
4.3.2 OLTC, SVRs and CBs Optimization 74
4.3.3 DERs Optimization 76
4.3.4 Case Study With Two Levels Algorithm 79
4.3.5 Final considerations about the two-levels algorithm . . 90
Appendix 92

Conclusions 93

Glossary **97**

Acronyms **99**

List of Figures **99**

List of Tables **102**

Bibliography **103**

Part I

Introduction to smart grids

Chapter 1

The Evolution of the Traditional Electrical System

Traditionally it is known that to produce electricity it is necessary to exploit a primary energy source, which is transformed into electricity in the production plants to be easily transported. After transport, it is made available to various users, in forms that can be used directly.
More precisely, the Italian electrical system Fig. 1.1 consists of four subsystems, namely production, transmission, distribution, and user.

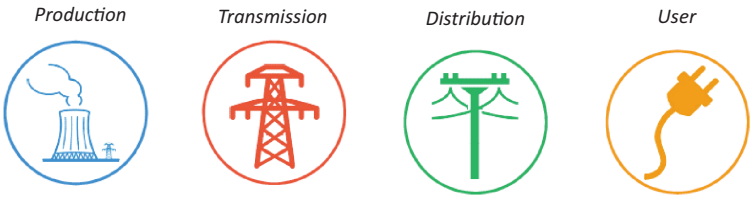

Figure 1.1: The subdivision of the Italian electrical system

This traditional electrical system structure is rapidly evolving towards smart grids.
Naturally, the main motivations behind this development are political and technical in nature:

- The growth of energy demand
- Environmental problems

- International climate agreements
- The diffusion of distributed generation
- The diffusion of new components and new technologies

In recent decades, the International Energy Agency has recorded a growth in the world energy consumption which is strongly correlated to emerging economies and population growth, because of the link between economic growth and primary energy energy consumption.

Since most energy is produced from fossil fuels, two fundamental problems arise.

First of all, a substantial increase in global CO2 emissions into the atmosphere is taking place with a consequent increase in global warming, responsible for climate change.

Secondly, the depletion of fuel reserves will affect future generations on energy security and costs, i.e. on the availability of energy reliable supplies at reasonable prices.

The energy sector has therefore begun to undergo a radical transformation, following the environment goals, which are evolving from the Kyoto protocol, to the Paris agreement and the "climate-energy" package. The search for solutions to atmospheric pollution and the consequent climate change is promoted, favoring DG from RES as a form of energy production with zero impact. The plants connected to the distribution networks Fig. 1.2 mainly exploit water, wind, solar irradiance and biomasses/biofuels as RESs.

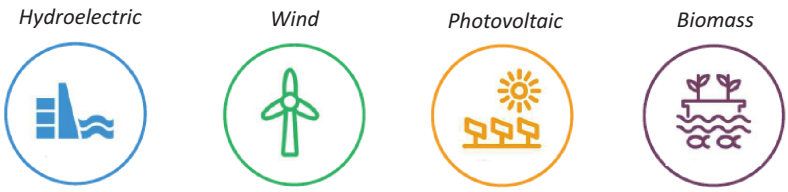

Figure 1.2: The Renewable Sources

Furthermore, in the field of electrical systems, new Information and Communication Technologies (ICT) and new components Fig. 1.3 with innovative features and functions are increasingly spreading, such as intelligent loads

Figure 1.3: The New Components

(e.g. shiftable, interruptible) and storage systems (e.g. electric vehicles) [1].

However, let us remember that the function of the electrical system is threefold:

1) supply the energy required by the load

2) balancing the powers instant by instant

3) in compliance with the constraints of proper functioning and power quality.

1.1 Differences Between the Traditional Electrical System and Smart Grids

Since its inception in the 1960s, the national electrical system has been conceived with a hierarchical structure Fig. 1.4 in which there is a relatively limited number of large production plants, capable of supplying energy and power to the loads through the transmission and distribution networks. Today, however, this paradigm is undergoing a deep transformation.

The correct operation of the electrical system is no longer guaranteed in the presence of production plants from renewable sources.

It is well known that production plants powered by renewable sources cannot be regulated as in most cases they exploit a primary energy source that is variable and random in nature. Therefore, a new additional cause of randomness is introduced in the electricity balance which is not linked to the variability of the loads.

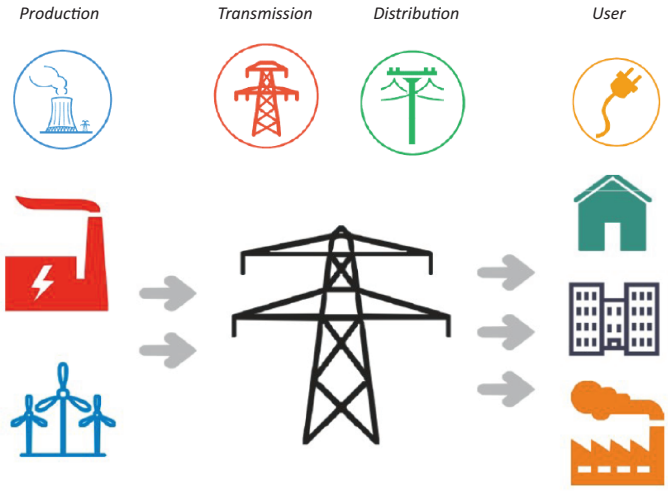

Figure 1.4: The Traditional Electrical System

Furthermore, the present-day control systems do not provide for the advanced regulation of the distribution systems and distributed generators. Indeed it could be possible to ask DGs to adjust the supply of electricity to load requests, also safeguarding the quality of the energy supply service, but it is possible only in presence of electric Energy Storage Systems (EES)) [2], [3].

For this reason, distribution systems must evolve and transform into the intelligent distribution networks of the future, named Smart Grids Fig. 1.5.

The smart grid is an electrical system to which are connected:

- Electricity production plants,
- Energy storage systems,
- Controlled and uncontrolled loads

and which is equipped with:

- monitoring and control systems,
- a communication infrastructure

On the one hand the strong penetration of the DGs by RESs guarantees a lower energy dependence on foreign sources, lower distribution losses and

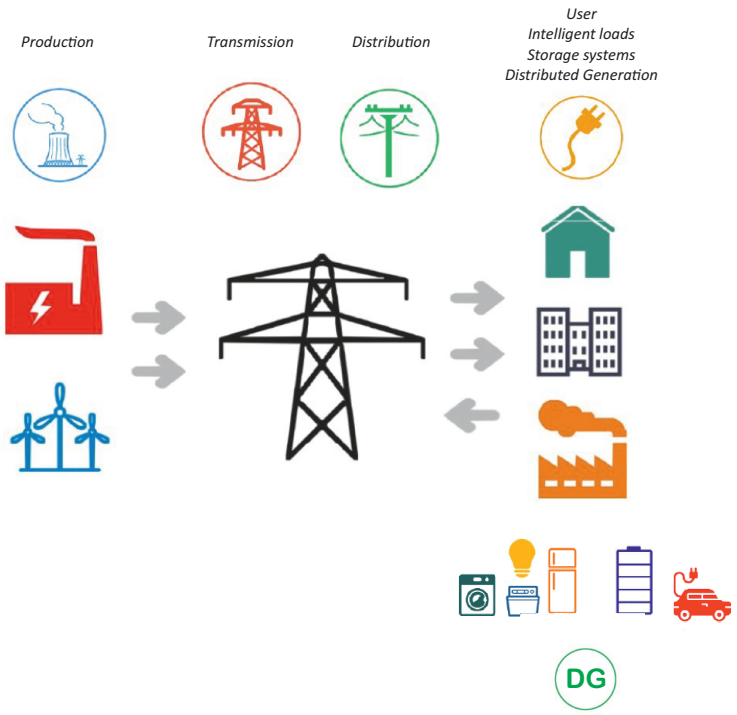

Figure 1.5: The New Electrical System

a reduction of greenhouse gas emissions into the atmosphere, on the other hand, it introduces new problems on the networks, in particularly distribution ones, accentuated by the random nature of the RESs. In fact, the distribution system completely changes its role and functions, being gradually destined to transform itself from a "passive" network to an "active" network. "in which the consumer also becomes a producer, with consequent bi-directionality of power flows [4].
Therefore, since the network has changed with respect to the traditional type, new technical problems have naturally emerged for voltage control [5]. New techniques must therefore be developed to ensure efficient, reliable, and safe operation of the distribution systems of the future [6].

1.2 The Problem of Voltage Regulation in Smart Grids

Changes in network operation from passive to active can cause nodal voltage limits to be violated, resulting in poor power quality [7]. The main problem consists in the fact that the DGs mainly use "intermittent" primary energy sources which can give rise to sudden and rapid injections of power causing over / under voltages. therefore for a correct operation of the network, it is necessary to be able to control the active and reative powers injected and absorbed defining a new control system of the distribution network [8], [9].

Present-day voltage regulation devices may not respond adequately to the numerous and rapid changes in voltage. In fact, conventional control devices such as on-load tap-changer of the transformer in HV / MV substations, step voltage regulators and capacitor banks, have too slow response times [10], [11], [12]. Then, the integration of new control devices is necessary.

It is therefore necessary to develop new flexible voltage control strategies to keep the nodal voltages within the admissible limits. Such strategies should be able to integrate the conventional control devices with the new devices present on the network, such as DGs, electric vehicles and controllable loads [13], [14]. These letter devices will be referred to as Distributed Energy Resources (DERs).

In this frame, an important issue is seeking economic solutions that do not require significant changes in the structure of the network but, at the same time, improve the flexibility of existing networks by exploiting the increasing number of DERs. It is therefore necessary to identify strategies for the management and control of the optimal distribution network [15], which is the focus of this Thesis.

Chapter 2

Control Strategies of Smart Grids

The new strategies for voltage control in distribution systems can be divided into two main categories, according to whether they rely or not on the use of a communication infrastructure [16], [8]:

- Local control,
- Communication-based control architectures.

In a local control Fig. 2.1, the controllers of both DERs and conventional Volt/Var devices use measurements at the point of common coupling (PCC) to individually elaborate and actuate a control action without requiring any information exchange among the DERs and between the DERs and a central controller.
The result is a globally non-optimal control of voltages, but it is the lowest-cost solution to start involving DERs in the voltage control of existing distribution networks. Unfortunately, the absence of coordination may introduce technical problems related to the interaction among controllers or even system instability.

In the communication-based control architectures, there are numerous advantages in coordinating the local actions of DERs through the data collected by smart meters. However, this represents a solution that requires multiple and costly investments in existing distribution systems [17].
The architectures based on communication [18] can in turn be classified into:

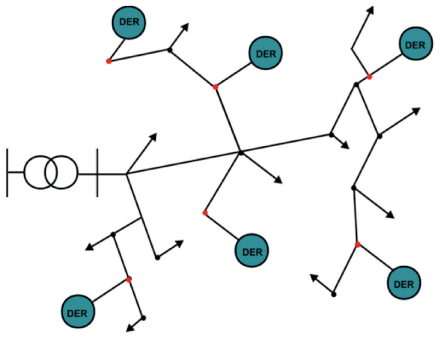

Figure 2.1: Local Control

- Centralized,
- Distributed,
- Decentralized.

The different characteristics of the three architectures in terms of optimal control results and of investment costs for the communication infrastructures are outlined in the following Sections.

2.1 Centralized control architecture

In a centralized architecture Fig. 2.2, a central control unit, typically located at the substation level, firstly solves a system voltage optimization control problem on the basis of the measurements collected from all the nodes/devices of the network; then, it sends the optimal set-points back to the local controller of both DERs and conventional Volt/Var devices. This approach yields the optimal solution but its implementation is very expensive requiring a large communication infrastructure with adequate bandwidth to exchange information quickly and accurately.

2.2 Distributed control architecture

In a distributed architecture Fig. 2.3, the controllers of both DERs and conventional Volt/Var devices use measurements at PCC to achieve local voltage regulation as in a local control, but they also exchange information

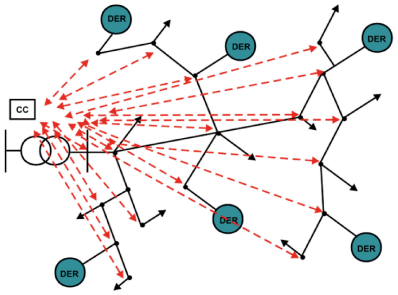

Figure 2.2: Centralized control architecture

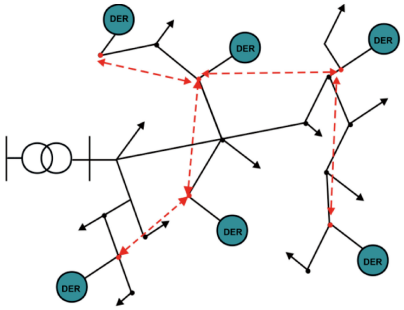

Figure 2.3: Distributed control architecture

with the controllers of the neighboring nodes for coordination purposes. This approach aims at overcoming the technical problems of the local control architecture, while limiting the investments for the communication infrastructure.

2.3 Decentralized control architecture

In a decentralized architecture Fig. 2.4, the distribution system is usually partitioned into Voltage Control Zones (VCZs). Referring to sensitivity matrices of nodal voltages with respect to active and reactive power injections by DERs, the VCZs are defined so that each VCZ contains nodes that are significantly coupled among each other and are weakly coupled with the nodes belonging to other VCZs; in the 'electric center' of a VCZ is placed the pilot node (PN), whose voltage variation best represents the variation of the voltage in the VCZ [19], [20]. In each VCZ a centralized zone controller is present which is located at the PNs, whereas the coordination among the various zone controllers is obtained by a distributed control. This approach

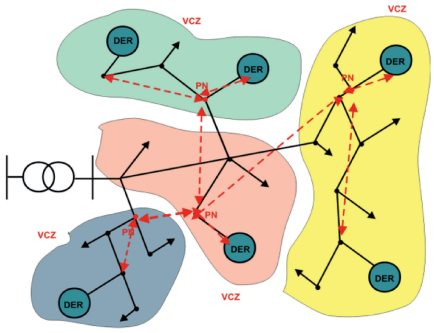

Figure 2.4: Decentralized Control

guarantees the optimal solution for each VCZ and requires a communication infrastructure lighter than the centralized control, expecially if a large number of DERs and Volt/Var devices is present.

Part II

Distribution System Modeling

Chapter 3

Linear modelling of the distribution system

In this part of the Thesis, attention is focused on linear modelling of the distribution system.
In the previous part, it has been evidenced that new voltage regulation systems with innovative control architectures are going to be implemented in distribution systems. In particular, a large number of DERs and Volt/Var control devices are expected to be connected to the networks and to be adequately controlled and coordinated. To develop the new voltage control architectures, the interaction among the various DERs and devices must be adequately analysed and modelled: it is the focus of this second part of the Thesis in view of the tackling voltage regulation problem in the third part.
As well known, power systems steady-state operation is typically modelled by the non-linear power flow equations. Then, exploiting the radial configuration typically adopted in distribution network operation, in this part of the Thesis some simple linear models available in literature for the distribution system operation are analyzed and extended to improve their accuracy.

3.1 Electric Equivalent Circuit of the Distribution System

Consider, as an example but without loss of generality, the LV distribution system shown in the Fig. 3.1.

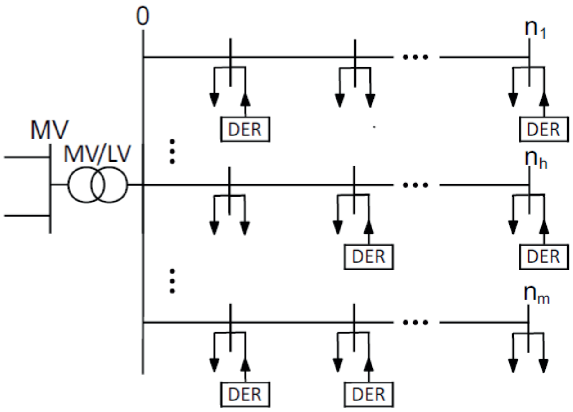

Figure 3.1: Low Voltage Distribution System with DERs

The system is composed of a MV/LV substation with m departing feeders from the LV busbar in the substation (node 0); the generic $h-th$ feeder is composed of n_h branches and at each branch uncontrolled loads and/or DERs are connected.

Fig. 3.2 represents the electrical circuit of the MV/LV power supply system in balanced operating conditions (unbalanced modelling is more complex and left to future research).

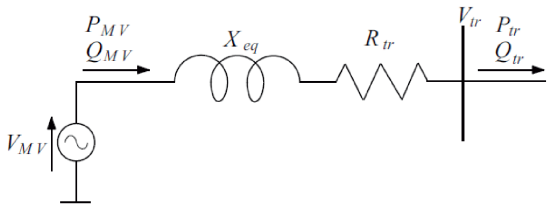

Figure 3.2: Electric equivalent circuit of the MV/LV Substation

Two electrical parameters characterize the equivalent circuit:

- the resistance R_{tr} of the MV/LV transformer;
- the equivalent impedance $X_{eq} = X_{tr} + X_{sc}$, where X_{tr} is the reactance

of the transformer and X_{sc} the short-circuit impedance of the MV node.

Three electric variables characterize the model at the MV node:

- the amplitude of the no-load voltage V_{MV} of the node, which is assumed to be assigned, representing the slack bus of the system;
- the input active power P_{MV};
- the input reactive power Q_{MV}.

Similarly the MV/LV transformer output is characterized by three electrical variables:

- the LV busbar voltage amplitude V_{tr};
- the outgoing active power P_{tr};
- the outgoing reactive power Q_{tr}.

In Fig. 3.3, in a similar way, it is represented by the electric circuit of the generic $j-th$ branch of the LV distribution system.

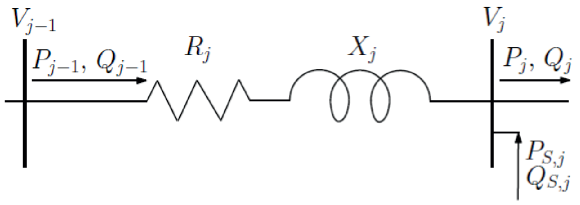

Figure 3.3: Electric equivalent circuit of the $j-th$ branch

Two electrical parameters characterize the branch equivalent circuit:

- the resistance R_j;
- the reactance X_j.

Three electrical variables characterize the branch at the sending node $j-1$:

- the nodal voltage amplitude V_{j-1};

- the incoming active power P_{j-1};
- the incoming reactive power Q_{j-1}.

Similarly, three electrical variables characterize the branch at the receiving node j,

- the nodal voltage amplitude V_j;
- the outgoing active power P_j;
- the outgoing reactive power Q_j;

Furthermore, two external variables or "enforcements" are included at the receiving node j, which are the active shunt power $P_{S,j}$ and the shunt reactive power $Q_{S,j}$ defined as:

$$\begin{aligned} P_{S,j} &= P_{der,j} - P_{L,j} \\ Q_{S,j} &= Q_{der,j} - Q_{L,j} \end{aligned}$$

being $P_{der,j}$ and $Q_{der,j}$, respectively, the active and reactive powers injected by the DER connected to the $j-th$ node, and $P_{L,j}$ and $Q_{L,j}$, respectively, the active and reactive powers absorbed by the uncontrolled load connected to the $j-th$ node.

The linear model of the LV distribution system can be obtained through the linearization of the load flow equations of the branches associated with the components of the LV distribution system represented in Fig 3.2 and Fig. 3.3. Then, imposing both boundary and coupling conditions, a closed-form solution of linearized DistFlow equations is obtained through the use of the chain rule [21]. Such a closed form represents the linear model of the distribution system with DER, and is expressed in terms of variations in the electrical variables of the LV networks (with respect to an initial operating point) as linear functions of DER injections. The construction occurs step by step: first, the model of a generic branch and a feeder composed of several branches is developed; then, the MT/BT model the power system is introduced and combined with the models of the power supplies, obtaining the model of the entire LV distribution system [21].

3.2 Branch Model

3.2.1 Exact non-linear model

The model of the $j-th$ branch, Fig. 3.3, is described by the well-known distribution load flow (*DistFlow*) equations for the steady-state operation [22]

$$\begin{cases} P_j &= P_{j-1} - \dfrac{R_j(P_{j-1}^2 + Q_{j-1}^2)}{V_{j-1}^2} + P_{s_j} \\ Q_j &= Q_{j-1} - \dfrac{X_j(P_{j-1}^2 + Q_{j-1}^2)}{V_{j-1}^2} + Q_{s_j} \\ V_j^2 &= V_{j-1}^2 - 2(R_j P_{j-1} + X_j Q_{j-1}) + \dfrac{(R_j^2 + X_j^2)(P_{j-1}^2 + Q_{j-1}^2)}{V_{j-1}^2} \end{cases} \tag{3.1}$$

These equations overcome the limits of the classical power flow formulation based on non-linear equations written for each node of the network (formulation used at the transmission level), but are valid only in the case of radial topology of the distribution network because voltage phases are not included in the representation.

3.2.2 Linearized model

To simplify the study it is possible to linearized the equations (3.1) around an initial operating point.

Let the vector of nodal variables x_j be defined as

$$x_j = (P_j, Q_j, V_j^2)^t$$

and the Jacobian matrix, which realizes the partial derivatives with respect to the three variables, be

$$J_j = \begin{bmatrix} \dfrac{\delta x_j}{\delta P_{j-1}} & \dfrac{\delta x_j}{\delta Q_{j-1}} & \dfrac{\delta x_j}{\delta V_{j-1}^2} \end{bmatrix} \tag{3.2}$$

The linearization (3.1) of the equations yields the following branch model

$$\Delta x_j = J_j \Delta x_{j-1} + (\Delta P_{s_j}, \Delta Q_{s_j}, 0)^t \tag{3.3}$$

with

- Δx_j is the variation of the electrical variables at the receiving node x_j with respect to the initial operating point x_j^0 as a function of the vector

$$\Delta x_j = x_j - x_j^0$$

- Δx_{j-1} is the variation of the electrical variables at the supplying node x_{j-1}, with respect to the initial operating point x_j^0

$$\Delta x_{j-1} = x_{j-1} - x_{j-1}^0$$

- J_j is the Jacobian matrix (3.2) evaluated in the initial operating point,
- ΔP_{S_j},ΔQ_{S_j} are the variations of the injections of the shunt active and reactive powers at the receiving node.

If the initial operating condition is characterized by the absence of DERs injections, then ΔP_{S_j},ΔQ_{S_j} are equal to the values $P_{der,j}$, $Q_{der,j}$ of the DERs active and reactive power injections at the receiving node, which are considered to be assigned enforcements.

3.2.3 Structural linear model

A particular case is the one in which the initial operating point is characterized not only by null powers injected by all the DERs connected to the LV distribution system but also by null powers absorbed by the uncontrolled loads. Then, all active and reactive power flows are null along the branches and the so-called *LinDistFlow* model is derived [23]. In particular the Jacobian matrix (3.2) reduces to the form

$$J_j = \begin{bmatrix} 1 & 0 & 0 \\ 0 & 1 & 0 \\ -2R_j & -2X_j & 1 \end{bmatrix}$$

which we refer to as "structural" model, because it does not depend on the initial values of electric variables, because the power flows are all null and, consequently, no voltage drop is present and voltages are all equal to the slack bus voltage. In this model, active and reactive losses are neglected and voltage drops approximated to linearly dependend on active and reactive power flows

3.2.4 Structural linear model with losses

To account for losses, which are neglected in the previous *LinDistFlow* or structural modeling, are integrated by adding an approximated term. The Jacobian matrix (3.2) is approximated to the sum of a structural part (3.4), hereinafter indicated with the superscript s, and a part including the losses, hereinafter indicated with the superscript $loss$, that is

$$J_j = J_j^s + J_j^{loss}$$

with

$$\begin{aligned} J_j^s &= \begin{bmatrix} 1 & 0 & 0 \\ 0 & 1 & 0 \\ -2R_j & -2X_j & 1 \end{bmatrix} \\ J_j^{loss} &= \begin{bmatrix} -2R_j \frac{P_{j-1}}{V_{j-1}^2}|_0 & R_j \frac{Q_{j-1}}{V_{j-1}^2}|_0 & 0 \\ -2X_j \frac{P_{j-1}}{V_{j-1}^2}|_0 & -2X_j \frac{Q_{j-1}}{V_{j-1}^2}|_0 & 0 \\ 0 & 0 & 0 \end{bmatrix} \end{aligned}$$

Defining the quantities α_p^j and α_q^j, representative of a weight linked to losses

$$\alpha_p^j = \frac{P_{j-1}}{V_{j-1}^2}|_0$$

$$\alpha_q^j = \frac{Q_{j-1}}{V_{j-1}^2}|_0$$

J_j^{loss} is written in compact form

$$J_j^{loss} = \begin{bmatrix} -2R_j\alpha_p^j & -2R_j\alpha_q^j & 0 \\ -2X_j\alpha_p^j & -2X_j\alpha_q^j & 0 \\ 0 & 0 & 0 \end{bmatrix}$$

In this model, the term of the voltage that is neglected is related to the last term in the voltage expression, see (3.1). It is reasonable because it is a term depending on the square value of the series impedance of the branch. Since series impedances value in *per unit* is usually of the order of 10^{-2}, the neglected term is of the order of 10^{-4}. Moreover, the dependency of the active and reactive power flows on the voltage variations is also neglected due to the limited variations of voltages. In fact these terms are related to the product of series impedances times the voltage variations, which in turn should result to be of the order of 10^{-4}.

3.3 Feeder Model

3.3.1 Structural linear model

The electric equivalent circuit of the h-th feeder of the LV distribution system is composed of a series of n_h branches. Then, the model of the feeder is composed of n_h equations of type (3.3):

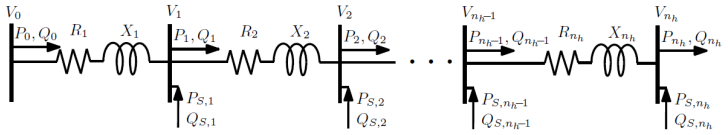

Figure 3.4: Electric Equivalent Circuit of the h-th Feeder

Consequently, the feeder model is composed of n_h equations of this type

$$\Delta x_j = J_j \Delta x_{j-1} + (\Delta P_{s_j}, \Delta Q_{s_j}, 0)^t$$

with $j = 0, ..., n_h$.

Applying the chain rule to this equation

$$\Delta x_j = M_j \Delta x_0 + \sum_{k=1}^{j} N_{j_k} (\Delta P_{s_k}, \Delta Q_{s_k}, 0)^t \tag{3.4}$$

Defining the matrices M_j

$$M_j = \coprod_{l=0}^{j-1} J_{j-l} = \begin{bmatrix} 1 & 0 & 0 \\ 0 & 1 & 0 \\ -2\sum_{l=1}^{j} R_l & -2\sum_{l=1}^{j} X_l & 1 \end{bmatrix}$$

The values of matrix N_{j_k} depend on j and k:

$$N_{j_k} = \coprod_{l=0}^{j-k-1} J_{j-l} = \begin{bmatrix} 1 & 0 & 0 \\ 0 & 1 & 0 \\ -2\sum_{l=k+1}^{j} R_l & -2\sum_{l=k+1}^{j} X_l & 1 \end{bmatrix} \quad \text{for } k < j;$$

$N_{j_k} = 0$ for $k > j$;
$N_{j_k} = I$ for $k = j$.

To obtain a defined problem, three additional conditions must be assigned. It derived from the behavior of the feeder at its borders. In particular, the voltage amplitude at the head of the feeder is imposed by the MV/LV supplying substation and the active and reactive powers flowing out of the end-node of the feeders are always null. The border conditions can be expressed in terms of variations of the electric nodal variables as

$$\begin{aligned} \Delta {V_0}^2 &= \Delta \widetilde{V_0}^2 \\ \Delta P_{n_h} &= 0 \\ \Delta Q_{n_h} &= 0 \end{aligned}$$

where $\Delta \widetilde{V_0}^2$ is the variation of the squared voltage amplitude imposed at the LV busbar by the MV/LV supplying substation [1].

Rewriting the equation (3.4) for $j = n_h$ and particularizing it for Δx_0

$$\begin{bmatrix} 0 \\ 0 \\ \Delta V_{n_h}^2 \end{bmatrix} = M_{n_h} \begin{bmatrix} \Delta P_0 \\ \Delta Q_0 \\ \Delta \widetilde{V}_0^2 \end{bmatrix} + \sum_{k=1}^{n_h} N_{j_k} \begin{bmatrix} \Delta {P_k}^{der} \\ \Delta {Q_k}^{der} \\ \Delta {V_k}^{2_{reg}} \end{bmatrix}$$

Considering the first two lines [2]

$$\begin{bmatrix} 0 \\ 0 \end{bmatrix} = \begin{bmatrix} \Delta P_0 \\ \Delta Q_0 \end{bmatrix} \sum_{k=1}^{n_h} \bar{N}_{n_h k} \begin{bmatrix} \Delta {P_k}^{der} \\ \Delta {Q_k}^{der} \\ \Delta {V_k}^{2_{reg}} \end{bmatrix}$$

then

$$\begin{bmatrix} \Delta P_0 \\ \Delta Q_0 \end{bmatrix} = -\sum_{k=1}^{n_h} \bar{N}_{n_h k} \begin{bmatrix} \Delta {P_k}^{der} \\ \Delta {Q_k}^{der} \\ \Delta {V_k}^{2_{reg}} \end{bmatrix} = -\sum_{k=1}^{n_h} \begin{bmatrix} 1 & 0 & 0 \\ 0 & 1 & 0 \end{bmatrix} \begin{bmatrix} \Delta {P_k}^{der} \\ \Delta {Q_k}^{der} \\ \Delta {V_k}^{2_{reg}} \end{bmatrix} = - \begin{bmatrix} \sum_{k=1}^{n_h} \Delta {P_k}^{der} \\ \sum_{k=1}^{n_h} \Delta {Q_k}^{der} \end{bmatrix}$$

[1] The symbol $\widetilde{}$ indicates an assigned value.

[2] The symbol $\bar{}$ represents the 2×2 principal minor composed of the first two rows and first two column of a matrix.

with $\bar{A}_k = -\bar{N}_{n_h k}$ and $\bar{a} = (0,0)^t$
Then it can be written

$$\Delta x_0 = -\sum_{k=1}^{n_h} \begin{bmatrix} 1 & 0 & 0 \\ 0 & 1 & 0 \\ 0 & 0 & 0 \end{bmatrix} \begin{bmatrix} \Delta {P_k}^{der} \\ \Delta {Q_k}^{der} \\ \Delta {V_k}^{2_{reg}} \end{bmatrix} + \begin{bmatrix} 0 \\ 0 \\ 1 \end{bmatrix} \Delta \widetilde{V_0}^2$$

consequentially

$$\Delta x_0 = \begin{bmatrix} -\sum\limits_{k=1}^{n_h} \Delta {P_k}^{der} \\ -\sum\limits_{k=1}^{n_h} \Delta {Q_k}^{der} \\ \Delta \widetilde{V}_0^2 \end{bmatrix}$$

Substituting this expression in the initial equation, obtain

$$\Delta x_j = M_j \begin{bmatrix} -\sum\limits_{k=1}^{n_h} \Delta {P_k}^{der} \\ -\sum\limits_{k=1}^{n_h} \Delta {Q_k}^{der} \\ \Delta \widetilde{V_0}^2 \end{bmatrix} + \sum_{k=1}^{n_h} N_{j_k} \begin{bmatrix} \Delta {P_k}^{der} \\ \Delta {Q_k}^{der} \\ \Delta {V_k}^{2_{reg}} \end{bmatrix}$$

by doing a series of steps, can write that Δx_j is equal to

$$\Delta x_j = -\sum_{k=1}^{n_h} M_j \begin{bmatrix} 1 & 0 & 0 \\ 0 & 1 & 0 \\ 0 & 0 & 0 \end{bmatrix} \begin{bmatrix} \Delta {P_k}^{der} \\ \Delta {Q_k}^{der} \\ \Delta {V_k}^{2_{reg}} \end{bmatrix} + M_j a \Delta \widetilde{V_0}^2 + \sum_{k=1}^{n_h} N_{j_k} \begin{bmatrix} \Delta {P_k}^{der} \\ \Delta {Q_k}^{der} \\ \Delta {V_k}^{2_{reg}} \end{bmatrix}$$

By grouping the terms

$$\Delta x_j = \sum_{k=1}^{n_h} (N_{j_k} - M_j \begin{bmatrix} 1 & 0 & 0 \\ 0 & 1 & 0 \\ 0 & 0 & 0 \end{bmatrix}) \begin{bmatrix} \Delta {P_k}^{der} \\ \Delta {Q_k}^{der} \\ \Delta {V_k}^{2_{reg}} \end{bmatrix} + M_j a \Delta \widetilde{V}_0^2$$

It can re-succeed the representative equation of the lateral model, referring to the sum of several branches, with $P^{der} = 0$ and $Q^{der} = 0$ at the end

$$\Delta x_j = \sum_{k=1}^{n_h} B_{j_k} \begin{bmatrix} \Delta {P_k}^{der} \\ \Delta {Q_k}^{der} \\ \Delta {V_k}^{2_{reg}} \end{bmatrix} + b_j \Delta \widetilde{V}_0^2$$

with

$$B_{jk} = N_{jk} - Mj \begin{bmatrix} 1 & 0 & 0 \\ 0 & 1 & 0 \\ 0 & 0 & 0 \end{bmatrix}$$

$$b_j = M_j a = \begin{bmatrix} 1 & 0 & 0 \\ 0 & 1 & 0 \\ -2\sum_{l=1}^{j} R_l & -2\sum_{l=1}^{j} X_l & 1 \end{bmatrix} \begin{bmatrix} 0 \\ 0 \\ 1 \end{bmatrix} = \begin{bmatrix} 0 \\ 0 \\ 1 \end{bmatrix} = a = b_0$$

In the equation, the vectors Δx_j of the variation of the electric variables at the receiving node of each branch belonging to the feeder are expressed as a function of

- The vectors $(\Delta P_{s_j}, \Delta Q_{s_j}, 0)^t$ of the DERs active and reactive power injections in all the nodes of the feeder through the matrices B_{jk};
- The variation $\Delta {V_0}^2$ of the squared voltage amplitude at the LV busbar of the supplying substation through the vector b_j.

It is interesting to to analyze what the matrix B_{jk} indicates whose value is different whose value is different depending on whether $k > j$ or $k \leq j$.

In the first case $k > j$ the injection of ΔP^{der} and ΔQ^{der} reduces P_j and Q_j by the same amount up to node j. Any voltage regulation in node k has no effect upstream. This phenomenon is best described by considering the expression of B_{jk}

$$B_{jk} = \begin{bmatrix} -1 & 0 & 0 \\ 0 & -1 & 0 \\ 2\sum_{l=1}^{j} R_l & 2\sum_{l=1}^{j} X_l & 0 \end{bmatrix} \qquad j = 0, ..., n_h \qquad k = 1, ..., n_h$$

In the second case $k \leq j$the injection of ΔP^{der} and ΔQ^{der} does not alter P_j and Q_j . the voltage drop is reduced to knot k. Any tension adjustment in node k has no effect on P_j and Q_j. This phenomenon is best described by considering the expression of B_{jk}

$$B_{jk} = \begin{bmatrix} 0 & 0 & 0 \\ 0 & 0 & 0 \\ 2\sum_{l=1}^{k} R_l & 2\sum_{l=1}^{k} X_l & 1 \end{bmatrix} \qquad j = 0, ..., n_h \qquad k = 1, ..., n_h.$$

3.3.2 Structural linear model with losses

In the modeling in the previous paragraph, only structural Jacobian matrices have been considered and losses were neglected.

A similar procedure can be followed for the linearized feeder model also in this case have a structural part, indicated below with the superscript s and one with inclusive of losses, indicated below with the superscript $loss$.

Keeping in mind the approximations that have been introduced in the branch structural model with losses, also in the following the procedure is applied neglecting the terms in which series impedances appear with a second or higher order.

Then, let us rewrite the feeder model and start from the definition of the matrices J_j, M_j and N_{jk}.
The Jacobian realizes by a structural component and a loss component, as follows

$$J_j = J_j^s + J_j^{loss} = \begin{bmatrix} 1 & 0 & 0 \\ 0 & 1 & 0 \\ -2R_j & -2X_j & 1 \end{bmatrix} + \begin{bmatrix} -2R_j \frac{P_{j-1}}{V_{j-1}^2}|_0 & -2R_j \frac{Q_{j-1}}{V_{j-1}^2}|_0 & 0 \\ -2X_j \frac{P_{j-1}}{V_{j-1}^2}|_0 & -2X_j \frac{Q_{j-1}}{V_{j-1}^2}|_0 & 0 \\ 0 & 0 & 0 \end{bmatrix}$$

The matrices M_j result to be

$$M_j = M_j^s + M_j^{loss} = \coprod_{l=0}^{j-1} J_{j-l} = \coprod_{l=0}^{j-1} (J_{j-l}^s + J_{j-l}^{loss}) =$$

$$= \begin{bmatrix} 1 & 0 & 0 \\ 0 & 1 & 0 \\ -2\sum_{l=1}^{j} R_l & -2\sum_{l=1}^{j} X_l & 1 \end{bmatrix} + \begin{bmatrix} -2\sum_{l=1}^{j} R_l \frac{P_{l-1}}{V_{l-1}^2}|_0 & -2\sum_{l=1}^{j} R_l \frac{Q_{l-1}}{V_{l-1}^2}|_0 & 0 \\ -2\sum_{l=1}^{j} X_l \frac{P_{l-1}}{V_{l-1}^2}|_0 & -2\sum_{l=1}^{j} X_l \frac{Q_{l-1}}{V_{l-1}^2}|_0 & 0 \\ 0 & 0 & 0 \end{bmatrix}$$

whereas matrices N_{jk} for all $k < j$

$$N_{jk} = N_{jk}^{s} + N_{jk}^{loss} = \coprod_{l=0}^{j-k-1} J_{j-l} = \coprod_{l=0}^{j-k-1} (J_{j-l}^{s} + J_{j-l}^{loss}) =$$

$$= \begin{bmatrix} 1 & 0 & 0 \\ 0 & 1 & 0 \\ -2\sum_{l=k+1}^{j} R_l & -2\sum_{l=k+1}^{j} X_l & 1 \end{bmatrix} + \begin{bmatrix} -2\sum_{l=k+1}^{j} R_l \frac{P_{l-1}}{V_{l-1}^2}|_0 & -2\sum_{l=k+1}^{j} R_l \frac{Q_{l-1}}{V_{l-1}^2}|_0 & 0 \\ -2\sum_{l=k+1}^{j} X_l \frac{P_{l-1}}{V_{l-1}^2}|_0 & -2\sum_{l=k+1}^{j} X_l \frac{Q_{l-1}}{V_{l-1}^2}|_0 & 0 \\ 0 & 0 & 0 \end{bmatrix}$$

To simplify the notation, the following quantities are defined

$$\beta_{R_p}^{j_k} = \sum_{l=k+1}^{j} R_l \frac{P_{l-1}}{V_{l-1}^2}$$

$$\beta_{R_q}^{j_k} = \sum_{l=k+1}^{j} R_l \frac{Q_{l-1}}{V_{l-1}^2}$$

$$\beta_{X_p}^{j_k} = \sum_{l=k+1}^{j} X_l \frac{P_{l-1}}{V_{l-1}^2}$$

$$\beta_{X_q}^{j_k} = \sum_{l=k+1}^{j} X_l \frac{Q_{l-1}}{V_{l-1}^2}$$

The specific case in which $k = 0$ is also considered

$$\beta_{R_p}^{j_0} = \sum_{l=1}^{j} R_l \frac{P_{l-1}}{V_{l-1}^2}$$

$$\beta_{R_q}^{j_0} = \sum_{l=1}^{j} R_l \frac{Q_{l-1}}{V_{l-1}^2}$$

$$\beta_{X_p}^{j_0} = \sum_{l=1}^{j} X_l \frac{P_{l-1}}{V_{l-1}^2}$$

$$\beta_{X_q}^{j_0} = \sum_{l=1}^{j} X_l \frac{Q_{l-1}}{V_{l-1}^2}$$

With this notation, let us proceed with the writing of M_j

$$M_j = M_j^{s} + M_j^{loss} = \coprod_{l=0}^{j-1} J_{j-l} = \coprod_{l=0}^{j-1} (J_{j-l}^{s} + J_{j-l}^{loss}) =$$

$$= \begin{bmatrix} 1 & 0 & 0 \\ 0 & 1 & 0 \\ -2\sum_{l=1}^{j} R_l & -2\sum_{l=1}^{j} X_l & 1 \end{bmatrix} + \begin{bmatrix} -2\beta_{R_p}^{j_0} & -2\beta_{R_q}^{j_0} & 0 \\ -2\beta_{X_p}^{j_0} & -2\beta_{X_q}^{j_0} & 0 \\ 0 & 0 & 0 \end{bmatrix} =$$

$$= \begin{bmatrix} 1 & 0 & 0 \\ 0 & 1 & 0 \\ -2\sum_{l=1}^{j} R_l & -2\sum_{l=1}^{j} X_l & 1 \end{bmatrix} - 2 \begin{bmatrix} \beta_{R_p}^{j_0} & \beta_{R_q}^{j_0} & 0 \\ \beta_{X_p}^{j_0} & \beta_{X_q}^{j_0} & 0 \\ 0 & 0 & 0 \end{bmatrix} =$$

$$= M_j^s - 2B^{j_0}$$

Let us instead consider N_{jk}. Remember that the value assumed by this matrix differs depending on j and k. In particular if $j = k$ then $N_{jk} = I$, if instead $j < k$ have $N_{jk} = 0$, if $j > k$ the matrix must be constructed and the steps are defined below

$$N_{jk} = N_{j_k}^s + N_{j_k}^{loss} = \coprod_{l=0}^{j-k-1} J_{j-l} = \coprod_{l=0}^{j-k-1} (J_{j-l}^s + J_{j-l}^{loss}) =$$

$$= \begin{bmatrix} 1 & 0 & 0 \\ 0 & 1 & 0 \\ -2\sum_{l=k+1}^{j} R_l & -2\sum_{l=k+1}^{j} X_l & 1 \end{bmatrix} + \begin{bmatrix} -2\beta_{R_p}^{j_k} & -2\beta_{R_q}^{j_k} & 0 \\ -2\beta_{X_p}^{j_k} & -2\beta_{X_q}^{j_k} & 0 \\ 0 & 0 & 0 \end{bmatrix} =$$

$$= \begin{bmatrix} 1 & 0 & 0 \\ 0 & 1 & 0 \\ -2\sum_{l=k+1}^{j} R_l & -2\sum_{l=k+1}^{j} X_l & 1 \end{bmatrix} - 2 \begin{bmatrix} \beta_{R_p}^{j_k} & \beta_{R_q}^{j_k} & 0 \\ \beta_{X_p}^{j_k} & \beta_{X_q}^{j_k} & 0 \\ 0 & 0 & 0 \end{bmatrix} =$$

$$= N_{j_k}^s - 2B^{j_k}$$

Now that have rewritten these matrices, let's replace them and find Δx_j

$$\Delta x_j = M_j \Delta x_0 + \sum_{k=1}^{n_h} N_{j_k} \Delta f_k =$$

$$= (M_j^s \Delta x_0 + M_j^{loss} \Delta x_0) + \sum_{k=1}^{n_h} (N_{j_k}^s \Delta f_k + N_{j_k}^{loss} \Delta f_k)$$

wher Δf_k represents the forcing. As done previously, to find Δx_j you need to find Δx_0. Then particularizes Δx_j for $j = n_h$ and only the first two lines are considered

$$\begin{bmatrix} 0 \\ 0 \\ \Delta V^2_{n_h} \end{bmatrix} = (M^s_{n_h} + M^{loss}_{n_h}) \begin{bmatrix} \Delta P_0 \\ \Delta Q_0 \\ \Delta \widetilde{V}^2_0 \end{bmatrix} + \sum_{k=1}^{n_h} (N^s_{nh_k} + N^{loss}_{nh_k}) \Delta f_k$$

so

$$\begin{bmatrix} 0 \\ 0 \end{bmatrix} = (\bar{M}^s_{n_h} + \bar{M}^{loss}_{n_h}) \begin{bmatrix} \Delta P_0 \\ \Delta Q_0 \end{bmatrix} + \sum_{k=1}^{n_h} (\bar{N}^s_{nh_k} + \bar{N}^{loss}_{nh_k}) \Delta f_k$$

From this last equation obtain Δx_0

$$\Delta x_0 = \begin{bmatrix} \Delta P_0 \\ \Delta Q_0 \end{bmatrix} = -(\bar{M}^s_{n_h} + \bar{M}^{loss}_{n_h})^{-1} [\sum_{k=1}^{n_h} (\bar{N}^s_{nh_k} + \bar{N}^{loss}_{nh_k}) \Delta f_k]$$

Now look for the value of $\bar{M}^{-1}_{n_h}$

$$\bar{M}_{n_h} = \bar{M}^s_{nh} + \bar{M}^{loss}_{n_h} = \begin{bmatrix} 1 - 2\beta^{nh_0}_{R_p} & -2\beta^{nh_0}_{R_q} \\ -2\beta^{nh_0}_{X_p} & 1 - 2\beta^{nh_0}_{X_q} \end{bmatrix} = I - 2\bar{B}^{nh_0}$$

To be able to invert the matrix, need to look for the determinant (obtained by neglecting higher order terms)

$$det(\bar{M}_{n_h}) = 1 - 2(\beta^{nh_0}_{R_p} + \beta^{nh_0}_{X_q})$$

Consequently

$$\bar{M}^{-1}_{n_h} = \frac{1}{det(\bar{M}_{n_h})} \bar{M}^*_{n_h} =$$

$$= \frac{1}{1 - 2(\beta^{nh_0}_{R_p} + \beta^{nh_0}_{X_q})} \begin{bmatrix} 1 - 2\beta^{nh_0}_{R_p} & 2\beta^{nh_0}_{R_q} \\ 2\beta^{nh_0}_{X_p} & 1 - 2\beta^{nh_0}_{X_q} \end{bmatrix} =$$

$$= \begin{bmatrix} 1 & 0 \\ 0 & 1 \end{bmatrix} + \frac{2}{det(\bar{M}_{nh})} \begin{bmatrix} \beta^{nh_0}_{R_p} & \beta^{nh_0}_{R_q} \\ \beta^{nh_0}_{X_p} & \beta^{nh_0}_{X_q} \end{bmatrix} =$$

$$= I + \frac{2}{det(\bar{M}_{n_h})} \bar{B}^{nh_0}$$

Start again from Δx_0, and rewrite this expression by replacing the obtained values

$$\Delta x_0 = \begin{bmatrix} \Delta P_0 \\ \Delta Q_0 \end{bmatrix} = -(\bar{M}^s_{nh} + \bar{M}^{loss}_{n_h})^{-1} [\sum_{k=1}^{n_h} (\bar{N}^s_{nh_k} + \bar{N}^{loss}_{nh_k}) \Delta f_k] =$$

$$= -(I + \frac{2}{det(\bar{M}_{n_h})}\bar{B}^{nh_0})[\sum_{k=1}^{n_h}(I - 2\bar{B}^{nh_k})\Delta f_k] =$$

$$= -(I + \frac{2}{det(\bar{M}_{n_h})}\bar{B}^{nh_0})[\sum_{k=1}^{n_h} I\Delta f_k - \sum_{k=1}^{n_h} 2\bar{B}^{nh_k}\Delta f_k] =$$

$$= -(I)(\sum_{k=1}^{n_h} I\Delta f_k) - (I)(-2\sum_{k=1}^{n_h} \bar{B}^{nh_k}\Delta f_k) -$$

$$-(\frac{2}{det(\bar{M}_{nh})}\bar{B}^{nh_0})(\sum_{k=1}^{n_h} I\Delta f_k) - (\frac{2}{det(\bar{M}_{n_h})}\bar{B}^{nh_0})(-\sum_{k=1}^{n_h} 2\bar{B}^{nh_k})\Delta f_k) =$$

$$= -\sum_{k=1}^{n_h}\Delta f_k + \sum_{k=1}^{n_h} 2\bar{B}^{nh_k}\Delta f_k - \sum_{k=1}^{n_h}\frac{2}{det(\bar{M}_{nh})}\bar{B}^{nh_0}\Delta f_k + \sum_{k=1}^{n_h}\frac{4}{det(\bar{M}_{n_h})}\bar{B}^{nh_0}\bar{B}^{nh_k}\Delta f_k =$$

$$= -\sum_{k=1}^{n_h} I\Delta f_k + \sum_{k=1}^{n_h}(2\bar{B}^{nh_k} - \frac{2}{det(\bar{M}_{n_h})}\bar{B}^{nh_0} + \frac{4}{det(\bar{M}_{n_h})}\bar{B}^{nh_0}\bar{B}^{nh_k})\Delta f_k$$

Two matrices are now defined: $\bar{S}$ the structural part and $\bar{L}^{nh_k}$ the losses part

$$\bar{S} = I$$

$$\bar{L}^{nh_k} = (2\bar{B}^{nh_k} - \frac{2}{det(\bar{M}_{n_h})}\bar{B}^{nh_0} + \frac{4}{det(\bar{M}_{n_h})}\bar{B}^{nh_0}\bar{B}^{nh_k})$$

Therefore, written in a concise manner

$$\Delta x_0 = \begin{bmatrix}\Delta P_0 \\ \Delta Q_0 \\ \Delta V_0^2\end{bmatrix} = -\sum_{k=1}^{n_h} S\Delta f_k + \sum_{k=1}^{n_h} L^{nh_k}\Delta f_k + \begin{bmatrix}0 \\ 0 \\ 1\end{bmatrix}\Delta\widetilde{V}_0^2$$

Found Δx_0, replace it in Δx_j and obtain

$$\Delta x_j = M_j\Delta x_0 + \sum_{k=1}^{n_h} N_{j_k}\Delta f_k =$$

$$= (M_j^s\Delta x_0 + M_j^{loss}\Delta x_0) + \sum_{k=1}^{n_h}(N_{j_k}^s\Delta f_k + N_{j_k}^{loss}\Delta f_k) =$$

$$= (M_j^s + M_j^{loss}) - \sum_{k=1}^{n_h} S\Delta f_k + \sum_{k=1}^{n_h} L^{nh_k}\Delta f_k + \begin{bmatrix}0 \\ 0 \\ 1\end{bmatrix}\Delta\widetilde{V}_0^2 + (N_{j_k}^s + N_{j_k}^{loss})\Delta f_k =$$

$$= -\sum_{k=1}^{n_h} M_j^s S \Delta f_k + \sum_{k=1}^{n_h} M_j^s L^{nh_k} \Delta f_k + M_j^s \begin{bmatrix} 0 \\ 0 \\ 1 \end{bmatrix} \Delta \widetilde{V}_0^2 -$$

$$-\sum_{k=1}^{n_h} M_j^{loss} S \Delta f_k + \sum_{k=1}^{n_h} M_j^{loss} L^{nh_k} \Delta f_k + M_j^{loss} \begin{bmatrix} 0 \\ 0 \\ 1 \end{bmatrix} \Delta \widetilde{V}_0^2 +$$

$$+\sum_{k=1}^{n_h} N_{j_k}^s \Delta f_k + \sum_{k=1}^{n_h} N_{j_k}^{loss} \Delta f_k$$

A series of steps are carried out to then group the terms without the losses and with

$$\Delta x_j = \sum_{k=1}^{n_h} (-M_j^s S + N_{jk}^s + M_j^s L^{nh_k} - M_j^{loss} S - M_j^{loss} L^{nh_k} + N_{j_k}^{loss}) \Delta f_k +$$

$$+ (M_j^s \begin{bmatrix} 0 \\ 0 \\ 1 \end{bmatrix} + M_j^{loss} \begin{bmatrix} 0 \\ 0 \\ 1 \end{bmatrix}) \Delta \widetilde{V}_0^2$$

define

$$B_{j_k} = B_{j_k}^s + B_{jk}^{loss} = (-M_j^s S + N_{j_k}^s) + (M_j^s L^{nh_k} - M_j^{loss} S + M_j^{loss} L^{nh_k} + N_{j_k}^{loss})$$

$$b_j = b_j^s + b_j^{loss} = (M_j^s \begin{bmatrix} 0 \\ 0 \\ 1 \end{bmatrix}) + (M_j^{loss} \begin{bmatrix} 0 \\ 0 \\ 1 \end{bmatrix})$$

Therefore rewrite Δx_j with the same formulation already used but in this case have the integration of the losses

$$\Delta x_j = \Delta x_j^s + \Delta x_j^{loss} = \sum_{k=1}^{n_h} B_{j_k}^s \Delta f_k + b_j^s \Delta \bar{V}_0^2 + \sum_{k=1}^{n_h} B_{j_k}^{loss} \Delta f_k + b_j^{loss} \Delta \bar{V}_0^2$$

Also in this case the expressions of $B_{j_k}^s$ and of B_{jk}^{loss} can be easily interpreted and constructed similarly to what has been explained at the end of the previous section for B_{j_k} in the case of structural linear model.

3.4 Lateral Model

For the sake of conciseness, the Lateral model is reported only for the case of the structural linear model; the same procedure can be followed also in the case that losses were considered.

3.4.1 Structural linear model

To specify the model feeder equations for each one of the m feeders, a superscript referring to the feeder number is added to the variables, matrices and vectors.

Then, the model equations for the $h-th$ feeders becomes

$$\Delta x_{h,j} = \sum_{k=1}^{n_h} B_{h,j_k} \Delta x_{h,k}^f + b_0 \Delta \widetilde{V}_{h,0}^2 \tag{3.5}$$

Where h represents the generic lateral and is $h = 1, ..., L$.
The external forcing of the node k of the lateral h is defined as follows

$$\Delta x_{h,k}^f = \begin{bmatrix} \Delta P_{h,k}^{inj} \\ \Delta Q_{h,k}^{inj} \\ \Delta V_{h,k}^{ext} \end{bmatrix}$$

The main feeder, on the other hand, is indicated with a subscript $h = 0$

$$\Delta x_{0,j} = \sum_{k=1}^{n_0} B_{0,j_k} \Delta x_{0,k}^f + b_0 \Delta \widetilde{V}_{0,0}^2 \tag{3.6}$$

To get a defined problem, as also done for the feeder, it is necessary to assign three additional conditions. They are derived from the behavior of the feeder at its borders. In particular, the magnitude of the voltage at the head of the power supply is imposed by the MV/LV power supply cabin and the active and reactive powers output from the terminal node of the feeders which however in this case are not zero.
Boundary conditions can be expressed in terms of variations in electricity nodal variables such as

$$P_{h,0} = -\sum_{k=1}^{n_h} P_{h,k}^{inj}, \quad Q_{h,0} = -\sum_{k=1}^{n_h} Q_{h,k}^{inj} \tag{3.7}$$

The variation of the squared voltage amplitude imposed at the LV busbar by the MV/LV supplying substation, which is equal to

$$\Delta\widetilde{V}^2_{h,0} = \Delta V^2_{0,n_0} \forall h = 1, ..., L \tag{3.8}$$

Equation (3.5) is correct except for imposing (3.8) while for (3.7) it is necessary to impose in the last node the active and reactive powers not equal to zero but to the sum of the starting powers at the laterals. Rewrite the maim feeder by imposing the (3.7), and in (3.7) rewrite $P_{h,0}$ and $Q_{h,0}$ obtained from (3.5) for $j = 0$

$$\Delta x_{h,0} = \sum_{k=1}^{n_h} B_{h,0_k} \Delta x^f_{h,k} + b_0 \Delta\widetilde{V}^2_{h,0}$$

with

$$B_{h,0k} = \begin{bmatrix} -1 & 0 & 0 \\ 0 & -1 & 0 \\ 0 & 0 & 0 \end{bmatrix} \quad and \quad b_0 = \begin{bmatrix} 0 \\ 0 \\ 1 \end{bmatrix}$$

As a result it is obtained

$$P_{h,0} = -\sum_{k=1}^{n_h} P^{inj}_{h,k}, \quad and \quad Q_{h,0} = -\sum_{k=1}^{n_h} Q^{inj}_{h,k}$$

Making the substitution in (3.7)

$$P_{0,n_0} = -\sum_{h=1}^{L}\sum_{k=1}^{n_h} P^{inj}_{h,k}, \quad and \quad Q_{0,n_0} = -\sum_{h=1}^{L}\sum_{k=1}^{n_h} Q^{inj}_{h,k}$$

These on-board conditions apply as in the case of the single feeder

$$\begin{bmatrix} -1 & 0 & 0 \\ 0 & -1 & 0 \end{bmatrix} \sum_{h=1}^{L}\sum_{k=1}^{n_h} \Delta x^f_{h,k} = \begin{bmatrix} \Delta P_{0,0} \\ \Delta Q_{0,0} \end{bmatrix} + \sum_{k=1}^{n_0} \bar{N}_{n_0,k} \Delta x^f_{0,k}$$

with

$$\bar{N}_{n_0,k} = \begin{bmatrix} 1 & 0 & 0 \\ 0 & 1 & 0 \end{bmatrix}$$

therefore

$$\begin{bmatrix}\Delta P_{0,0}\\ \Delta Q_{0,0}\end{bmatrix} = -\begin{bmatrix}1 & 0 & 0\\ 0 & 1 & 0\end{bmatrix}\Delta x^f_{0,k} + \begin{bmatrix}-1 & 0 & 0\\ 0 & -1 & 0\end{bmatrix}\sum_{h=1}^{L}\sum_{k=1}^{n_h}\Delta x^f_{h,k}$$

In this way, obtain the equation

$$\begin{bmatrix}\Delta P_{0,0}\\ \Delta Q_{0,0}\end{bmatrix} = \begin{bmatrix}-1 & 0 & 0\\ 0 & -1 & 0\end{bmatrix}\sum_{h=0}^{L}\sum_{k=1}^{n_h}\Delta x^f_{h,k}$$

As done for the single feeder, replace to obtain $\Delta x_{0,0}$

$$\Delta x_{0,0} = -\begin{bmatrix}1 & 0 & 0\\ 0 & 1 & 0\\ 0 & 0 & 0\end{bmatrix}\sum_{h=0}^{L}\sum_{k=1}^{n_h}\Delta x^f_{h,k} + \begin{bmatrix}0\\ 0\\ 1\end{bmatrix}\Delta\widetilde{V}^2_{0,0}$$

Therefore find the $\Delta x_{0,j}$ in the main feeder

$$\Delta x_{0,j} = -M_{0,j}\begin{bmatrix}1 & 0 & 0\\ 0 & 1 & 0\\ 0 & 0 & 0\end{bmatrix}\sum_{h=0}^{L}\sum_{k=1}^{n_h}\Delta x^f_{h,k} + \begin{bmatrix}0\\ 0\\ 1\end{bmatrix}\Delta\widetilde{V}^2_{0,0} + \sum_{k=1}^{n_0}N_{0,jk}\Delta x^f_{0,k} =$$

$$= -\begin{bmatrix}1 & 0 & 0\\ 0 & 1 & 0\\ -2\sum_{l=1}^{j}R_l & -2\sum_{l=1}^{j}X_l & 0\end{bmatrix}\sum_{h=0}^{L}\sum_{k=1}^{n_h}\Delta x^f_{h,k} + \begin{bmatrix}0\\ 0\\ 1\end{bmatrix}\Delta\widetilde{V}^2_{0,0} + \sum_{k=1}^{n_0}N_{0,jk}\Delta x^f_{0,k} =$$

$$= -\bar{M}_{0,j}\sum_{h=1}^{L}\sum_{k=1}^{n_h}\Delta x^f_{h,k} + \begin{bmatrix}0\\ 0\\ 1\end{bmatrix}\Delta\widetilde{V}^2_{0,0} + \sum_{k=1}^{n_h}\left(-\bar{M}_{0,j} + N_{0,jk}\right)\Delta x^f_{0,k}$$

Define

$$B_{0,j_{n_0}} = -\bar{M}_{0,j} \quad for \quad k > j \quad and \quad B_{0,j_k} = \left(-\bar{M}_{0,j} + N_{0,jk}\right)$$

The variable Δx_0 can be written in the form

$$\Delta x_{0,j} = B_{0,j_{n_0}}\sum_{h=1}^{L}\sum_{k=1}^{n_h}\Delta x^f_{h,k} + \sum_{k=1}^{n_0}B_{0,j_k}\Delta x^f_{0,k} + \begin{bmatrix}0\\ 0\\ 1\end{bmatrix}\Delta\widetilde{V}^2_{0,0} \tag{3.9}$$

Now,the part on the main feeder concluded, imposed (3.8) in the (3.5). It particularize (3.9) for $j = n_0$ in order to obtain $\Delta\widetilde{V}^2_{0,n_0}$ which appears in (3.8)

$$\Delta x_{0,n_0} = B_{0,j_{n_0}} \sum_{h=1}^{L} \sum_{k=1}^{n_h} \Delta x_{h,k}^f + \sum_{k=1}^{n_0} B_{0,n_{0_k}} \Delta x_{0,k}^f + \begin{bmatrix} 0 \\ 0 \\ 1 \end{bmatrix} \Delta \widetilde{V}_{0,0}^2$$

The third line is rewritten using the subscript p instead of h, which represents the right side of (3.8).

$$\begin{aligned} \Delta V_{0,n_0}^2 = & \quad \begin{bmatrix} 2\sum_{l=1}^{n_0} R_l & 2\sum_{l=1}^{n_0} X_l & 0 \end{bmatrix} \sum_{p=1}^{L} \sum_{k=1}^{n_p} \Delta x_{p,k}^f + \\ & + \quad \sum_{k=1}^{n_0} \begin{bmatrix} 2\sum_{l=1}^{n_0} R_l & 2\sum_{l=1}^{n_0} X_l & 1 \end{bmatrix} \Delta x_{0,k}^f + \Delta \widetilde{V}_{0,0}^2 \end{aligned} \tag{3.10}$$

Substituting the (3.8) in the (3.5)

$$\Delta x_{h,j} = \sum_{k=1}^{n_h} B_{h,j_k} \Delta x_{h,k}^f + \begin{bmatrix} 0 \\ 0 \\ 1 \end{bmatrix} \Delta V_{0,n_0}^2 =$$

$$= \sum_{k=1}^{n_h} B_{h,j_k} \Delta x_{h,k}^f + \begin{bmatrix} 0 \\ 0 \\ 1 \end{bmatrix} \begin{bmatrix} 2\sum_{l=1}^{n_0} R_l & 2\sum_{l=1}^{n_0} X_l & 0 \end{bmatrix} \sum_{p=1}^{L} \sum_{k=1}^{n_p} \Delta x_{p,k}^f +$$

$$+ \sum_{k=1}^{n_0} b_0 \begin{bmatrix} 2\sum_{l=1}^{k} R_l & 2\sum_{l=1}^{k} X_l & 1 \end{bmatrix} \Delta x_{0,k}^f + b_0 \Delta \widetilde{V}_{0,0}^2 =$$

$$= \sum_{k=1}^{n_h} B_{h,j_k} \Delta x_{h,k}^f + \begin{bmatrix} 0 & 0 & 0 \\ 0 & 0 & 0 \\ 2\sum_{l=1}^{n_0} R_l & 2\sum_{l=1}^{n_0} X_l & 0 \end{bmatrix} \sum_{p=1}^{L} \sum_{k=1}^{n_p} \Delta x_{p,k}^f +$$

$$+ \sum_{k=1}^{n_0} \begin{bmatrix} 0 & 0 & 0 \\ 0 & 0 & 0 \\ 2\sum_{l=1}^{k} R_l & 2\sum_{l=1}^{k} X_l & 1 \end{bmatrix} \Delta x_{0,k}^f + b_0 \Delta \widetilde{V}_{0,0}^2 =$$

$$= \sum_{k=1}^{n_h} B_{h,j_k} \Delta x_{h,k}^f \begin{bmatrix} 0 & 0 & 0 \\ 0 & 0 & 0 \\ 2\sum_{l=1}^{n_0} R_l & 2\sum_{l=1}^{n_0} X_l & 0 \end{bmatrix} \sum_{p=1\neq h}^{L} \sum_{k=1}^{n_p} \Delta x_{p,k}^f +$$

$$\sum_{k=1}^{n_h} \begin{bmatrix} 0 & 0 & 0 \\ 0 & 0 & 0 \\ 2\sum_{l=1}^{n_0} R_l & 2\sum_{l=1}^{n_0} X_l & 0 \end{bmatrix} \Delta x_{h,k}^f + \sum_{k=1}^{n_0} \begin{bmatrix} 0 & 0 & 0 \\ 0 & 0 & 0 \\ 2\sum_{l=1}^{k} R_l & 2\sum_{l=1}^{k} X_l & 1 \end{bmatrix} \Delta x_{0,k}^f +$$

$$b_0 \Delta \widetilde{V}_{0,0}^2$$

Define

$$\bar{B}_{0,n_0} = \begin{bmatrix} 0 & 0 & 0 \\ 0 & 0 & 0 \\ 2\sum_{l=1}^{n_0} R_l & 2\sum_{l=1}^{n_0} X_l & 0 \end{bmatrix}$$

and

$$B_{0,n_0 k} = \begin{bmatrix} 0 & 0 & 0 \\ 0 & 0 & 0 \\ 2\sum_{l=1}^{k} R_l & 2\sum_{l=1}^{k} X_l & 1 \end{bmatrix}$$

After this series of steps the lateral model is obtained

$$\begin{aligned} \Delta x_{h,j} &= B_{0,n_0} + \sum_{p=1\neq h}^{L} \sum_{k=1}^{n_p} \Delta x_{p,k}^f + \sum_{k=1}^{n_0} B_{0,n_0 k} \Delta x_{0,k}^f + b_0 \Delta \widetilde{V}_{0,0}^2 + \\ &+ \sum_{k=1}^{n_h} (B_{h,j_k} + B_{0,n_0}) \Delta x_{h,k}^f \end{aligned} \tag{3.11}$$

On the first two rows of equation (3.11) there are non-zero values that are equal to -1 only for B_{h,j_k}, i.e. for those DERs present on lateral h considered downstream of branch j.

On the third lines however, have an equivalent model of a single feeder made from the main plus the lateral h, adding all the active and reactive power forcing injected by the DER into the node $(0, n_0)$.

It is possible construct the matrices B_{h,j_k} by referring to the equivalent model for branch (h, j) and the (3.9) for the main feeder, it refers to the

equivalent model on which the data is construct the B_{0,j_k} as in the case of a single feeder.

Therefore, the Linearized Lateral Model can also be constructed in a similar way by adding the losses.

3.5 Structural Load Flow Algorithm

An efficient algorithm is presented to evaluate the sensitivity matrices of the active and reactive power flows and of the voltages to DERs injections and to the action of voltage control devices. For the sake of conciseness, the algorithm is presented with reference to the structural linear model of the distribution system, but can easily be extended to account for losses in an approximated way as described in the previous sections.
The code used is present in each step in the Appendix.

The general block diagram is reported in Fig. 3.5 and in the reminder each step of the procedure is analysed.

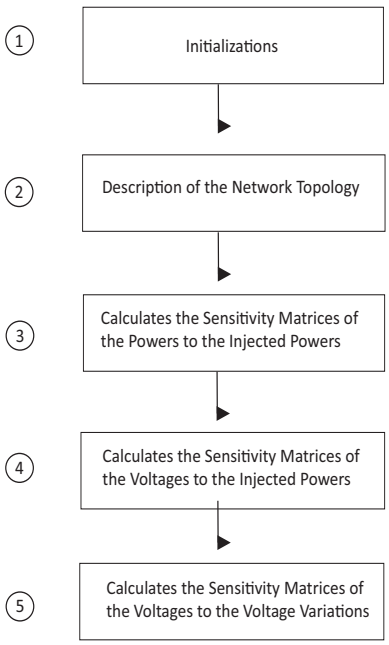

Figure 3.5: Flow Chart Algorithm

For the sake of clarity but without loss of generality, reference is made to the distribution network represented in Fig. 3.1. In Fig. 3.6 for better understanding, a branch, a feeder, and a lateral are highlighted, respectively, in yellow, blue and red colors.

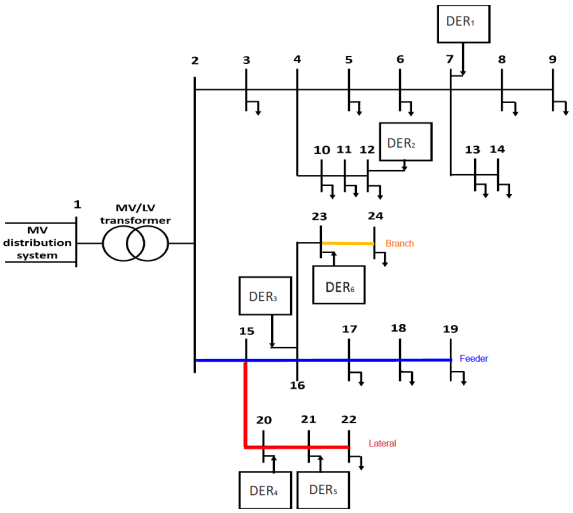

Figure 3.6: Highlighted Network Division

3.5.1 Initializations

The smallest element of the LV distribution network is precisely consider: the branch. The algorithm needs the following initializations: the definitions of the slack node, the number of branches, then the starting and arrival node of the branch and finally the resistance and reactance of each branch.

3.5.2 Description of the Network Topology

A fundamental step to arrive at the construction of the matrices is the definition of the network topology. In particular for each branch a path must be defined, that is, it is necessary to define the sequence of branches to go upstream from the branch in question to the slack node. Therefore, to define the path of each branch, the path is evaluated backwards by finding the branch that presents as ending node the initial node of the branch under consideration. In Fig. 3.7, there is a graphical representation of a path

chosen as an example.

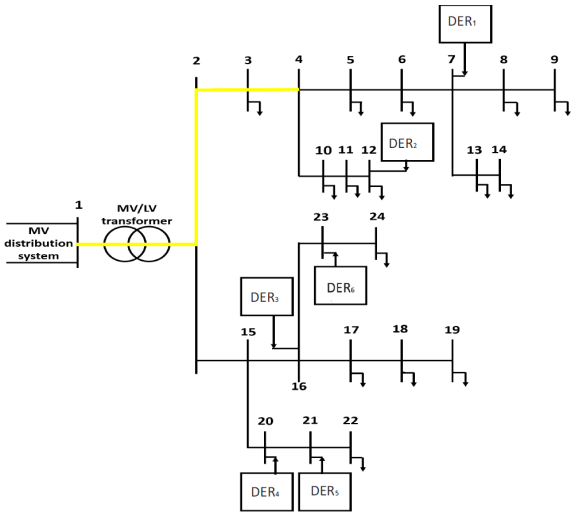

Figure 3.7: Path for the branch $3-4$

So to go from branch 4 to the slack, in this example represented by branch 1, this path highlighted in yellow is created. The algorithm, therefore, iterate this reasoning for each branch of the network.

Therefore, in order to define the path for each branch, the path backwards to the slack is carried out. It considers the starting node of the branch and sees for which other branches it is the arrival node. The iteration ends when slack is reached. Sequences are therefore obtained, in which the branch itself is present first and then all those upstream up to the CS (fixed to slack).

3.5.3 Evaluation of the Sensitivity Matrices of the Powers to the Injected Powers

Once the paths have been defined, the algorithm continues by calculating the sensitivity matrices of the power flows to the powers injections.

Let's assume, as shown in Fig. 3.8, that the DER_2 injects power (active or reactive, as the reasoning is equivalent).

If there is an active power injection in a branch of the network, the power that flows in the branch itself and also in the branches that belong to the path of the considered branch, upstream to the slack node. Assuming there are no losses, a power injection of 1 p.u leads to a reduction (by convection) of 1 p.u in the power on these branches.

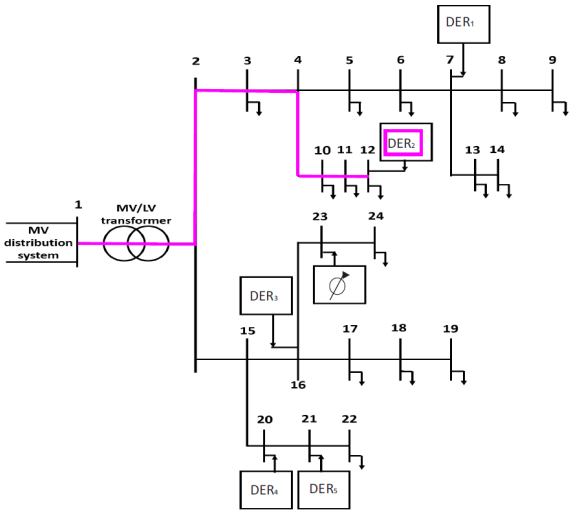

Figure 3.8: Graphic Example n. 1 for the Calculation of Matrix $\mathbf{T}_P^{Pder}$

Therefore, to build the matrix, the value -1 inserted in correspondence with all the branches upstream of the one where the injection took place. The other branches, on the contrary, are not affected by the power injection and therefore have a null value.
The construction occurs in an identical manner in the case of a reactive power injection.

3.5.4 Evaluation of the Sensitivity Matrices of the Voltages to the Injected Powers

To define the construction of the voltage matrix with respect to power injections, active or reactive,the reasoning is different. For example, an injection of power into the branch is assumed, as in Fig. 3.8.

The voltage drop at that point equal to the sum of the resistances of the branches present in the path times 2 and times the ΔP. the reasoning is identical in the case of reactive power injection but the sum of the reactances of the branches on the path is considered.

However, the remaining values of the matrix are not zero. Therefore, by injecting power into a branch, do not have variations in active and reactive power in the branches not belonging to the path, but certainly have a variation in the voltage for these branches. The algorithm then define which branches are in common and replace, for all subsequent branches, the voltage

sensitivity coefficients of the last branch in common.

At this point, we have a value for all the elements of the path matrix.

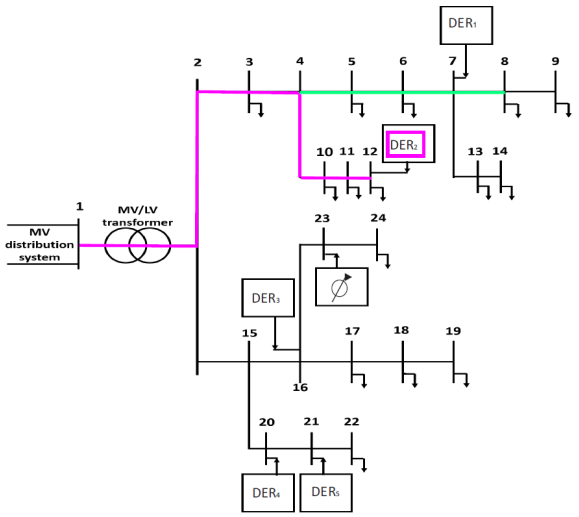

Figure 3.9: Graphic Example n. 2 for the Calculation of Matrix $\mathbf{T}_V^{Pder}$ and $\mathbf{T}_V^{Qder}$

Therefore referring to the Fig. 3.9, the power injection of DER_2 not change in power on branch 8 but, naturally, there change in voltage. Therefore the algorithm define for branches 5,6,7 and 8, the voltage sensitivity coefficient of branch 4 being the branch in common with the path.

3.5.5 Evaluation of the Sensitivity Matrix of the Voltages to the Voltage Regulators action

At this point calculate the sensitivity matrices of the voltages to the VRs. It is assumed that have the VRs that provides a voltage step in the $24th$ branch, in Fig. 3.10.

The steps of the algorithm build the matrix composed of unitary values for the branches whose path include the branch in question (on green line) and null values for the remaining branches.

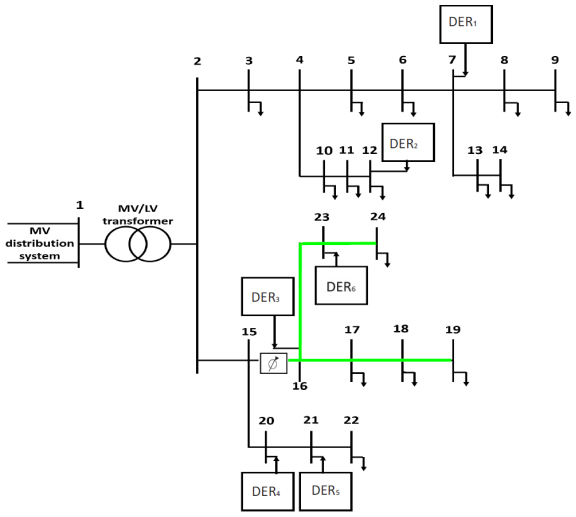

Figure 3.10: Graphic Example for the Calculation of Matrix $\mathbf{T}_V^{V_{RT}}$

Appendix

Structural Load Flow Algorithm

```
%% initializations

pf=loadcase('European_Enel_237_riord_caseA');
n_branch=length(pf.branch(:,1));
node_par=pf.branch(:,1);
node_arr=pf.branch(:,2);
nodes=pf.bus(:,1);
n_node=length(nodes);
slack=pf.bus(find(pf.bus(:,2)==3),1);
R_branch=pf.branch(:,3);
X_branch=pf.branch(:,4);

    % calculate the path from each node to the slack in terms of
    branches

    for n=1:n_branch
        path_branch{n}=[n];
        current_node=node_par(n);
        index=find(node_arr==current_node);
        while ~isempty(index);
            path_branch{n}=[path_branch{n}; index];
            current_node=node_par(index);
            index=find(node_arr==current_node);
        end
    end
```

```
% calculate the sensitivity matrix of the power flows

T_P_Pder=zeros(n_branch,n_node-1);
for n=1:n_branch
    T_P_Pder(path_branch{n},n)=-1.0;
end
T_Q_Qder=T_P_Pder;



% calculates the sensitivity matrices of the voltages to the
powers

T_V_Pder=zeros(n_branch,n_branch);
T_V_Qder=zeros(n_branch,n_branch);
for n=1:n_branch
    Lpath=length(path_branch{n});
    Rtot=0.0; Xtot=0.0;
    for nb=Lpath:-1:1;
        current_branch=path_branch{n}(nb);
        Rtot=Rtot+2*R_branch(current_branch);
        T_V_Pder(current_branch,n)=Rtot;
        Xtot=Xtot+2*X_branch(current_branch);
        T_V_Qder(current_branch,n)=Xtot;
    end
end


for n=1:n_branch
    for nb=1:n_branch
        if T_V_Pder(nb,n)==0
            last_index=0;
            Lpath=length(path_branch{nb});
            for nbb=Lpath:-1:1

index=find(path_branch{n}==path_branch{nb(nbb));
if ~isempty(index) last_index=path_branch{n(index);
            end
            end
            T_V_Pder(nb,n)=T_V_Pder(last_index,n);
            T_V_Qder(nb,n)=T_V_Qder(last_index,n);
        end
    end
end


 % calculates the sensitivity matrices of the voltages to the
 VR voltages

 T_V_VRT=eye(n_branch,n_branch);
 for n=1:n_branch
     for nb=1:n_branch
         index=find(path_branch{nb}==n);
         if ~isempty(index) T_V_VRT(nb,n)=1.0; end
     end
 end
```

Part III

The voltage optimization problem in smart grids

Chapter 4

Decentralized Voltage Optimization Problem

The basic voltage optimization problem is expressed in a centralized form and it is taken as a starting point for moving to the decentralized formulations.

The centralized Voltage Optimization Problem (VOP) minimizes the voltage deviations from their reference values; the equality constraints are the PF equations of the network; the inequality constraints are the limits of the nodal voltages and of the DG reactive powers, yielding the classical optimal reactive power flow (ORPF) problem:

$$\begin{aligned} &\min_{Q_{k_1},\ldots,Q_{k_{N_{DG}}}} \sum_{i=1}^{N}(V_i^2 - V_{i,\text{ref}}^2)^2 \\ &\text{subject to} \\ &\quad \text{PF equations} \\ &\quad V_{i,\min} \le V_i \le V_{i,\max} \qquad i = 1,\ldots,N \\ &\quad Q_{k,\min} \le Q_k \le Q_{k,\max} \quad k = k_1,\ldots,k_{N_{DG}} \end{aligned} \tag{4.1}$$

where V_i and $V_{i,\text{ref}}$ are, respectively, the nodal voltage amplitude and its reference value at the i-th node of the grid; $[V_{i,\min}, V_{i,\max}]$ and $[Q_{k,\min}, Q_{k,\max}]$ are the admissible ranges of variation of the nodal voltage amplitudes and of the reactive powers offered by DGs, respectively; N and N_{DG} are the numbers of nodes of the network and of the DGs, respectively; and $\{k_1,\ldots,k_{N_{DG}}\}$ is a subset of $\{1,\ldots,N\}$ including only the nodes of the network with DGs. The VOP (4.1) is a non-linear programming problem of large dimension which

provides the best solution of the voltage control problem but presents possible convergence problems, due to the non linear PF equations and the large dimension.

To reduce the complexity of the problem [24], the PF equations in (4.1) are linearized by the method proposed in [25] or the various linear approximations proposed in literature and recalled in the previous Part II.
Let:

$$\mathbf{y}^{\mathrm{T}} = \{\Delta V_1^2, \ldots, \Delta V_N^2\}$$
$$\mathbf{x}^{\mathrm{T}} = \{\Delta Q_{k_1}, \ldots, \Delta Q_{k_{N_{dg}}}\}$$

be the vectors of the variations of the nodal voltages and of the DG reactive powers from an initial working condition, respectively. Then, (4.1) can be written in the matrix form as:

$$\begin{aligned} &\min_{\mathbf{x}} \frac{1}{2}\mathbf{y}^{\mathrm{T}}\mathbf{y} - \mathbf{y}_{\mathrm{ref}}{}^{\mathrm{T}}\mathbf{y} \\ &\text{subject to} \\ &\quad \mathbf{y} = \mathbf{\Gamma}\mathbf{x} \\ &\quad \mathbf{y}_{\min} \leq \mathbf{y} \leq \mathbf{y}_{\max} \\ &\quad \mathbf{x}_{\min} \leq \mathbf{x} \leq \mathbf{x}_{\max} \end{aligned} \tag{4.2}$$

where $\mathbf{\Gamma}$ is the sensitivity matrix of the nodal voltages to the DG reactive powers; $\mathbf{y}_{\mathrm{ref}}$ is the vector of the variations of the reference values; $[\mathbf{y}_{\min}, \mathbf{y}_{\max}]$ and $[\mathbf{x}_{\min}, \mathbf{x}_{\max}]$ are the operating constraints of the network and DGs, respectively. By using the linearized PF equations in the objective function, (4.2) changes into

$$\begin{aligned} &\min_{\mathbf{x}} \frac{1}{2}\mathbf{x}^{\mathrm{T}}\mathbf{H}\mathbf{x} - \mathbf{h}^{\mathrm{T}}\mathbf{x} \\ &\text{subject to} \\ &\quad \mathbf{y}_{\min} \leq \mathbf{\Gamma}\mathbf{x} \leq \mathbf{y}_{\max} \\ &\quad \mathbf{x}_{\min} \leq \mathbf{x} \leq \mathbf{x}_{\max} \end{aligned} \tag{4.3}$$

where: $\mathbf{H} = \mathbf{\Gamma}^{\mathrm{T}}\mathbf{\Gamma}$ and $\mathbf{h}^{\mathrm{T}} = \mathbf{y}_{\mathrm{ref}}\mathbf{\Gamma}^{\mathrm{T}}$. Since $\mathbf{H}$ is a symmetric and positive definite matrix, the objective function is strictly convex and (4.3) presents a global minimum. With respect to (4.1), the drawback is the approximation of the solution whereas the benefit is the absence of convergence problem in finding the numerical solution. Anyway, problem (4.3) is still a centralized VOP requiring large investments.

4.1 Decentralized VOP with ADMM

Firstly, a linear method for the steady-state analysis of distribution networks is used to formulate a centralized voltage optimization problem of a network partitioned into voltage control zones. Then, overlapping variables are introduced and the lack of strict convexity of the objective function is handled by adopting the iterative method of multipliers. Finally, a fully decentralized problem is obtained by applying the alternate direction multiplier method (ADMM); it results in a quadratic programming problem to be solved in each area with a limited number of scalar variables to swap.

A decentralized VOP is a valid alternative to reduce the high investment cost of the centralized solution. The first stage is to divide the distribution network into several VCZs by a partitioning method [26], [10], [20] . For the sake of readability, only two VCZs, indicated as VCZ_1 and VCZ_2, are considered; by the way it is without loss of generality, because the results can be extended to a larger number of VCZs. For each VCZ a PN is identified, indicated as PN_1 and PN_2 [27–29]. In the following subscripts 1 and 2 specify the electrical quantities in, respectively, VCZ_1 and VCZ_2.

It is assumed that VCZ_1 (VCZ_2) is equipped with a Control Center (C.C.) that acquires the measurement of the voltage amplitude of PN_1 (PN_2); then, the C.C. of VCZ_1 (VCZ_2) solves a zone VOP exchanging data with the C.C. of VCZ_2 (VCZ_1) and, eventually, sends the set-points to the reactive power controllers of the DGs in VCZ_1(VCZ_2). Such an approach limits the measurements from the field and the data exchange among zone C.C.s and DGs. In the following, (4.2) is revisited to get its decentralized formulation. To this aim:

- it is rewritten for a grid partitioned into two VCZs;
- additional variables are introduced;
- the Lagrange Multipliers (MMs) is applied to solve the dual problem working on the Augmented Lagrangian function (LA);
- the ADMM is applied to achieve a decentralized solution.

4.1.1 VOP Partitioning

Let $\mathbf{u}_1$ ($\mathbf{u}_2$) be the vectors of variational variables including the voltage amplitude of PN_1 (PN_2) and the reactive powers of the DGs in VCZ_1 (VCZ_2); in the first step, (4.2) is rewritten as, see Appendix

$$\begin{aligned} &\min_{\mathbf{u}_1,\mathbf{u}_2} F(\mathbf{u}_1) + F(\mathbf{u}_2) \\ &\text{subject to} \\ &\mathbf{e}_{11}^{\mathrm{T}}\mathbf{u}_1 + \mathbf{e}_{12}^{\mathrm{T}}\mathbf{u}_2 = 0 \quad \mathbf{e}_{21}^{\mathrm{T}}\mathbf{u}_1 + \mathbf{e}_{22}^{\mathrm{T}}\mathbf{u}_2 = 0 \\ &\mathbf{u}_{1\min} \leq \mathbf{u}_1 \leq \mathbf{u}_{1\max} \quad \mathbf{u}_{2\min} \leq \mathbf{u}_2 \leq \mathbf{u}_{2\max} \end{aligned} \tag{4.4}$$

In comparison with (4.2), the objective function in (4.4) accounts only for the voltages of the PNs with separable terms; then, it can be distributed between the two VCZs together with the inequality constraints. As a drawback, the objective function remains convex but not in a strict sense. Then, problem (4.4) presents local minimum points. Moreover, (4.4) is still not fully-decentralized, because the equality constraints are not separable. In fact, the first equality constraint highlights the influence of the injections of the reactive powers of the DGs in both VCZ_1 and VCZ_2 on the voltage amplitude of the PN_1; a similar consideration stands for the second equality constraint.

4.1.2 Additional Variables

To better handle the coupling constraints, additional scalar variables z_{11}, z_{12}, z_{21} and z_{22} are introduced in (4.4), see Appendix

4.1.3 Method of Multipliers

To overcome the lack of strict convexity of the objective function, the dual optimization problem, working on the LA function related to the coupling constraints, is used and iteratively solved by the MMs [30], see Appendix. Even if the MMs permits to handle the lack of strict convexity of the objective function, the presence of the quadratic terms in the Augmented Lagrangian [31–33]function still makes the problem nonseparable among the two VCZs.

4.1.4 Alternating Direction Method of Multipliers

Finally, the ADMM [30], [34], [35] is used to decompose the VOP into separable problems so as to obtain the optimization problem to be solved by each zone C.C. and the data exchange between the two C.C.s, see Appendix In particular, in each iteration of ADMM, the zone C.C. of VCZ_1 solves the following quadratic programming problem:

$$\begin{aligned} &\min_{\mathbf{u}_1} \frac{1}{2}{\mathbf{u}_1}^{\mathrm{T}}\mathbf{H}_1\mathbf{u}_1 - {\mathbf{h}_1}^{\mathrm{T}}\mathbf{u}_1 \\ &\text{subject to} \\ &\quad \mathbf{u}_{1,\min} \leq \mathbf{u}_1 \leq \mathbf{u}_{1,\max} \end{aligned} \tag{4.5}$$

and the zone C.C. of VCZ_2 solves the following quadratic programming problem:

$$\begin{aligned} &\min_{\mathbf{u}_2} \frac{1}{2}{\mathbf{u}_2}^{\mathrm{T}}\mathbf{H}_2\mathbf{u}_2 - {\mathbf{h}_2}^{\mathrm{T}}\mathbf{u}_2 \\ &\text{subject to} \\ &\quad \mathbf{u}_{2,\min} \leq \mathbf{u}_2 \leq \mathbf{u}_{2,\max} \end{aligned} \tag{4.6}$$

where $\mathbf{H}_1$ and $\mathbf{H}_2$ depend on the sensitivity coefficients in $\mathbf{\Gamma}$; $\mathbf{h}_1$ and $\mathbf{h}_2$ depend on the values $\mathbf{u}_1^*$ and $\mathbf{u}_2^*$ of the variables obtained in the previous step and on the Lagrange multipliers λ_1, λ_2, which are updated according to:

$$\lambda_1 = \lambda_1^* + cw_1 \tag{4.7}$$

$$\lambda_2 = \lambda_2^* + cw_2 \tag{4.8}$$

where w_1, w_2 are calculated by:

$$w_1 = \tfrac{1}{2}\left(\mathbf{e}_{11}^{\mathrm{T}}\,\mathbf{u}_1 + \mathbf{e}_{12}^{\mathrm{T}}\,\mathbf{u}_2\right) \tag{4.9}$$

$$w_2 = \tfrac{1}{2}\left(\mathbf{e}_{21}^{\mathrm{T}}\,\mathbf{u}_1 + \mathbf{e}_{22}^{\mathrm{T}}\,\mathbf{u}_2\right) \tag{4.10}$$

The ADMM is implemented by a distributed algorithm whose steps are Fig. 4.1:

i. initialize $k = 0$, $\mathbf{u}_1 = 0$, $\mathbf{u}_2 = 0$, $\lambda_1 = 0$, $\lambda_2 = 0$, and choose c;

ii. $k = k + 1$;

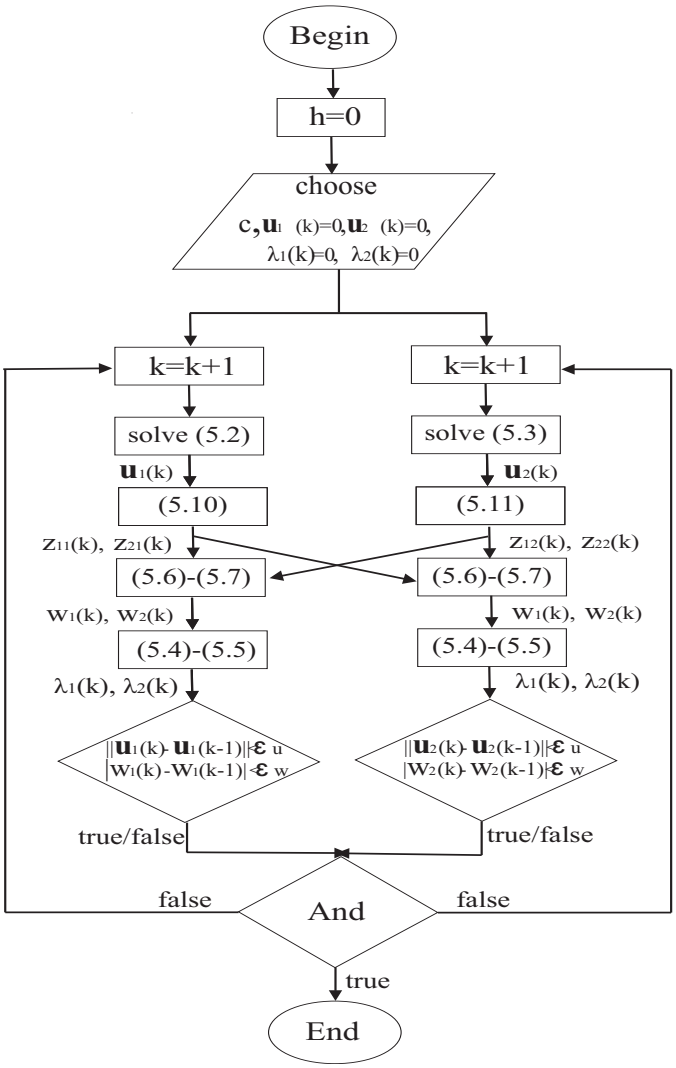

Figure 4.1: Decentralized Algorithm (ADMM)

iii. VCZ_1 and VCZ_2 solve in parallel the minimization problems (4.5) and (4.6), respectively, obtaining the vectors $\mathbf{u}_1(k)$, $\mathbf{u}_2(k)$;

iv. VCZ_1 evaluates the scalars z_{11} and z_{21} (see (4.13) in Appendixand VCZ_2 evaluates the scalars z_{12} and z_{22} (see (4.14) in Appendix

v. VCZ_1 receives z_{12} and z_{22} from VCZ_2, while VCZ_2 receives z_{11} and z_{21} from VCZ_1; VCZ_1 and VCZ_2 separately calculate w_1 and w_2 according to (4.9)-(4.10);

vi. both VCZ_1 and VCZ_2 separately evaluate λ_1 and λ_2 according to (4.7)-(4.8);

vii. VCZ_1 checks if $\|\mathbf{u}_1(k)-\mathbf{u}_1(k-1)\| < \epsilon_u$ and $|w_1(k)-w_1(k-1)| < \epsilon_w$; VCZ_2 if $\|\mathbf{u}_2(k)-\mathbf{u}_2(k-1)\| < \epsilon_u$ and $|w_2(k)-w_2(k-1)| < \epsilon_w$ (being ϵ_u and ϵ_w predefined tolerances);

viii. if the output of step vii. is true for both problems then stop and $\mathbf{u}_1(k)$ and $\mathbf{u}_2(k)$ are the solutions; else go back to step ii. and start a new iteration.

By applying the ADMM, the VOP to be solved by each VCZ is a quadratic programming problem of reduced dimension (see (4.5) and (4.6)); the adopted method allows to cope with the lack of strict convexity of the objective functions, assuring convergence. Furthermore, the data exchange between the two C.C.s is limited to two scalar values (z_{11}, z_{21}, z_{22} and z_{12}) at each iteration, Fig. 4.1. It is worth noticing that the choice of the penalty parameter c can reduce the number of iterations to converge.

4.1.5 Case Study with ADMM

The 24-nodes distribution network, supplied by a 20/0.4 kV substation and including six DGs, Fig. 4.2, is clustered in two VCZs as in [6]. Details about electrical parameters of the network and the loads are also reported in [6].

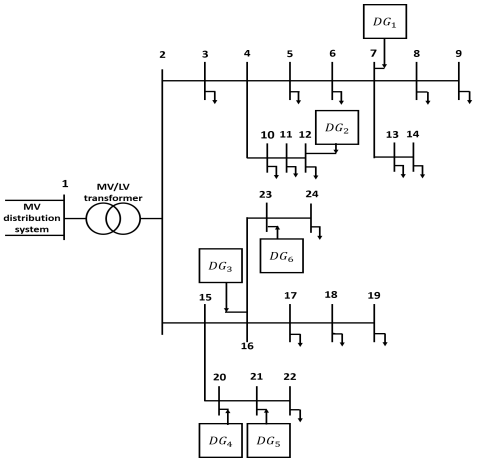

Figure 4.2: Distribution system

Tests have been carried out to verify the performance of the proposed decentralized algorithm, referred to as the *decentralized VOP* in the reminder. In all the tests the *decentralized VOP* has reached convergence; the choice of the penalty parameter c has impact only on the number of iterations to

reach convergence. The parameter c can vary in the range of values from 0.1 to 10: in particular, it has been fixed $c = 0.1$, which has proved to be the best choice. In the following some relevant results are reported referring to the following three cases:

- *Case 1*: V_{MV}=0.99 p.u. and S_{load}=70%S_{load}^{rated};
- *Case 2*: V_{MV}=1.025 p.u. and S_{load}=60%S_{load}^{rated};
- *Case 3*: V_{MV}=0.985 p.u. and S_{load}=50%S_{load}^{rated}.

Concerning the operating conditions of the DG_s, Tab. 4.1 reports the values of the active power injections for all the three cases, and the range of possible variation of the reactive powers.

Table 4.1: Active Power Injections and Reactive Power Ranges for DGs (ADMM)

Power	**Case**	DG_1	DG_2	DG_3	DG_4	DG_5	DG_6
Active (MW)	1	0.020	0.015	0.025	0.015	0.015	0.010
	2	0.010	0.005	0.005	0.025	0.003	0.002
	3	0.018	0.012	0.022	0.012	0.012	0.007
Reactive (MVAr)	1/2/3	±0.0150	±0.0113	±0.0188	±0.0113	±0.0113	±0.0075

The accuracy of the solutions provided by the *decentralized VOP* is analyzed and compared with those of other centralized methods; The improvement of the voltage profiles obtained by the *decentralized VOP* is shown with respect to the case without any kind of VOP; The convergence characteristics of the *decentralized VOP* are compared with the ones of a previously-proposed decentralized algorithm [6].

The accuracy of the solutions obtained by the *decentralized VOP* must be compared with a reference case. To this aim, the ORPF problem is assumed as the *benchmark VOP* and its objective function as a voltage profile index (VPI). The ORPF problem is solved using MATPOWER package considering all the reference values of the nodal voltages equal to 1.0 p.u.. In

Tab. 4.5 the values of the VPI obtained by the *decentralized VOP* for the three cases are reported and compared with the *benchmark VOP*. For the sake of completeness, Tab. 4.5 reports also the values of the VPI obtained by solving the centralized VOP problem *using quadprog function in MATLAB environment*, indicated as the *VCZ-based VOP*. This latter VOP adopts the same objective function and the same linear model of the distribution system as the *decentralized VOP*, but its solution is centralized. Comparing the VPI values of the first and second column in Tab. 4.5, it is evident that in all cases the solutions obtained by the *VCZ-based VOP* present larger values than the corresponding solutions of the *benchmark VOP*: it is due to the different objective function limited to PN_s and to the linear model of the distribution system adopted in the *VCZ-based VOP*. Comparing the VPI values of the second and third column in Tab. 4.5, it is evident that the *decentralized VOP* provides solutions that are very similar to the ones of the *VCZ-based VOP* in terms of VPI values. Comparing the *decentralized VOP* to the *benchmark VOP*, it can be stated that the order of magnitude of the VPI values is the same for all the cases and, consequently, that a good level of accuracy of the solution has been achieved.

The solutions obtained by the *decentralized VOP* in terms of reactive powers injected by DGs are imposed in the distribution system load flow to obtain the resulting voltage profiles along the feeders. Such profiles are compared with the ones obtained by the *benchmark VOP* as well as with the ones obtained assuming no VOP solution, that is imposing null reactive powers injected by DGs.

For the *Case 1*, the voltage profiles of VCZ_1 and VCZ_2 are shown in Figs. 4.3 and 4.4, respectively; similarly, Figs. 4.5 and 4.6 shown the voltage profiles for the *Case 2* and Figs. 4.7 and 4.8 for the *Case 3*.

From the figures, it is evident the improvement of the voltage profiles when an optimization is performed and the proximity of those obtained by the *decentralized VOP* to the ones obtained by the *benchmark VOP*.

The convergence characteristics of the *decentralized VOP* is analyzed with reference to the number of iterations *to reach convergence* and to the numerical solution.

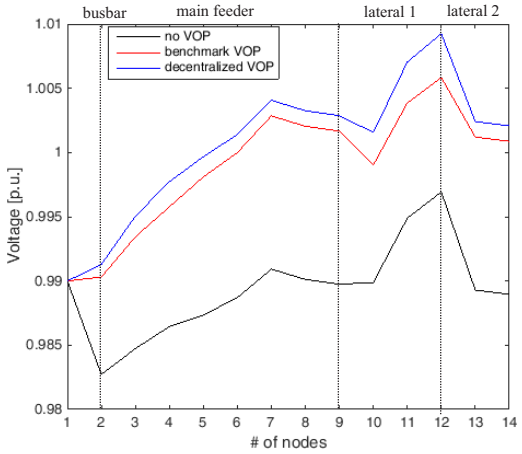

Figure 4.3: Case 1: voltage profile in VCZ_1 (ADMM)

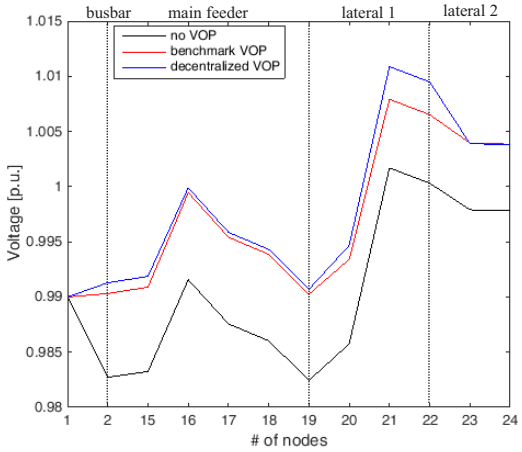

Figure 4.4: Case 1: voltage profile in VCZ_2 (ADMM)

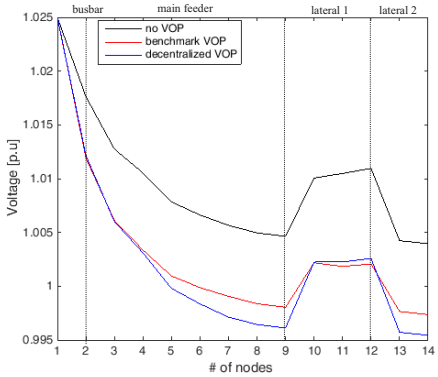

Figure 4.5: Case 2: voltage profile in VCZ_1 (ADMM)

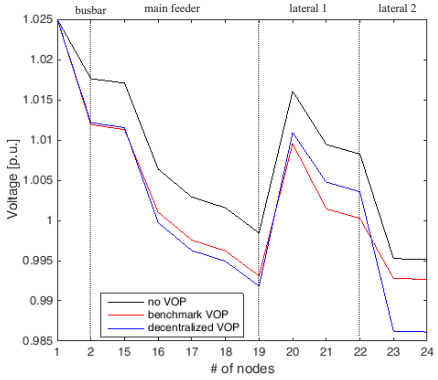

Figure 4.6: Case 2: voltage profile in VCZ_2 (ADMM)

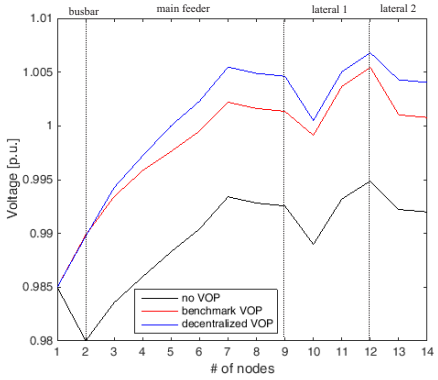

Figure 4.7: Case 3: voltage profile in VCZ_1 (ADMM)

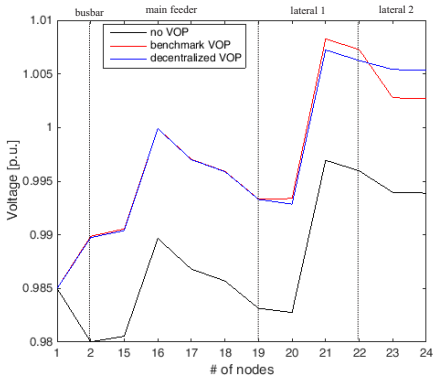

Figure 4.8: Case 3: voltage profile in VCZ_2 (ADMM)

Table 4.2: Voltage Profile Index [$10^{-}3$ *p.u.*] (ADMM)

Case	*benchmark VOP*	*VCZ-based VOP*	*decentralized VOP*
1	2.18	2.82	2.74
2	1.91	2.99	3.65
3	1.84	2.35	2.36

Table 4.3: Number of iterations and Voltage Profile Index (ADMM)

Case	Number of iterations		VPI [$10^{-}3$ *p.u.*]	
	decentralized GS	*decentralized VOP*	*decentralized GS*	*decentralized VOP*
1	68	8	3.14	2.74
2	35	9	3.55	3.65
3	36	20	2.76	2.36

For the sake of comparison, the results obtained by using the decentralized algorithm proposed in [6] are also reported. This algorithm, in the following the *decentralized GS*, solves the dual problem of (4.4) by a decentralized Gauss-Seidel method. In Tab. 4.6 the number of iterations and the values of the VPI of the obtained numerical solutions are reported for all the 3 cases. Comparing the values obtained by the two decentralized algorithms, it can be stated that in all the cases the *decentralized VOP* reaches, with less iterations, a numerical solution which is more accurate with respect to the *decentralized GS*.

4.1.6 Final considerations about ADMM

Using, therefore, the method of alternating direction of multipliers, a quadratic programming problem of limited dimension was iteratively solved in each voltage control zone and the coordination was obtained by exchanging only two scalar quantities between the pilot nodes. The algorithm implementing the iterative method has also been presented. The proposed approach ensures convergence of the voltage optimization problem with a limited number of iterations. Of course this method can be easily extended to a network partitioned into a greater number of clusters.

Appendix

VOP partitioning

Let y_1 (y_2) be the variation of the *squared* nodal voltage at the PN_1 (PN_2), that is $y_1 = \Delta V^2_{PN_1}$ and $y_2 = \Delta V^2_{PN_2}$ and $\mathbf{x}_1$ ($\mathbf{x}_2$) the subset of $\mathbf{x}$ related to the DGs in VCZ_1 (VCZ_2). Then, (4.2) can be rewritten by distributing the variables between the two zones as:

$$\begin{aligned} &\min_{\mathbf{x}_1,\mathbf{x}_2} \quad \tfrac{1}{2}\, y_1^2 - y_{1\text{ref}}\, y_1 + \tfrac{1}{2}\, y_2^2 - y_{2\text{ref}}\, y_2 \\ &\text{subject to} \\ &y_1 = \mathbf{\Gamma}_{11}\mathbf{x}_1 + \mathbf{\Gamma}_{12}\mathbf{x}_2 \quad y_2 = \mathbf{\Gamma}_{21}\mathbf{x}_1 + \mathbf{\Gamma}_{22}\mathbf{x}_2 \\ &y_{1\text{min}} \le y_1 \le y_{1\text{max}} \qquad y_{2\text{min}} \le y_2 \le y_{2\text{max}} \\ &\mathbf{x}_{1\text{min}} \le \mathbf{x}_1 \le \mathbf{x}_{1\text{max}} \qquad \mathbf{x}_{2\text{min}} \le \mathbf{x}_2 \le \mathbf{x}_{2\text{max}} \end{aligned} \tag{4.11}$$

where $\mathbf{\Gamma}_{11}$, $\mathbf{\Gamma}_{12}$, $\mathbf{\Gamma}_{21}$ and $\mathbf{\Gamma}_{22}$ are submatrices of $\mathbf{\Gamma}$. Indicating as:

$$\mathbf{u}_1{}^{\mathrm{T}} = \begin{pmatrix} y_1 & \mathbf{x}_1^{\mathrm{T}} \end{pmatrix} \quad \text{and} \quad \mathbf{u}_2{}^{\mathrm{T}} = \begin{pmatrix} y_2 & \mathbf{x}_2^{\mathrm{T}} \end{pmatrix} \tag{4.12}$$

(4.11) can be rewritten in the compact form (4.4) being

$$\begin{aligned} F(\mathbf{u}_1) &= \tfrac{1}{2}\mathbf{u}_1^{\mathrm{T}}\mathbf{A}_1\mathbf{u}_1 + \mathbf{b}_1^{\mathrm{T}}\mathbf{u}_1 \\ F(\mathbf{u}_2) &= \tfrac{1}{2}\mathbf{u}_2^{\mathrm{T}}\mathbf{A}_2\mathbf{u}_2 + \mathbf{b}_2^{\mathrm{T}}\mathbf{u}_2 \end{aligned}$$

$$\begin{aligned} \mathbf{e}_{11}^{\mathrm{T}} &= \begin{pmatrix} 1 & -\mathbf{\Gamma}_{11} \end{pmatrix} \quad \mathbf{e}_{12}^{\mathrm{T}} = \begin{pmatrix} 0 & -\mathbf{\Gamma}_{12} \end{pmatrix} \\ \mathbf{e}_{21}^{\mathrm{T}} &= \begin{pmatrix} 1 & -\mathbf{\Gamma}_{21} \end{pmatrix} \quad \mathbf{e}_{22}^{\mathrm{T}} = \begin{pmatrix} 0 & -\mathbf{\Gamma}_{22} \end{pmatrix} \end{aligned}$$

with:

$$\mathbf{A}_1 = \mathbf{A}_2 = \begin{pmatrix} 1 & 0 & 0 \\ 0 & 0 & 0 \\ 0 & 0 & 0 \end{pmatrix} \quad \begin{aligned} \mathbf{b}_1^{\mathrm{T}} &= \begin{pmatrix} y_{1\text{ref}} & 0 & 0 \end{pmatrix} \\ \mathbf{b}_2^{\mathrm{T}} &= \begin{pmatrix} y_{2\text{ref}} & 0 & 0 \end{pmatrix} \end{aligned}$$

Additional variables

To handle the coupling between VCZ_1 and VCZ_2 additional scalar variables are defined:

$$z_{11} = \mathbf{e}_{11}^{\mathrm{T}}\mathbf{u}_1 \quad \text{and} \quad z_{21} = \mathbf{e}_{21}^{\mathrm{T}}\mathbf{u}_1 \tag{4.13}$$

$$z_{12} = \mathbf{e}_{12}^{\mathrm{T}}\mathbf{u}_2 \quad \text{and} \quad z_{22} = \mathbf{e}_{22}^{\mathrm{T}}\mathbf{u}_2 \tag{4.14}$$

Assigning z_{11}, z_{21} to VCZ_1 and z_{22}, z_{12} to VCZ_2, (4.4) is rewritten as:

$$
\begin{aligned}
&\min_{\mathbf{u}_1,\mathbf{u}_2} F(\mathbf{u}_1) + F(\mathbf{u}_2) \\
&\text{subject to} \\
&\quad z_{11} + z_{12} = 0 \quad z_{21} + z_{22} = 0 \\
&\quad z_{11} = \mathbf{e}_{11}^{\mathrm{T}}\mathbf{u}_1 \quad z_{12} = \mathbf{e}_{12}^{\mathrm{T}}\mathbf{u}_2 \\
&\quad z_{21} = \mathbf{e}_{21}^{\mathrm{T}}\mathbf{u}_1 \quad z_{22} = \mathbf{e}_{22}^{\mathrm{T}}\mathbf{u}_2 \\
&\quad \mathbf{u}_{1\min} \le \mathbf{u}_1 \le \mathbf{u}_{1\max} \quad \mathbf{u}_{2\min} \le \mathbf{u}_2 \le \mathbf{u}_{2\max}
\end{aligned}
\tag{4.15}
$$

In (4.15) equations that couple the two VCZs are the first two and are expressed in the additional scalar variables z_{11}, z_{12}, z_{21} and z_{22} rather than vectors $\mathbf{u}_1$ and $\mathbf{u}_2$ as in (4.4).

Method of Multipliers

The dual optimization problem of (4.15) is formulated, using the Augmented Lagrangian function related to some of the equality constraints. The dual problem is iteratively solved by the MMs; it consists of successive minimizations of the problem (4.16) followed by the updates of the Lagrange multipliers p_{11}, p_{12}, p_{21} and p_{22} in (4.17) so as to minimize the Augmented Lagrangian within adequate precision [30], that is:

$$
\begin{aligned}
&\min_{\substack{\mathbf{u}_1,z_{11},z_{12}\\ \mathbf{u}_2,z_{21},z_{22}}} \\
&\quad F(\mathbf{u}_1) + F(\mathbf{u}_2) \\
&\quad + p_{11}(z_{11} - \mathbf{e}_{11}^{\mathrm{T}}\mathbf{u}_1) + p_{12}(z_{12} - \mathbf{e}_{12}^{\mathrm{T}}\mathbf{u}_2) \\
&\quad + p_{21}(z_{21} - \mathbf{e}_{21}^{\mathrm{T}}\mathbf{u}_1) + p_{22}(z_{22} - \mathbf{e}_{22}^{\mathrm{T}}\mathbf{u}_2) \\
&\quad + \tfrac{c}{2}(z_{11} - \mathbf{e}_{11}^{\mathrm{T}}\mathbf{u}_1)^2 + \tfrac{c}{2}(z_{12} - \mathbf{e}_{12}^{\mathrm{T}}\mathbf{u}_2)^2 \\
&\quad + \tfrac{c}{2}(z_{21} - \mathbf{e}_{21}^{\mathrm{T}}\mathbf{u}_1)^2 + \tfrac{c}{2}(z_{22} - \mathbf{e}_{22}^{\mathrm{T}}\mathbf{u}_2)^2 \\
&\text{subject to} \\
&\quad z_{11} + z_{12} = 0 \quad z_{21} + z_{22} = 0 \\
&\quad \mathbf{u}_{1\min} \le \mathbf{u}_1 \le \mathbf{u}_{1\max} \quad \mathbf{u}_{2\min} \le \mathbf{u}_2 \le \mathbf{u}_{2\max}
\end{aligned}
\tag{4.16}
$$

with:

$$
\begin{aligned}
p_{11} &= p_{11}^* + c(z_{11} - \mathbf{e}_{11}^{\mathrm{T}}\mathbf{u}_1) \quad p_{12} = p_{12}^* + c(z_{12} - \mathbf{e}_{12}^{\mathrm{T}}\mathbf{u}_2) \\
p_{21} &= p_{21}^* + c(z_{21} - \mathbf{e}_{21}^{\mathrm{T}}\mathbf{u}_1) \quad p_{22} = p_{22}^* + c(z_{22} - \mathbf{e}_{22}^{\mathrm{T}}\mathbf{u}_2)
\end{aligned}
\tag{4.17}
$$

where c is the penalty parameter and * indicates the value assumed by the variable at the previous step.

Alternating Direction Method of Multipliers (ADMM)

The ADMM [30] is an iterative algorithm that decomposes (4.16)-(4.17) between the two VCZs according to:

$$\underline{\text{VCZ}_1}$$

$$\begin{aligned} \min_{\mathbf{u}_1} \quad & F(\mathbf{u}_1) + \lambda_1 \mathbf{e}_{11}^{\mathrm{T}} \mathbf{u}_1 + \lambda_2 \mathbf{e}_{21}^{\mathrm{T}} \mathbf{u}_1 \\ & + \tfrac{c}{2} (\mathbf{e}_{11}^{\mathrm{T}} (\mathbf{u}_1 - \mathbf{u}_1{}^*) + w_1^*)^2 \\ & + \tfrac{c}{2} (\mathbf{e}_{21}^{\mathrm{T}} (\mathbf{u}_1 - \mathbf{u}_1{}^*) + w_2^*)^2 \\ \text{subject to} & \\ & \mathbf{u}_{1\min} \leq \mathbf{u}_1 \leq \mathbf{u}_{1\max} \end{aligned} \tag{4.18}$$

$$\underline{\text{VCZ}_2}$$

$$\begin{aligned} \min_{\mathbf{u}_2} \quad & F(\mathbf{u}_2) + \lambda_1 \mathbf{e}_{12}^{\mathrm{T}} \mathbf{u}_2 + \lambda_2 \mathbf{e}_{22}^{\mathrm{T}} \mathbf{u}_2 \\ & + \tfrac{c}{2} (\mathbf{e}_{12}^{\mathrm{T}} (\mathbf{u}_2 - \mathbf{u}_2{}^*) + w_1^*)^2 \\ & + \tfrac{c}{2} (\mathbf{e}_{22}^{\mathrm{T}} (\mathbf{u}_2 - \mathbf{u}_2{}^*) + w_2^*)^2 \\ \text{subject to} & \\ & \mathbf{u}_{2\min} \leq \mathbf{u}_2 \leq \mathbf{u}_{2\max} \end{aligned} \tag{4.19}$$

whereas the Lagrange multipliers are updated according to:

$$\lambda_1 = \lambda_1^* + c\, w_1 \qquad \lambda_2 = \lambda_2^* + c\, w_2 \tag{4.20}$$

with w_1, w_2 calculated as:

$$w_1 = \tfrac{1}{2} \big(\mathbf{e}_{11}^{\mathrm{T}} \mathbf{u}_1 + \mathbf{e}_{12}^{\mathrm{T}} \mathbf{u}_2 \big) \tag{4.21}$$

$$w_2 = \tfrac{1}{2} \big(\mathbf{e}_{21}^{\mathrm{T}} \mathbf{u}_1 + \mathbf{e}_{22}^{\mathrm{T}} \mathbf{u}_2 \big) \tag{4.22}$$

The minimization problems (4.18)-(4.19) are rewritten in the compact form (4.5)-(4.6) with

$$\mathbf{H}_1 = \mathbf{A}_1 + c \begin{pmatrix} 1 & -\Gamma_{11} \\ -\Gamma_{11}^{\mathrm{T}} & \Gamma_{11}^{\mathrm{T}} \Gamma_{11} \end{pmatrix} + c \begin{pmatrix} 0 & 0 \\ 0 & \Gamma_{21}^{\mathrm{T}} \Gamma_{21} \end{pmatrix}$$

$$\mathbf{H}_2 = \mathbf{A}_2 + c \begin{pmatrix} 1 & -\Gamma_{22} \\ -\Gamma_{22}^{\mathrm{T}} & \Gamma_{22}^{\mathrm{T}} \Gamma_{22} \end{pmatrix} + c \begin{pmatrix} 0 & 0 \\ 0 & \Gamma_{12}^{\mathrm{T}} \Gamma_{12} \end{pmatrix}$$

$$\begin{aligned} \mathbf{h}_1^{\mathrm{T}} = {} & b_1^{\mathrm{T}} + \lambda_1 \mathbf{e}_{11}^{\mathrm{T}} + \lambda_2 \mathbf{e}_{21}^{\mathrm{T}} \\ & + c\, \mathbf{e}_{11}^{\mathrm{T}} (w_1 - \mathbf{u}_1^* \mathbf{e}_{11})^{\mathrm{T}} + c\, \mathbf{e}_{21}^{\mathrm{T}} (w_2 - \mathbf{u}_1^* \mathbf{e}_{21}^{\mathrm{T}}) \\ \mathbf{h}_2^{\mathrm{T}} = {} & b_2^{\mathrm{T}} + \lambda_1 \mathbf{e}_{12}^{\mathrm{T}} + \lambda_2 \mathbf{e}_{22}^{\mathrm{T}} \\ & + c\, \mathbf{e}_{22}^{\mathrm{T}} (w_2 - \mathbf{u}_2^* \mathbf{e}_{22})^{\mathrm{T}} + c\, \mathbf{e}_{12}^{\mathrm{T}} (w_1 - \mathbf{u}_2^* \mathbf{e}_{12}^{\mathrm{T}}) \end{aligned}$$

with w_1, w_2 and λ_1, λ_2 being updated according to (4.21)-(4.22) and (4.20), respectively.

4.2 Decentralized VOP with APP

The centralized VOP is revisited to get its decentralized formulation using the Auxiliary Problem Principle (APP). To this aim:

A. the centralized VOP is rewritten for the network partitioning in VCZs;

B. the new VOP is reformulated as an unconstrained VOP by using the Augmented Lagrangian (LA) solved by the MMs;

C. the unconstrained VOP is decomposed and solved by applying the APP.

4.2.1 VOP Partitioning

As in [6], the distribution network is divided into VCZs by adopting a network partitioning method [10, 26]. In the following only two VCZs (VCZ_1, VCZ_2) are considered; by the way, it is without loss of generality, because the results can be extended to a larger number of VCZs. For each VCZ a PN is identified (PN_1, PN_2) [27]. The VOP is reformulated with a new objective function. It takes into account only the deviation of the nodal voltages at the PNs from their reference values. By distributing the variables between the two VCZs, the VOP is rewritten as

$$\begin{aligned} &\min_{\mathbf{x}_1,\mathbf{x}_2} \frac{1}{2} y_1^2 - y_{1\text{ref}}\, y_1 + \frac{1}{2} y_2^2 - y_{2\text{ref}}\, y_2 \\ &\text{subject to} \\ &\quad y_1 = \mathbf{\Gamma}_{11}\mathbf{x}_1 + \mathbf{\Gamma}_{12}\mathbf{x}_2 \qquad y_2 = \mathbf{\Gamma}_{21}\mathbf{x}_1 + \mathbf{\Gamma}_{22}\mathbf{x}_2 \\ &\quad y_{1\min} \le y_1 \le y_{1\max} \qquad y_{2\min} \le y_2 \le y_{2\max} \\ &\quad \mathbf{x}_{1\min} \le \mathbf{x}_1 \le \mathbf{x}_{1\max} \qquad \mathbf{x}_{2\min} \le \mathbf{x}_2 \le \mathbf{x}_{2\max} \end{aligned} \tag{4.23}$$

where $y_1(y_2)$ is the variation of the voltage at $PN_1(PN_2)$; $y_{1\text{ref}}(y_{2\text{ref}})$ the variation of the voltage reference value at $PN_1(PN_2)$; $\mathbf{x}_1\,(\mathbf{x}_2)$ the vector of the variations of the set-points of the DG reactive power controllers in $VCZ_1(VCZ_2)$; $\mathbf{\Gamma}_{11}\,(\mathbf{\Gamma}_{22})$ a submatrix of $\mathbf{\Gamma}$ that relates the squared nodal voltage at $PN_1(PN_2)$ to the reactive powers injected by the DGs in same VCZ; $\mathbf{\Gamma}_{12}\,(\mathbf{\Gamma}_{21})$ a submatrix of $\mathbf{\Gamma}$ that relates the squared nodal voltage

at $PN_1(PN_2)$ to the reactive powers injected by the DGs in other VCZ; $[y_{1\min}, y_{1\max}]$ ($[y_{2\min}, y_{2\max}]$) the admissible range of variation of $y_1(y_2)$; $[\mathbf{x}_{1\min}, \mathbf{x}_{1\max}]$ ($[\mathbf{x}_{2\min}, \mathbf{x}_{2\max}]$) the vector of the admissible range of variation of $\mathbf{x}$. While the objective function in (4.23) can be distributed between the two VCZs, the equality constraints presents coupling terms and, then, cannot be separated. To allow easier management of coupling constraints, the overlapping variables w_{12} and w_{21} are introduced and (4.23) is rewritten by introducing some additional constraints assuring consistency of the problem as

$$\begin{aligned}
&\min_{\mathbf{x}_1,\mathbf{x}_2} \frac{1}{2} y_1^2 - y_{1\text{ref}}\, y_1 + \frac{1}{2} y_2^2 - y_{2\text{ref}}\, y_2 \\
&\text{subject to} \\
&\quad y_1 = \mathbf{\Gamma}_{11}\mathbf{x}_1 + w_{12} \qquad y_2 = \mathbf{\Gamma}_{22}\mathbf{x}_2 + w_{21} \\
&\quad w_{12} = \mathbf{\Gamma}_{12}\mathbf{x}_2 \qquad\quad w_{21} = \mathbf{\Gamma}_{21}\mathbf{x}_1 \\
&\quad y_{1\min} \le y_1 \le y_{1\max} \qquad y_{2\min} \le y_2 \le y_{2\max} \\
&\quad \mathbf{x}_{1\min} \le \mathbf{x}_1 \le \mathbf{x}_{1\max} \qquad \mathbf{x}_{2\min} \le \mathbf{x}_2 \le \mathbf{x}_{2\max}
\end{aligned} \tag{4.24}$$

Finally, by substituting the coupling constraints in the objective function and by introducing the vectors ${\mathbf{z}_1}^{\mathrm{T}} = (\mathbf{x}_1\ w_{12})$ and ${\mathbf{z}_2}^{\mathrm{T}} = (\mathbf{x}_2\ w_{21})$, (4.24) can be rewritten in matrix form

$$\begin{aligned}
&\min_{\mathbf{z}_1,\mathbf{z}_2} F(\mathbf{z}_1) + F(\mathbf{z}_2) \\
&\text{subject to} \\
&\quad \mathbf{e}_{11}^{\mathrm{T}}\mathbf{z}_1 + \mathbf{e}_{12}^{\mathrm{T}}\mathbf{z}_2 = 0 \qquad \mathbf{e}_{21}^{\mathrm{T}}\mathbf{z}_1 + \mathbf{e}_{22}^{\mathrm{T}}\mathbf{z}_2 = 0 \\
&\quad y_{1\min} \le \mathbf{c}_1^{\mathrm{T}}\mathbf{z}_1 \le y_{1\max} \qquad y_{2\min} \le \mathbf{c}_2^{\mathrm{T}}\mathbf{z}_2 \le y_{2\max} \\
&\quad \mathbf{z}_{1\min} \le \mathbf{D}_1\mathbf{z}_1 \le \mathbf{z}_{1\max} \qquad \mathbf{z}_{2\min} \le \mathbf{D}_2\mathbf{z}_2 \le \mathbf{z}_{2\max}
\end{aligned} \tag{4.25}$$

with $F(\mathbf{z}_1)$, $F(\mathbf{z}_2)$, $\mathbf{e}_{11}^{\mathrm{T}}$, $\mathbf{e}_{12}^{\mathrm{T}}$, $\mathbf{e}_{21}^{\mathrm{T}}$, $\mathbf{e}_{22}^{\mathrm{T}}$, $\mathbf{c}_1^{\mathrm{T}}$, $\mathbf{c}_2^{\mathrm{T}}$, $\mathbf{D}_1$, $\mathbf{D}_2$ defined in Appendix.The VOP (4.25) is still not fully-decentralized, because the equality constraints are not separable. Moreover, it presents local minimum points because, considering only the PNs, the objective function remains convex but not in a strict sense.

4.2.2 Method of Multipliers

To overcome the lack of strict convexity, the dual optimization problem based on the AL function is used and iteratively solved by the MMs [30]. It consists of successive minimizations of the following not constrained problem

$$\begin{aligned}
&\min_{\mathbf{z}_1,\mathbf{z}_2} F(\mathbf{z}_1) + F(\mathbf{z}_2) + \lambda_1 f_{12} + \lambda_2 f_{21} + \frac{c}{2} f_{12}^2 + \frac{c}{2} f_{21}^2 \\
&\text{subject to} \\
&y_{1\min} \leq \mathbf{c}_1^{\mathrm{T}} \mathbf{z}_1 \leq y_{1\max} \quad y_{2\min} \leq \mathbf{c}_2^{\mathrm{T}} \mathbf{z}_2 \leq y_{2\max} \\
&\mathbf{z}_{1\min} \leq \mathbf{D}_1 \mathbf{z}_1 \leq \mathbf{z}_{1\max} \quad \mathbf{z}_{2\min} \leq \mathbf{D}_2 \mathbf{z}_2 \leq \mathbf{z}_{2\max}
\end{aligned} \tag{4.26}$$

where c is the penalty parameters and with

$$f_{12} = \mathbf{e}_{11}^{\mathrm{T}} \mathbf{z}_1 + \mathbf{e}_{12}^{\mathrm{T}} \mathbf{z}_2 \quad f_{21} = \mathbf{e}_{21}^{\mathrm{T}} \mathbf{z}_1 + \mathbf{e}_{22}^{\mathrm{T}} \mathbf{z}_2 \tag{4.27}$$

followed by updates of the Lagrange multipliers[1]

$$\lambda_1 = \lambda_1^* + \rho f_{12} \qquad \lambda_2 = \lambda_2^* + \rho f_{21} \tag{4.28}$$

where ρ is a positive parameter. Although the MMs permits to handle the lack of strict convexity of the objective function, the presence of the quadratic terms in the AL function still makes the VOP (4.26) not separable among the two VCZs.

4.2.3 Auxiliary Problem Principle

The APP [31, 32, 38] is used to decompose the centralized VOP into subproblems that must be solved by each Zone Control Center (ZCC) and to coordinate the solutions of subproblems toward the solution of the overall problem. The APP adds an auxiliary function $K(\mathbf{z}_1, \mathbf{z}_2)$ to the objective function and replaces the quadratic terms of the AL with a linear approximation around the solution of the previous step. Applying APP to the master problem (4.26), the following auxiliary problem is derived[2]

$$\begin{aligned}
&\min_{\mathbf{z}_1,\mathbf{z}_2} K(\mathbf{z}_1, \mathbf{z}_2) \\
&\quad + \big(\epsilon F'(\mathbf{z}_1^*) - K'(\mathbf{z}_1^*)\big)\mathbf{z}_1 + \big(\epsilon F'(\mathbf{z}_2^*) - K'(\mathbf{z}_2^*)\big)\mathbf{z}_2 \\
&\quad + \epsilon(\lambda_1^* + c f_{12}^*) f_{12} + \epsilon(\lambda_2^* + c f_{21}^*) f_{21} \\
&\quad \text{subject to} \\
&\quad y_{1\min} \leq \mathbf{c}_1^{\mathrm{T}} \mathbf{z}_1 \leq y_{1\max} \quad y_{2\min} \leq \mathbf{c}_2^{\mathrm{T}} \mathbf{z}_2 \leq y_{2\max} \\
&\quad \mathbf{z}_{1\min} \leq \mathbf{D}_1 \mathbf{z}_1 \leq \mathbf{z}_{1\max} \quad \mathbf{z}_{2\min} \leq \mathbf{D}_2 \mathbf{z}_2 \leq \mathbf{z}_{2\max}
\end{aligned} \tag{4.29}$$

where ϵ is a positive parameter and the Lagrange multipliers are updated with (4.28). The auxiliary function is chosen as

$$K(\mathbf{z}_1, \mathbf{z}_2) = \tfrac{1}{2} \mathbf{z}_1^{\mathrm{T}} \mathbf{K}_1 \mathbf{z}_1 \; + \; \tfrac{1}{2} \mathbf{z}_2^{\mathrm{T}} \mathbf{K}_2 \mathbf{z}_2 \tag{4.30}$$

[1] The symbol * indicates the value assumed in the previous step.

[2] The symbol $'$ indicates the derivative.

being $\mathbf{K}_1$ and $\mathbf{K}_2$ suitably-chosen positive-definite matrices. The choice of a $K(\mathbf{z}_1, \mathbf{z}_2)$ strictly convex assures the existence and uniqueness of the solution to (4.29). Furthermore, a $K(\mathbf{z}_1, \mathbf{z}_2)$ additive, together with the first-order approximation of the quadratic terms of the LA, permit to split (4.29) into independent subproblems. Applying the APP (see Appendixfor details), in VCZ_1 it is solved the following quadratic programming problem

$$\begin{aligned} &\min_{\mathbf{z}_1} \frac{1}{2}\mathbf{z}_1^{\mathrm{T}}\mathbf{K}_1\mathbf{z}_1 - \mathbf{k}_1^{\mathrm{T}}\mathbf{z}_1 \\ &\text{subject to} \\ &\quad y_{1\min} \leq \mathbf{c}_1^{\mathrm{T}}\mathbf{z}_1 \leq y_{1\max} \quad \mathbf{z}_{1\min} \leq \mathbf{D}_1\mathbf{z}_1 \leq \mathbf{z}_{1\max} \end{aligned} \tag{4.31}$$

and in VCZ_2

$$\begin{aligned} &\min_{\mathbf{z}_2} \frac{1}{2}\mathbf{z}_2^{\mathrm{T}}\mathbf{K}_2\mathbf{z}_2 - \mathbf{k}_2^{\mathrm{T}}\mathbf{z}_2 \\ &\text{subject to} \\ &\quad y_{2\min} \leq \mathbf{c}_2^{\mathrm{T}}\mathbf{z}_2 \leq y_{2\max} \quad \mathbf{z}_{2\min} \leq \mathbf{D}_2\mathbf{z}_2 \leq \mathbf{z}_{2\max} \end{aligned} \tag{4.32}$$

where $\mathbf{k}_1$ and $\mathbf{k}_2$ are defined as

$$\begin{aligned} \mathbf{k}_1^{\mathrm{T}} &= \epsilon(\mathbf{z}_1^{*\mathrm{T}}\mathbf{A}_1 - \mathbf{b}_1^{\mathrm{T}}) - \mathbf{z}_1^{*\mathrm{T}}\mathbf{K}_1 + \epsilon\lambda_1\mathbf{e}_{11}^{\mathrm{T}} + \epsilon\lambda_2\mathbf{e}_{21}^{\mathrm{T}} + \\ &\quad + \epsilon c f_{12}^{*}\mathbf{e}_{11}^{\mathrm{T}} + \epsilon c f_{21}^{*}\mathbf{e}_{21}^{\mathrm{T}} \\ \mathbf{k}_2^{\mathrm{T}} &= \epsilon(\mathbf{z}_2^{*\mathrm{T}}\mathbf{A}_2 - \mathbf{b}_2^{\mathrm{T}}) - \mathbf{z}_2^{*\mathrm{T}}\mathbf{K}_2 + \epsilon\lambda_1\mathbf{e}_{12}^{\mathrm{T}} + \epsilon\lambda_2\mathbf{e}_{22}^{\mathrm{T}} + \\ &\quad + \epsilon c f_{12}^{*}\mathbf{e}_{12}^{\mathrm{T}} + \epsilon c f_{21}^{*}\mathbf{e}_{22}^{\mathrm{T}} \end{aligned}$$

and, then, depend, respectively, on the values of $\mathbf{z}_1^*$, $\mathbf{z}_2^*$ assumed in the previous step and on the Lagrange multipliers λ_1, λ_2, which are updates with (4.28). Subproblems are iteratively solved to reach convergence; the convergence characteristics are strictly related to the choice of the parameters ϵ, c, ρ [33].

The APP is implemented by a distributed algorithm whose steps are Fig.4.9:

i. initialize the step counter $h = 0$, together with $\mathbf{z}_1 = 0$, $\mathbf{z}_2 = 0$, $\lambda_1 = 0$, $\lambda_2 = 0$; choose ϵ, c, ρ and fix the tollerances τ_f and τ_z;

ii. $h = h + 1$;

iii. VCZ_1 and VCZ_2 solve in parallel the minimization problems (4.31) and (4.32), obtaining respectively the vectors $\mathbf{z}_1(h)$ and $\mathbf{z}_2(h)$;

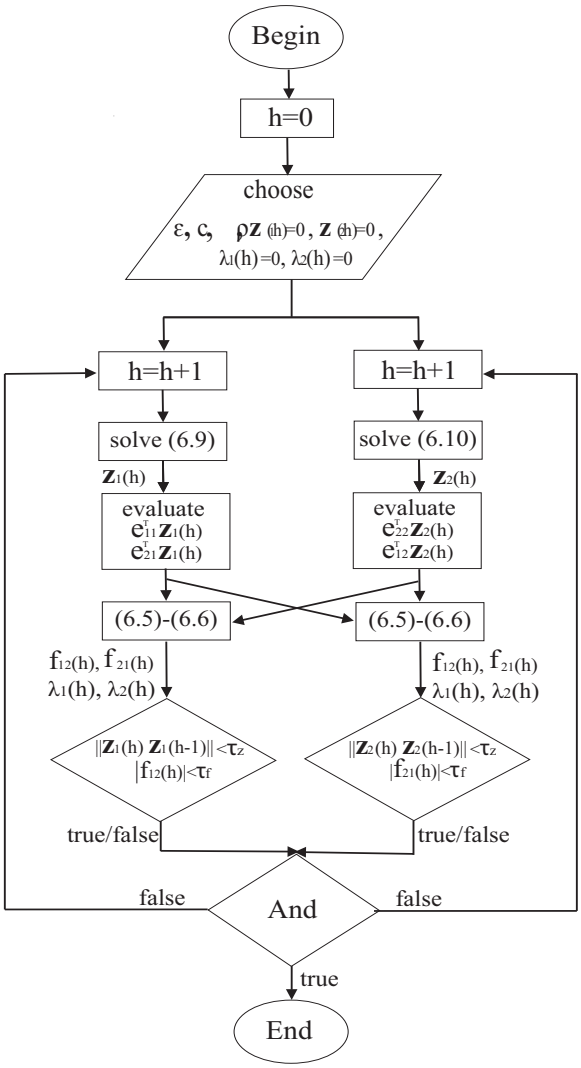

Figure 4.9: Decentralized Algorithm (APP)

iv. VCZ_1 evaluates the two scalar values $\mathbf{e}_{11}^{\mathrm{T}}\mathbf{z}_1(h)$ and $\mathbf{e}_{21}^{\mathrm{T}}\mathbf{z}_1(h)$, while VCZ_2 evaluates the two scalar values $\mathbf{e}_{22}^{\mathrm{T}}\mathbf{z}_2(h)$ and $\mathbf{e}_{12}^{\mathrm{T}}\mathbf{z}_2(h)$; the two zones exchange each other the evaluated values;

v. VCZ_1 and VCZ_2 calculate in parallel both the values $f_{12}(h)$ and $f_{21}(h)$ by (4.27), and both the values of $\lambda_1(h)$ and $\lambda_2(h)$ by (4.28);

vi. VCZ_1 (VCZ_2) checks if errors $|f_{12}(h)|$ ($|f_{21}(h)|$) are smaller than τ_f and the variations of the elements of $\mathbf{z}_1(h)$ ($\mathbf{z}_2(h)$) with respect to the previous iteration are smaller than τ_z; if false, go back to step ii.; otherwise stop.

In conclusion, by applying the APP, the VOP to be solved by each VCZ is a quadratic programming problem of small dimension, that can be easily be solved presenting a global minimum. Furthermore, the data exchange between the two ZCC at each iteration is limited to a set of two scalar values, respectively ($\mathbf{e}_{11}^{\mathrm{T}}\mathbf{z}_1$, $\mathbf{e}_{21}^{\mathrm{T}}\mathbf{z}_1$) and ($\mathbf{e}_{22}^{\mathrm{T}}\mathbf{z}_2$, $\mathbf{e}_{12}^{\mathrm{T}}\mathbf{z}_2$).

4.2.4 Case Study with APP

The 24-nodes distribution network with DGs in Fig. 4.2 is considered. A 20/0.4 kV substation, equipped with a 0.250 MVA transformer, feeds a 0.4 kV network composed of two main feeders, each one with two laterals. The electrical parameters of the network and the loads are reported in [6]. The LV network has been partitioned into two VCZs as in [6].

Tests have been carried out to verify the performance of the proposed APP decentralized algorithm, referred to as the *decentralized APP* in the reminder. In all the tests the *decentralized APP* has reached convergence; the choice of the penalty parameter c has impact only on the number of iterations to reach convergence. The parameter c can vary in the range of values from 0.1 to 10: in particular, in the tried APP algorithm, $c = 0.1$ has proved to be the best choice.

In the following some relevant results are reported referring to the following four cases:

- *Case 1*: V_{MV}=0.99 p.u. and S_{load}=70%S_{load}^{rated};
- *Case 2*: V_{MV}=1.025 p.u. and S_{load}=60%S_{load}^{rated};
- *Case 3*: V_{MV}=0.975 p.u. and S_{load}=50%S_{load}^{rated};
- *Case 4*: V_{MV}=1.04 p.u. and S_{load}=50%S_{load}^{rated}.

Concerning the operating conditions of the DGs, Tab. 4.4 reports the values of the active power injections for all the four cases, and the range of possible variation of the reactive powers.

The accuracy of the solutions is evaluated by comparing the value of the objective function obtained by the *decentralized APP* with those obtained

Table 4.4: Active Power Injections and Reactive Power Ranges for DGs (APP)

Power	**Case**	DG_1	DG_2	DG_3	DG_4	DG_5	DG_6
Active (MW)	1	0.02	0.015	0.025	0.015	0.015	0.01
	2	0.01	0.005	0.005	0.025	0.003	0.002
	3/4	0.018	0.012	0.022	0.012	0.012	0.007
Reactive (MVAr)	1/2/3/4	±0.015	±0.0113	±0.0188	±0.0113	±0.0113	±0.0075

Table 4.5: Comparison of the objective functions [$p.u.$] (APP)

Case	*VCZ-based VOP*	*decentralized ADMM*	*decentralized APP*
1	$< 10^{-8}$	$< 10^{-8}$	$< 10^{-8}$
2	$< 10^{-8}$	$< 10^{-8}$	$< 10^{-8}$
3	$5.658*10^{-6}$	$5.658*10^{-6}$	$5.659*10^{-6}$
4	$1.891*10^{-3}$	$1.891*10^{-3}$	$1.891*10^{-3}$

by the other methods, namely *VCZ-based VOP* and *decentralized ADMM*. All the methods work on the PNs but

- the *decentralized APP* solves the VOP (4.23) with a decentralized approach by means of the APP algorithm.
- the *VCZ-based VOP* solves the VOP (4.23) with a centralized approach;
- the *decentralized ADMM* solves the VOP (4.23) with a decentralized approach by means of the by the Alternating Direction Method of Multipliers (ADMM).

All the three methods solved the VOP in (4.23) with *quadprog* function of MATPOWER package in MATLAB environment.

In Tab. 4.5 the values of the objective functions obtained by the *decentralized APP* for the four cases are reported and compared with those of the

VCZ-based VOP and the *decentralized ADMM*. For the *Case 1* and *Case 2* all the three methods are able to guarantee that the solution accuracy goes below the value of 10^{-8}[p.u.], which represents the threshold value to assure that the method freely converged to the solution. The solutions obtained by the *VCZ-based VOP* present the best minimization of the objective function with respect to the corresponding solutions of both decentralized methods. The situation is different for *Case 3* and *Case 4*, where all the three algorithms get to the same minimization values; this is due to saturation of reactive power capabilities of the DG inverters. All the three methods are not longer free to get to the desired solution but the convergence of each algorithm is bound by the reactive power limits imposed by DG inverters. Nevertheless, it can be stated that the *decentralized APP*, when saturation conditions do not occur, provides a satisfactory level of accuracy of the VOP solution, bringing the optimization function to negligible values.

Tab. 4.6 reports the number of iterations to reach convergence of the two decentralized approaches for all the four cases. Comparing the values obtained by the two decentralized algorithms, it can be stated that in *Case 1* and *Case 2* the *decentralized ADMM* is faster to reach convergence with respect to *decentralized APP*, which, on the other hand, is the fastest in *Case 3* and *Case 4*. More in general, the behaviour of the *decentralized APP* proves to be more stable than the one of the *decentralized ADMM*; in fact, also when saturation occurs, the number of iterations stays almost unaltered for the *decentralized APP*, whereas evidently increases for the *decentralized ADMM*.

About the convergence, a further investigation is based on the analysis of errors on coupling constraints, see (4.27), for both the decentralized algorithms. Fig. 4.10 reports the trends of the maximum error versus the number of iterations in *Case 2* and *Case 4*. In the first steps of the iteration process, the error increases to reach a peak value and successively goes down. The convergence of both algorithms is complete when the value of the error on coupling constraints goes down to 10^{-4}. In *Case 2*, especially for the *decentralized ADMM* algorithm, the peak value is lower and the descent phase is faster than in *Case 4*. As evident from Fig. 4.10, the *decentralized APP* shows a more consistent behaviour than the *decentralized ADMM*.

Table 4.6: Number of iterations to reach convergence (APP)

Case	*decentralized ADMM*	*decentralized APP*
1	7	17
2	8	14
3	24	18
4	38	19

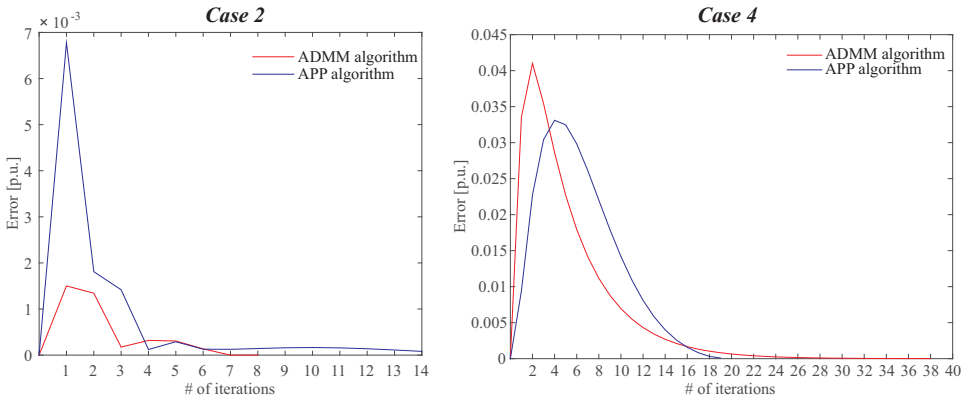

Figure 4.10: Error vs. n° of iterations: *Case 2* (right), *Case 4* (left) (APP)

The *decentralized APP* profiles are compared with the ones obtained by the classical *benchmark ORPF* (which solves the VOP (4.23) with non linear power flow equations) well as with the ones obtained assuming no VOP solution (that is imposing null reactive powers injected by DGs).

In Fig. 4.11 the voltage profiles are reported for VCZ_1 and VCZ_2 with reference to *Case 1*; likewise Figs. 4.12, 4.13, 4.14 with reference to, respectively, *Case 2*, *Case 3*, *Case 4*. In all the analyzed cases, the *decentralized APP* guarantees a voltage profile which is quite close to that of the *benchmark ORPF*; moreover, its improvement of the voltage profiles with respect to the case of no VOP solution is always evident. Fig. 4.14 clearly shows how, in *Case 4*, the voltage profiles of the *decentralized APP* and the *benchmark ORPF* are overlapped one with the other: this occurrence is due to the fact that the reactive power solutions, for both algorithms, saturate the reactive power capabilities of all the DG inverters.

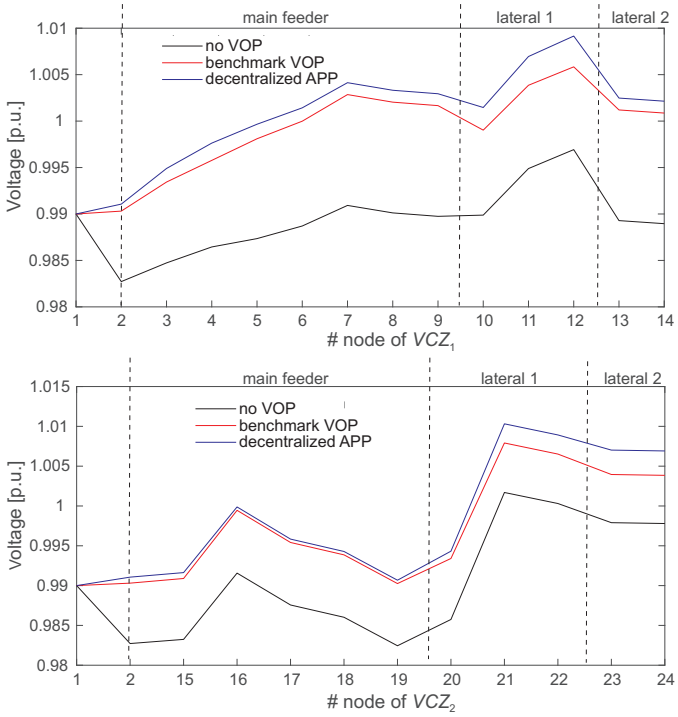

Figure 4.11: Voltage profile in *Case 1*: VCZ_1 (top) VCZ_2 (bottom) (APP)

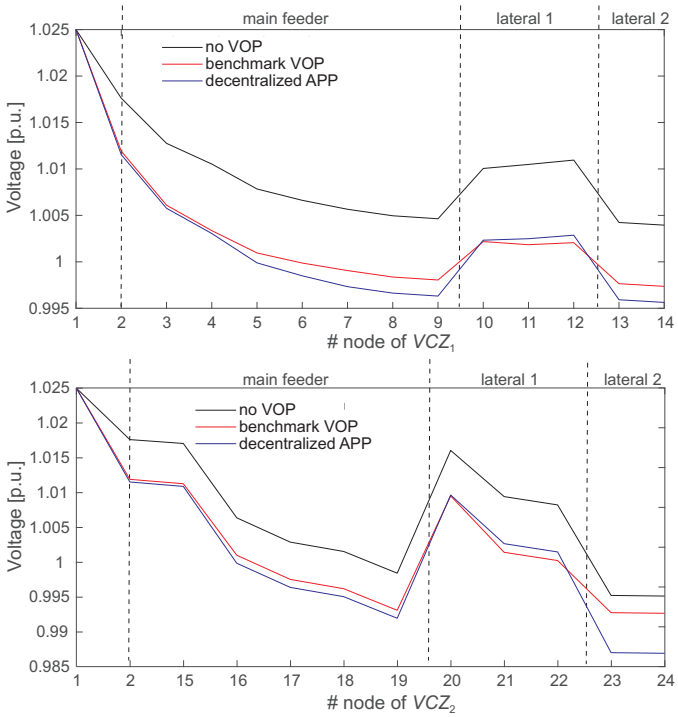

Figure 4.12: Voltage profile in *Case 2*: VCZ_1 (top) VCZ_2 (bottom) (APP)

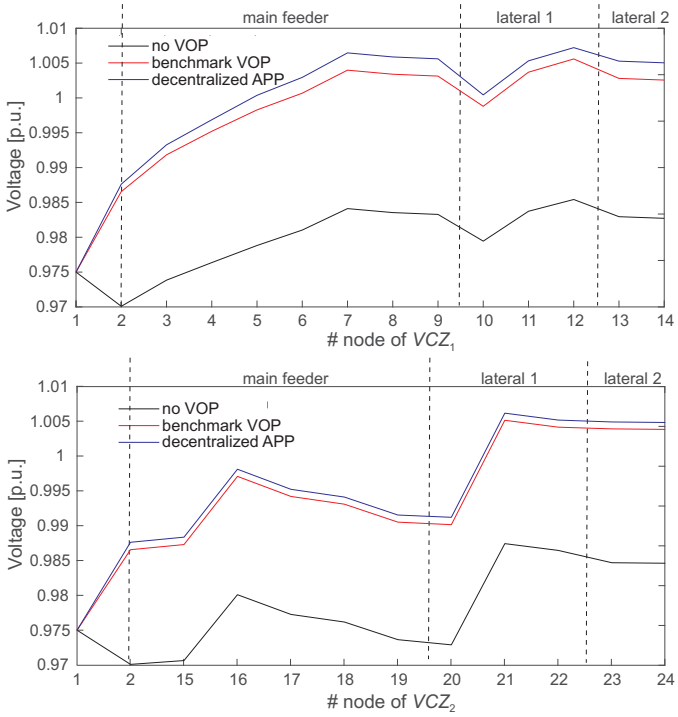

Figure 4.13: Voltage profile in *Case 3*: VCZ_1 (top) VCZ_2 (bottom) (APP)

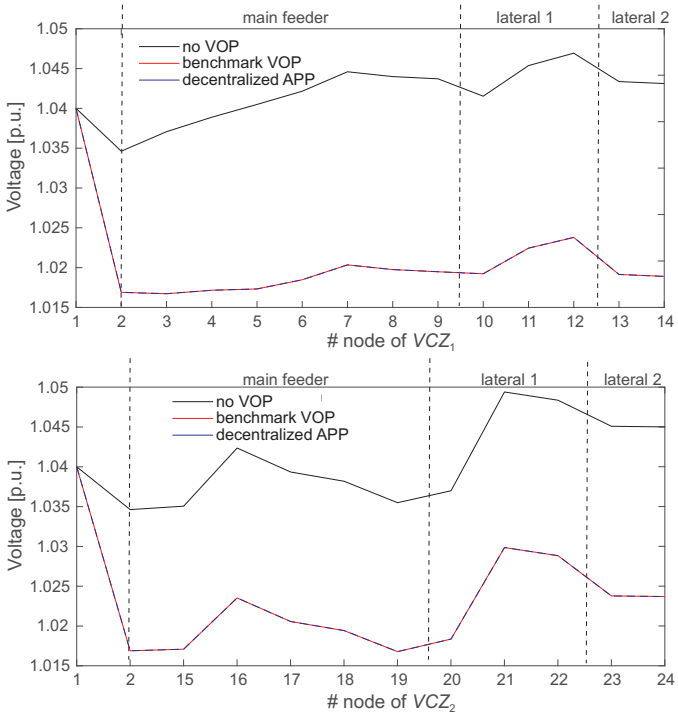

Figure 4.14: Voltage profile in *Case 4*: VCZ_1 (top) VCZ_2 (bottom) (APP)

4.2.5 Final considerations about APP

The main advantage of the proposed distributed algorithm is that it achieves the global optimal solution by iteratively solving strictly-positive definite quadratic subproblems of small dimension. To this aim, first the network is partitioned in voltage control zones and then the voltages at the pilot nodes are optimized by determining the best reactive powers injected by the DGs of the related zones. To account for the coupling among the different zones, the zonal subproblems are iteratively solved after exchanging a limited amount of data (two scalar values). The tests on a 24-nodes LV distribution grid with six DGs have shown a significant improvement of the voltage profile.

Appendix

VOP partitioning

$$
\begin{aligned}
&F(\mathbf{z}_1) = \tfrac{1}{2}\mathbf{z}_1^{\mathrm{T}}\mathbf{A}_1\mathbf{z}_1 - \mathbf{b}_1^{\mathrm{T}}\mathbf{z}_1 \quad F(\mathbf{z}_2) = \tfrac{1}{2}{\mathbf{z}_2}^{\mathrm{T}}\mathbf{A}_2\mathbf{z}_2 - {\mathbf{b}_2}^{\mathrm{T}}\mathbf{z}_2 \\
&\mathbf{e}_{11}^{\mathrm{T}} = (0 \;\; 1) \quad \mathbf{e}_{12}^{\mathrm{T}} = (-\boldsymbol{\Gamma}_{12} \;\; 0) \\
&\mathbf{e}_{21}^{\mathrm{T}} = (-\boldsymbol{\Gamma}_{21} \;\; 0) \quad {\mathbf{e}_{22}}^{\mathrm{T}} = (0 \;\; 1) \\
&\mathbf{A}_1 = \begin{pmatrix} \boldsymbol{\Gamma}_{11}^{\mathrm{T}}\boldsymbol{\Gamma}_{11} & \boldsymbol{\Gamma}_{11}^{\mathrm{T}} \\ \boldsymbol{\Gamma}_{11} & 1 \end{pmatrix} \mathbf{A}_2 = \begin{pmatrix} \boldsymbol{\Gamma}_{22}^{\mathrm{T}}\boldsymbol{\Gamma}_{22} & \boldsymbol{\Gamma}_{22}^{\mathrm{T}} \\ \boldsymbol{\Gamma}_{22} & 1 \end{pmatrix} \\
&\mathbf{b}_1^{\mathrm{T}} = (y_{1\mathrm{ref}}\boldsymbol{\Gamma}_{11} \;\; y_{1\mathrm{ref}}) \quad \mathbf{b}_2^{\mathrm{T}} = (y_{2\mathrm{ref}}\boldsymbol{\Gamma}_{22} \;\; y_{2\mathrm{ref}}) \\
&\mathbf{c}_1^{\mathrm{T}} = (\boldsymbol{\Gamma}_{11} \;\; 1) \qquad \mathbf{c}_2^{\mathrm{T}} = (\boldsymbol{\Gamma}_{22} \;\; 1) \\
&\mathbf{D}_1 = diag(\mathbf{1} \;\; 1) \qquad \mathbf{D}_2 = diag(\mathbf{1} \;\; 1)
\end{aligned}
$$

Auxiliary Problem Principle (APP)

Using (4.30) and deriving K and F, (4.29) is rewritten as:

$$
\begin{aligned}
&\min_{\mathbf{z}_1,\mathbf{z}_2} \tfrac{1}{2}\mathbf{z}_1^{\mathrm{T}}\mathbf{K}_1\mathbf{z}_1 + \tfrac{1}{2}\mathbf{z}_2^{\mathrm{T}}\mathbf{K}_2\mathbf{z}_2 \\
&\quad +\epsilon(\mathbf{z}_1^{*\mathrm{T}}\mathbf{A}_1 - \mathbf{b}_1^{\mathrm{T}})\mathbf{z}_1 + \epsilon(\mathbf{z}_2^{*\mathrm{T}}\mathbf{A}_2 - \mathbf{b}_2^{\mathrm{T}})\mathbf{z}_2 + \\
&\quad -\mathbf{z}_1^{*\mathrm{T}}\mathbf{K}_1\mathbf{z}_1 - \mathbf{z}_2^{*\mathrm{T}}\mathbf{K}_2\mathbf{z}_2 + \epsilon\lambda_1^* f_{12} + \epsilon\lambda_2^* f_{21} + \\
&\quad +\epsilon c f_{12}^* f_{12} + \epsilon c f_{21}^* f_{21} \\
&\text{subject to} \qquad\qquad (4.33) \\
&\quad y_{1\min} \le \mathbf{c}_1^{\mathrm{T}}\mathbf{z}_1 \le y_{1\max} \quad y_{2\min} \le \mathbf{c}_2^{\mathrm{T}}\mathbf{z}_2 \le y_{2\max} \\
&\quad \mathbf{z}_{1\min} \le \mathbf{D}_1\mathbf{z}_1 \le \mathbf{z}_{1\max} \quad \mathbf{z}_{2\min} \le \mathbf{D}_2\mathbf{z}_2 \le \mathbf{z}_{2\max}
\end{aligned}
$$

where the Lagrange multipliers are updates according to (4.28). The APP (4.33) is decomposed into two subproblems as:

VCZ$_1$

$$\begin{aligned}
&\min_{\mathbf{z}_1} \tfrac{1}{2}\mathbf{z}_1^{\mathrm{T}}\mathbf{K}_1\mathbf{z}_1 + \epsilon(\mathbf{z}_1^{*\mathrm{T}}\mathbf{A}_1 - \mathbf{b}_1^{\mathrm{T}})\mathbf{z}_1 - \mathbf{z}_1^{*\mathrm{T}}\mathbf{K}_1\mathbf{z}_1 + \\
&\quad +\epsilon\lambda_1^*\mathbf{e}_{11}^{\mathrm{T}}\mathbf{z}_1 + \epsilon\lambda_2^*\mathbf{e}_{21}^{\mathrm{T}}\mathbf{z}_1 + \epsilon c f_{12}^*\mathbf{e}_{11}^{\mathrm{T}}\mathbf{z}_1 + \epsilon c f_{21}^*\mathbf{e}_{21}^{\mathrm{T}}\mathbf{z}_1 \\
&\text{subject to} \\
&\quad y_{1\min} \le \mathbf{c}_1^{\mathrm{T}}\mathbf{z}_1 \le y_{1\max} \quad \mathbf{z}_{1\min} \le \mathbf{D}_1\mathbf{z}_1 \le \mathbf{z}_{1\max}
\end{aligned} \tag{4.34}$$

VCZ$_2$

$$\begin{aligned}
&\min_{\mathbf{z}_2} \tfrac{1}{2}\mathbf{z}_2^{\mathrm{T}}\mathbf{K}_2\mathbf{z}_2 + \epsilon(\mathbf{z}_2^{*\mathrm{T}}\mathbf{A}_2 - \mathbf{b}_2^{\mathrm{T}})\mathbf{z}_2 - \mathbf{z}_2^{*\mathrm{T}}\mathbf{K}_2\mathbf{z}_2 + \\
&\quad +\epsilon\lambda_1^*\mathbf{e}_{12}^{\mathrm{T}}\mathbf{z}_2 + \epsilon\lambda_2^*\mathbf{e}_{22}^{\mathrm{T}}\mathbf{z}_2 + \epsilon c f_{12}^*\mathbf{e}_{12}^{\mathrm{T}}\mathbf{z}_2 + \epsilon c f_{21}^*\mathbf{e}_{22}^{\mathrm{T}}\mathbf{z}_2 \\
&\text{subject to} \\
&\quad y_{2\min} \le \mathbf{c}_2^{\mathrm{T}}\mathbf{z}_2 \le y_{2\max} \quad \mathbf{z}_{2\min} \le \mathbf{D}_2\mathbf{z}_2 \le \mathbf{z}_{2\max}
\end{aligned} \tag{4.35}$$

where the Lagrange multipliers are updates according to (4.28). Eventually the minimization problems (4.34)-(4.35) can be rewritten in a compact quadratic form defining

$$\begin{aligned}
\mathbf{k}_1^{\mathrm{T}} &= \epsilon(\mathbf{z}_1^{*\mathrm{T}}\mathbf{A}_1 - \mathbf{b}_1^{\mathrm{T}}) - \mathbf{z}_1^{*\mathrm{T}}\mathbf{K}_1 + \epsilon\lambda_1\mathbf{e}_{11}^{\mathrm{T}} + \epsilon\lambda_2\mathbf{e}_{21}^{\mathrm{T}} + \\
&\quad +\epsilon c f_{12}^*\mathbf{e}_{11}^{\mathrm{T}} + \epsilon c f_{21}^*\mathbf{e}_{21}^{\mathrm{T}} \\
\mathbf{k}_2^{\mathrm{T}} &= \epsilon(\mathbf{z}_2^{*\mathrm{T}}\mathbf{A}_2 - \mathbf{b}_2^{\mathrm{T}}) - \mathbf{z}_2^{*\mathrm{T}}\mathbf{K}_2 + \epsilon\lambda_1\mathbf{e}_{12}^{\mathrm{T}} + \epsilon\lambda_2\mathbf{e}_{22}^{\mathrm{T}} + \\
&\quad +\epsilon c f_{12}^*\mathbf{e}_{12}^{\mathrm{T}} + \epsilon c f_{21}^*\mathbf{e}_{22}^{\mathrm{T}}
\end{aligned}$$

4.3 Decentralized VOP with two-levels algorithm

This chapter deals with the problem of optimizing voltage profiles in distribution networks adopting a two-levels algorithm. Firstly, the network is divided into several weakly-coupled VCZs with PN. Hence, partitioning is used to optimize the voltage profiles of distribution systems on the plot of a coordinated approach based on two time scales. At the first level, a centralized VOP is solved, minimizing the distance of the bus voltages at the PNs from their reference values and subject to linearized power flow equations, to fix the switch positions under load (OLTC) and step voltage regulators

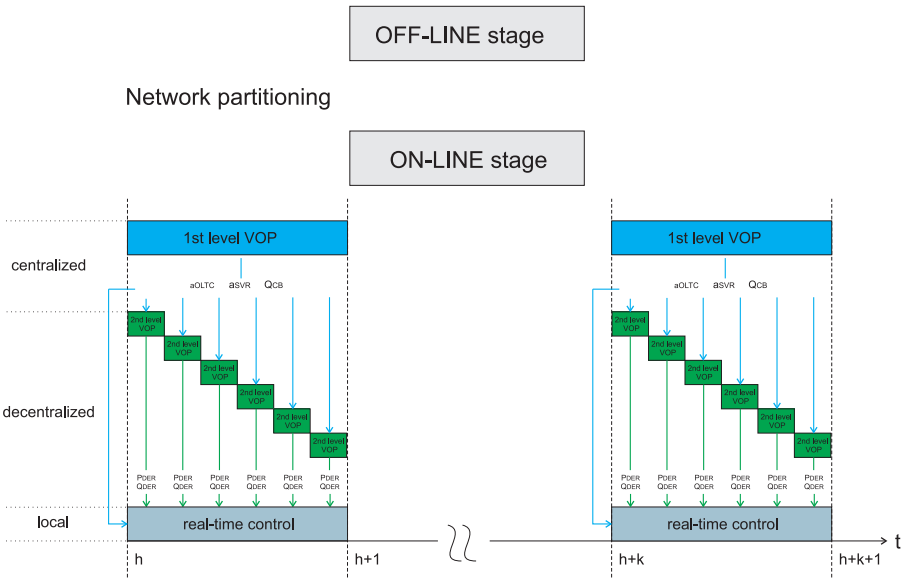

Figure 4.15: Representation of the VOP Formulation (Two-Levels)

(SVR), and the reactive powers supplied by capacitor banks (CB). At the second level, the VOP is implemented according to a decentralized approach, in which the solution is obtained by applying a distributed algorithm based on the alternate direction multiplier method (ADMM). It optimizes the voltage at the PN in each VCZ by acting on the active and reactive powers supplied by the DER present in the VCZ; VCZ solutions are driven to the global optimization of the entire distribution system by a limited data exchange between the PNs.

4.3.1 Voltage Optimitation Problem Formulation

The distribution network includes a OLTC at the supplying substation, M_{svr} and M_{cb} along the feeders, and M_{der}. The proposed formulation of the VOP consists of two stages: firstly, the network is partitioned in VCZs off-line; then, the representation in VCZs is used to optimize the voltage profiles of the distribution systems by solving a two-levels on-line VOP that aims at defining the optimal set-points of conventional and unconventional Voltage Control Devices (VCDs). A representation of the formulation of the proposed VOP is highlighted in Fig. 4.15. The operation in real-time of the local controllers is not treated in this work.

A Network partitioning;

The grid is partitioned into N_{vcz} VCZs with PNs by using the zoning methodology in [10].
The division of the network in VCZs requires the definition of electrical distances, which are a measure of the electrical connectedness among the nodes of the grid.
The most common methods to evaluate the electrical distances use the sensitivities of the nodal voltages to power injections [26,39]. In [10] the sensitivity coefficients are derived from the linear method for the steady-state analysis of the distribution system in [25].
Starting from an initial operating point, the linear method provides the sensitivity coefficients that linearly relate the variations of the active and the reactive powers out-flowing the nodes of the grid and of the squared nodal voltages to the variations of the powers injected in all the nodes of the grid, independently from the number and position of the DERs in a specific configuration.
In [10], the electrical distances are evaluated considering the sensitivities of the nodal voltages to active and reactive power injections, that can be taken into account separately or simultaneously. Once the electrical distances have been evaluated, nodes with similar electrical distances are grouped to form a VCZ by using the hierarchical clustering algorithm in [27].
In each VCZ a PN is identified, that is the node whose voltage variation best represents the voltage variations of all the nodes in the VCZ; the identification uses the algorithm in [20] to evaluate the proximity of each node to all the other nodes belonging to the same VCZ. Finally, the best number of VCZs is chosen by using the Silhouette index, that is the most widely-used index for evaluating the number of VCZs in the partition when hierarchical algorithms are applied. In practice, among different partitions of the network that present similar values of the Silhouette index, the choice can be based also on the criterion of guaranteeing a minimal number of VCDs in each VCZ.
In such a way, the partition of the network is fixed and it is extracted from structural characteristic of the network. Obviously, if different configurations of the topology of the network are possible, then different partitions can be evaluated off-line. Such an approach allows to reduce the computational effort of auxiliary service analysis in distribution network without degrading

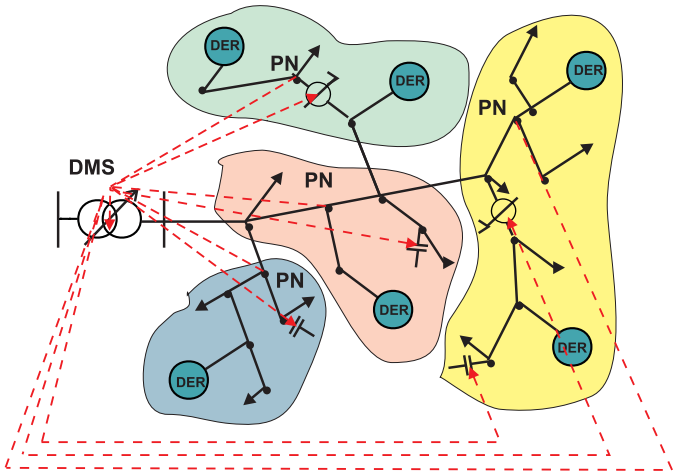

Figure 4.16: Information Exchange in the First Level VOP.

the performance of the clustering, thanks to the high accuracy of the linear method adopted for evaluating electrical distances [40].

B First level VOP;

At the first level a slow time-scale optimization is performed to fix the tap positions of both OLTC and SVRs, and the reactive power provided by CBs. The first level VOP is implemented according to a centralized approach. It measures the voltage amplitudes at the PNs and, solving a constrained linearized optimization problem that minimizes the deviation of the squared voltage amplitude at the PNs, $V^2_{pn_i}$, from their reference values, $V^2_{pn_{i,\mathrm{ref}}}$, defines the optimal set-points of the OLTC tap position, a_{oltc}, the M_{svr} tap positions of the SVRs, a_{svr_j}, and the M_{cb_t} reactive powers of the CBs, Q_{cb_t} then, such set-points are sent to the PNs for performing the second level VOP Fig. 4.15. The information exchange related to the adopted centralized approach is highlighted in Fig. 4.16.

C Second level VOP;

At the second level a fast time-scale optimization is performed to fix the set-points of the DER active and reactive power controllers. The second level the VOP is implemented according to a decentralized approach which is executed with the updated values of the set-points acquired from the first level. In each VCZ a centralized VOP is solved at its PN. Referring

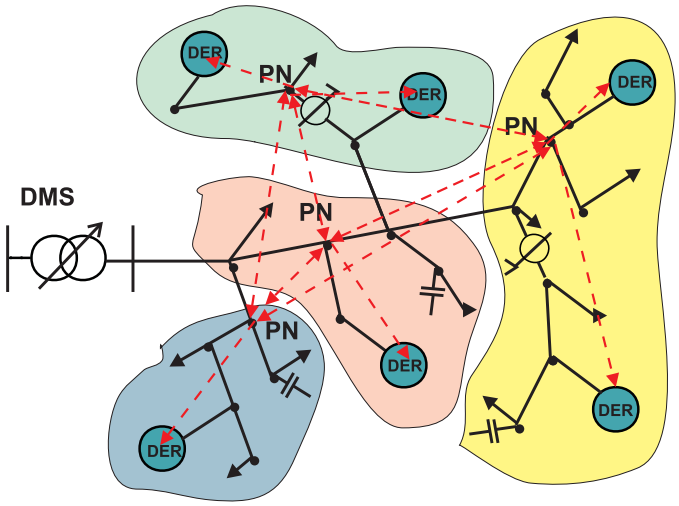

Figure 4.17: Information Exchange in the Second Level VOP.

to the i-th VCZ, by measuring the bus voltage at the PN, a constrained linearized optimization problem that minimizes the only deviation of $V^2_{pn_i}$ from $V^2_{pn_{i,\text{ref}}}$ is solved in order to define the optimal set-points of the active power P_{der_k} and the reactive power Q_{der_k} of DERs. The decentralized solution is achieved iteratively by exchanging scalar variables between PNs. The information exchange of the second level VOP related to the adopted decentralized approach is highlighted in Fig. 4.17.

4.3.2 OLTC, SVRs and CBs Optimization

The centralized VOP solved at the first level is

$$\min_{\substack{a_{oltc},\ a_{svr_1},\ldots,a_{M_{svr}} \\ Q_{cb_1},\ldots,Q_{cb_{M_{svr}}}}} \sum_{i=1}^{N_{vcz}} (V^2_{pn_i} - V^2_{pn_{i,\text{ref}}})^2$$

subject to (4.36)

PF equations

$$V^2_{pn_{i,\min}} \leq V^2_{pn_i} \leq V^2_{pn_{i,\max}} \qquad i = 1, \ldots, N_{vcz}$$

$$a_{oltc_{\min}} \leq a_{oltc} \leq a_{oltc_{\max}}$$

$$a_{svr_{j,\min}} \leq a_{svr_j} \leq a_{svr_{j,\max}} \qquad j = 1, \ldots, M_{svr}$$

$$Q_{cb_{t,\min}} \leq Q_{cb_t} \leq Q_{cb_{t,\max}} \qquad t = 1, \ldots, M_{cb}$$

where the optimal solution must satisfy PF equations and the operational limits on PN voltages, on the tap positions of OLTC and of SVRs and on

the CBs reactive power.

Using an extended version of the linear model in [25] in place of PF equations, (4.36) is rewritten in a variational form with respect to the initial operating point as

$$\begin{aligned}
&\min_{\substack{\Delta a^2_{oltc},\ \Delta a^2_{svr_1},\ldots,\Delta a^2_{M_{svr}} \\ \Delta Q_{cb_1},\ldots,\Delta Q_{cb_{M_{svr}}}}} \sum_{i=1}^{N_{vcz}} (\Delta V^2_{pn_i} - \Delta V^2_{pn_{i,\mathrm{ref}}})^2 \\
&\text{subject to} \qquad (4.37)\\
&\Delta V^2_{pn_i} = \Gamma^{oltc}_i \Delta V^2_{oltc} + \sum_{j=1}^{M_{svr}} \Gamma^{svr}_{ij}\ \Delta V^2_{svr_j} + \sum_{t=1}^{M_{cb}} \Gamma^{cb}_{it}\ \Delta Q_{cb_t} \\
&\quad \Delta V^2_{pn_{i,\min}} \le \Delta V^2_{pn_i} \le \Delta V^2_{pn_{i,\max}} \qquad i = 1,\ldots,N_{vcz} \\
&\quad \Delta V^2_{oltc} = s^{oltc} \Delta a^2_{oltc} \\
&\quad \Delta a_{oltc_{\min}} \le \Delta a_{oltc} \le \Delta a_{oltc_{\max}} \\
&\quad \Delta V^2_{svr_j} = s^{svr}_j \Delta a^2_{svr_j} \qquad j = 1,\ldots,M_{svr} \\
&\quad \Delta a_{svr_{j,\min}} \le \Delta a_{svr_j} \le \Delta a_{svr_{j,\max}} \qquad j = 1,\ldots,M_{svr} \\
&\quad \Delta Q_{cb_{t,\min}} \le \Delta Q_{cb_t} \le \Delta Q_{cb_{t,\max}} \qquad t = 1,\ldots,M_{cb}
\end{aligned}$$

where Γ^{oltc}_i, Γ^{svr}_{ij}, and Γ^{cb}_{it} are the sensitivities of the bus voltage at the i-th PN to, respectively, the squared voltage at the terminal bus of the OLTC, ΔV^2_{oltc}, to the squared voltage at the terminal bus of the j-th SVR, $\Delta V^2_{svr_j}$, and to the reactive power injected by the t-th CB. The voltages ΔV^2_{oltc} and $\Delta V^2_{svr_j}$ are related to the corresponding tap positions Δa^2_{oltc} and $\Delta a^2_{svr_j}$ by the sensitivities s^{oltc} and s^{svr}_j, respectively.

Defining the vector $\mathbf{y}$ of the PN voltages and the vector $\mathbf{x}_c$ of set-points of the conventional voltage control devices

$$\begin{aligned}
\mathbf{y}^{\mathrm{T}} &= \{\Delta V^2_{pn_1},\ldots,\Delta V^2_{pn_{N_{vcz}}}\} \\
\mathbf{x}_c^{\mathrm{T}} &= \{\Delta a^2_{oltc}, \Delta a^2_{svr_1},\ldots,\Delta a^2_{svr_{M_{svr}}}, \Delta Q_{cb_1},\ldots,\Delta Q_{cb_{M_{cb}}}\}
\end{aligned}$$

the VOP (4.37) is rewritten in a matrix form as

$$\begin{aligned}
&\min_{\mathbf{x}_c} \frac{1}{2} {\mathbf{x}_c}^{\mathrm{T}} \mathbf{H}_c \mathbf{x}_c - {\mathbf{h}_c}^{\mathrm{T}} \mathbf{x}_c \\
&\text{subject to} \qquad (4.38)\\
&\qquad \mathbf{y}_{\min} \le \mathbf{y} \le \mathbf{y}_{\max} \\
&\qquad \mathbf{x}_{c,\min} \le \mathbf{x}_c \le \mathbf{x}_{c,\max}
\end{aligned}$$

where

$$\mathbf{H}_c = \mathbf{\Gamma}_c{}^{\mathrm{T}}\mathbf{\Gamma}_c \qquad \mathbf{h}_c = \mathbf{y}_{\mathrm{ref}}\mathbf{\Gamma}_c{}^{\mathrm{T}}$$
$$\mathbf{\Gamma}_c = \begin{pmatrix} \mathbf{\Gamma}^{oltc} s^{oltc} & \mathbf{\Gamma}^{svr} S^{svr} & \mathbf{\Gamma}^{cb} \end{pmatrix}$$

4.3.3 DERs Optimization

The VOP at the second level is initially formulated in a centralized manner. Then, it is reformulated according to a decentralized approach to obtain separable VOPs in each VCZ. Finally, a distributed algorithm is implemented to provide the VOP solution by exchanging scalar variables between PNs.

A Centralized formulation;

The VOP minimizes the same objective function as the one of the first level but acts on the active and reactive powers of the unconventional control devices, that is

$$\min_{\substack{P_{der_1},\ldots,P_{der_{M_{der}}} \\ Q_{der_1},\ldots,Q_{der_{M_{der}}}}} \sum_{i=1}^{N_{vcz}} (V^2_{pn_i} - V^2_{pn_{i,\mathrm{ref}}})^2$$

subject to (4.39)

PF equations

$$V^2_{pn_{i,\min}} \le V^2_{pn_i} \le V^2_{pn_{i,\max}} \qquad i = 1,\ldots,N_{vcz}$$
$$P_{der_k,\min} \le P_{der_k} \le P_{der_k,\max} \qquad k = 1,\ldots,M_{der}$$
$$Q_{der_k,\min} \le Q_{der_k} \le Q_{der_k,\max} \qquad k = 1,\ldots,M_{der}$$

The optimal solution must satisfy PF equations and limits on the PN voltages and on the operational range of DERs. It is worth noting that the VOP (4.39) is a not-strictly convex constrained quadratic problem, because the objective function only refers to the voltages of the PNs. Always using the linear model in [25] in place of PF equations, (4.39) is rewritten in a variational form with respect to the initial operating point and, then, rewritten in a matrix form. Defining the vector $\mathbf{x}_u$ of set-points of the unconventional voltage control devices

$$\mathbf{x}_u^{\mathrm{T}} = \{\Delta P_{der_1},\ldots,\Delta P_{der_{M_{der}}},\Delta Q_{der_1}\ldots,\Delta Q_{der_{M_{der}}}\}$$

the VOP (4.39) is rewritten in a matrix form as

$$\begin{aligned} &\min_{\mathbf{x}_u} \frac{1}{2}{\mathbf{x}_u}^{\mathrm{T}}\mathbf{H}_u\mathbf{x}_u - {\mathbf{h}_u}^{\mathrm{T}}\mathbf{x}_u \\ &\text{subject to} \\ &\qquad \mathbf{y}_{\min} \leq \mathbf{y} \leq \mathbf{y}_{\max} \\ &\qquad \mathbf{x}_{u,\min} \leq \mathbf{x}_u \leq \mathbf{x}_{u,\max} \end{aligned} \tag{4.40}$$

where

$$\mathbf{H}_u = {\mathbf{\Gamma}_u}^{\mathrm{T}}\mathbf{\Gamma}_u \qquad \mathbf{h}_u = \mathbf{y}_{\mathrm{ref}}{\mathbf{\Gamma}_u}^{\mathrm{T}}$$
$$\mathbf{\Gamma}_u = \begin{pmatrix} \mathbf{\Gamma}^{P^{der}} & \mathbf{\Gamma}^{Q^{der}} \end{pmatrix}$$

B Decentralized formulation;

The VOP (4.40) is reformulated in a decentralized manner extending the method proposed in [36]. In particular, the lack of strict convexity of the VOP (4.39) is overcome by iteratively solving a dual centralized VOP working on the augmented Lagrangian function by the method of multipliers. Then, the dual centralized VOP is decomposed into separable problems by applying the ADMM.

Referring to the i-th VCZ, let the vector $\mathbf{u}_i$ be defined, including all the variables, namely the PN nodal voltage and the set-points of the unconventional voltage devices connected to the VCZ

$$\mathbf{u}_i^{\mathrm{T}} = \{\Delta V_{pn_i}^2, \mathbf{x}_i^{\mathrm{T}}\}$$

At each iteration, each VCZ firstly solves a centralized VOP which optimizes the voltage at the PN acting only on its local unconventional control devices

$$\begin{aligned} &\min_{\mathbf{u}_i} \frac{1}{2}{\mathbf{u}_i}^{\mathrm{T}}\mathbf{H}_i\mathbf{u}_i - {\mathbf{h}_i}^{\mathrm{T}}\mathbf{u}_i \\ &\text{subject to} \\ &\qquad \mathbf{u}_{i,\min} \leq \mathbf{u}_i \leq \mathbf{u}_{i,\max} \end{aligned} \tag{4.41}$$

with

$$\mathbf{H}_i = f_i(\mathbf{\Gamma}_u, c)$$
$$\mathbf{h}_i = g_i(\mathbf{\Gamma}_u, c, \lambda_1, \ldots, \lambda_{N_{vcz}})$$

where c is the penalty parameter and λ_i are the Lagrange multipliers. The expressions of $\mathbf{H}_i$ and $\mathbf{h}_i$ are in Appendix. Then, the solutions of (4.41)

obtained in the various VCZs are used to update the Lagrange multipliers according to

$$\lambda_i = \lambda_i^* + c\, w_i \qquad i = 1, \ldots, N_{vcz} \tag{4.42}$$

where $*$ indicates the value assumed by a variable in the previous step of iteration, and

$$w_i = \frac{1}{N_{vcz}} \big(\mathbf{e}_{ii}^{\mathrm{T}} \mathbf{u}_i + \sum_{\substack{j=1 \\ j \neq i}}^{N_{vcz}} \mathbf{e}_{ij}^{\mathrm{T}} \mathbf{u}_j \big) = \frac{1}{N_{vcz}} \big(z_{ii} + \sum_{\substack{j=1 \\ j \neq i}}^{N_{vcz}} z_{ij} \big) \tag{4.43}$$

The expressions of $\mathbf{e}_{ii}^{\mathrm{T}}$, $\mathbf{e}_{ij}^{\mathrm{T}}$ are in Appendix

C Distributed algorithm for decentralized solution;

It is possible to implement a distributed algorithm that provides the solution of VOP (4.41)–(4.42) by exchanging only scalar variables among PNs of each VCZ. The main steps of such an algorithm are described in the following and highlighted in Fig. 4.18.

i. Initialize the step counter $h = 0$ and $\mathbf{u}_i = 0$ and $\lambda_i = 0$; choose c and fix the tolerance τ;

ii. $h = h + 1$;

iii. each VCZ solve in parallel with the other VCZs the VOP (4.41), obtaining the vectors $\mathbf{u}_i$;

iv. each VCZ evaluates the additional scalar variables $z_{ii} = \mathbf{e}_{ii}^{\mathrm{T}} \mathbf{u}_i$ and $z_{ji} = \mathbf{e}_{ji}^{\mathrm{T}} \mathbf{u}_i$;

v. each VCZ provides the scalars z_{ii} and z_{ji} to the other VCZs and receives from them the scalars z_{jj} and z_{ij};

vi. each VCZ evaluates λ_i using (4.43) and (4.42);

vii. each VCZ checks if the changes of the values of $\mathbf{u}_i$ with respect to the ones of the previous iteration are small enough, that is $|\mathbf{u}_i(h) - \mathbf{u}_i(h-1)| < \tau$;

viii. if the output of step vii. is true for all the problems then stop and $\mathbf{u}_i(h)$ are the solutions; else go back to step ii. and start a new iteration.

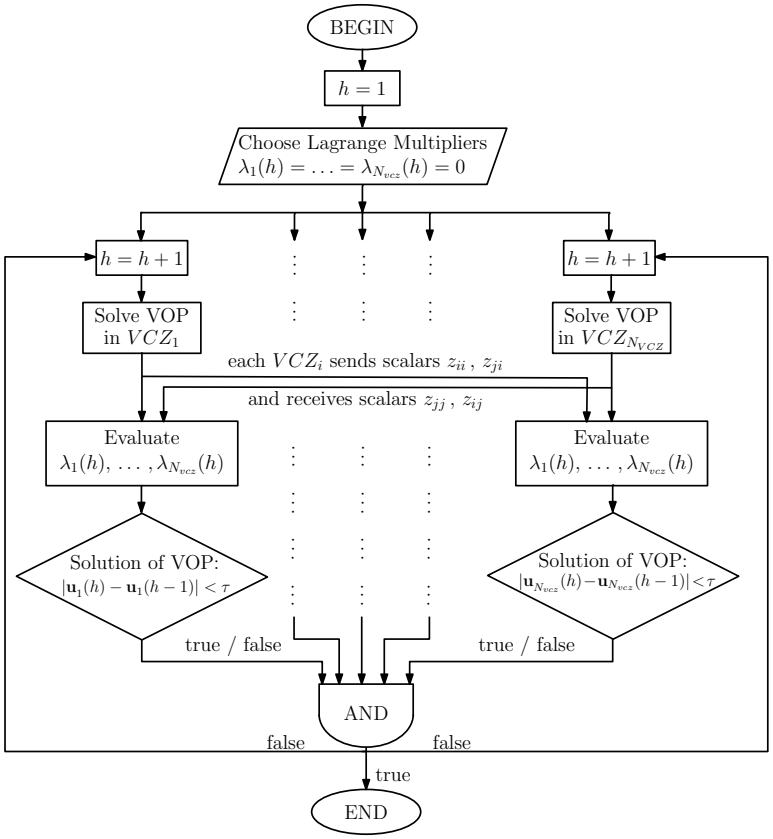

Figure 4.18: Distributed Algorithm (Two-Levels)

4.3.4 Case Study With Two Levels Algorithm

The distribution system under study is the IEEE 123-bus feeder which operates at a nominal MV voltage of 4.16 kV. To apply the proposed methodology, the distribution network is converted into a three-phase balanced system. The load connected to the network in rated operating conditions is equal to 3.49 MW and 1.17 MVAr for total active and reactive powers, respectively. The MV feeder is supplied by a 115/4.16 kV substation and the HV busbar is assumed as the slack bus with rated voltage amplitude.

The following conventional VCDs of the original test feeder are included: the OLTC on the substation transformer, the SVR #4 along the line segment 160-67, and the four CBs. The tap positions of both OLTC and SVR can vary in the range from 0.95 p.u. to 1.05 with 20 positions; CBs can be entirely connected or disconnected.

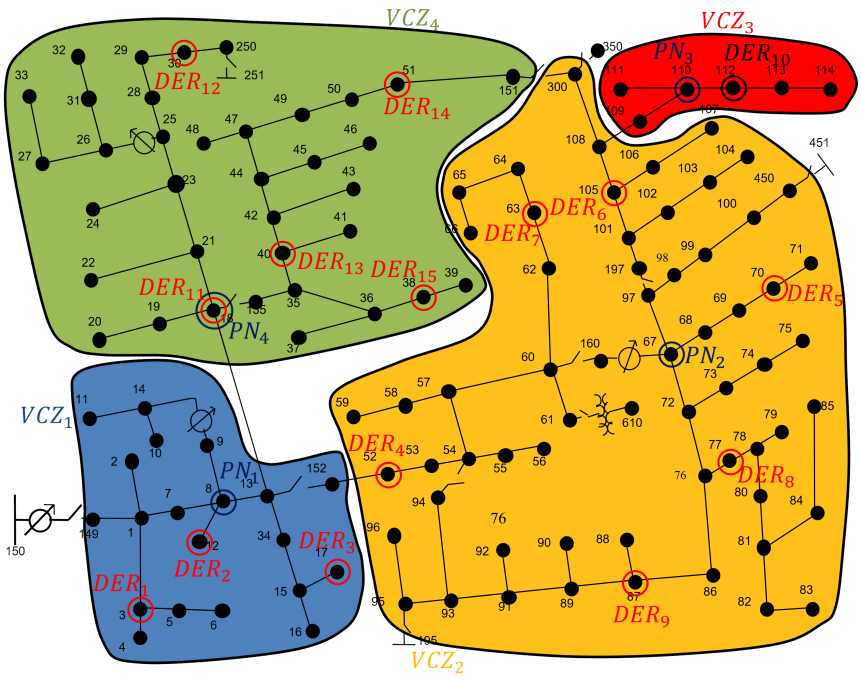

Figure 4.19: The 123-bus test feeder with DERs, VCZs and PNs (Two-Levels)

Concerning the DERs, 15 PVSs, each one of 250 kW peak active power, are connected to the grid at nodes 3, 12, 17, 52, 70, 105, 63, 77, 87, 112, 18, 30, 40, 51 and 38 as reported in Fig. 4.19. In addition, at the premises of 8 out of the 15 PV systems a EESS is installed. The unconventional VCDs consist of the 15 reactive power controllers of the PV systems and of the 8 active power controllers of the EESSs. In particular, the reactive power of the PV systems can be controlled in the range ±100 kVAr, whereas each EESS can vary the active power exchanged with the network in the range ±50 kW. Finally, the references values of the nodal voltages at the PNs are fixed equal to 1.0 p.u. and the allowable range of the nodal voltages is [0.95,1.05].

The linear model in [25] is applied to evaluate the sensitivity coefficients of the electrical variables to the powers injected in all the nodes of the grid. The starting point to linearize PF equations and to obtain such sensitivity coefficients is: voltage amplitude of the HV busbar equal to 1.025 p.u.; loads equal to 100 % of their rated values; OLTC and SVR transformer ratios equal

Table 4.7: Values of the Silhouette index for various network partioning (Two-Levels)

	Number of VCZs				
	3	4	5	6	7
Index	0.464	0.537	0.491	0.490	0.442

to 1.0; CBs switched off; and no DGs and EESSs connected to the grid. The electrical distances are evaluated using the sensitivities of the squared nodal voltages to the only reactive power injections, due to the R/X ratio of the MV network. Then nodes are merged into a number of VCZs ranging from 3 to 7. Table 4.7 reports the Silhouette indices evaluated for the different partitions. The Silhouette index present similar values; it reaches its maximum value for a network partitioned in 4 VCZs. The 4 resulting VCZs and the corresponding PNs are highlighted in Fig. 4.19. Such a partition corresponds to have a good distribution of VCDs in each VCZs thanks to the large number of DERs (i.e. 3 PVSs and 2 EESSs in VCZ_1; 1 SVR, 4 CBs, 6 PVSs and 3 EESSs in VCZ_2; 1 PVS and 1 EESS in VCZ_3; 5 PVSs and 2 EESSs in VCZ_4.)

The results of time simulations are reported to give evidence of the effective action of the proposed two-levels VOP.

The initial operating point of the IEEE 123-bus feeder is: loads equal to 80 % of the rated values; each PVS produces 200 kW with unity power factor (for a total generation equal to 3.0 MW); no active power injected/absorbed by EESSs; OLTC ratio and SVR ratio equal to 1.0; no CBs connected to the network; such a case will be referred in the following to as Case A.

The first level VOP provides the optimal set-points of the conventional VCDs, which are shown in Table 4.8. Analysing the results, it is evident the increment of the OLTC tap position and the slight increase of the SVR tap position; also, only one CB is switched on.

Acquiring the optimal set-points of the unconventional VCDs from the first level, the second level VOP provides the optimal set-points of DERs, which are shown in Table 4.9. It is evident that all the EESSs contribute to voltage optimization absorbing or injecting active power as well as all the

Table 4.8: Optimal set-points of conventional VCDs for different cases (Two-Levels)

Set-points	Case A	Case B	Case C	Case D	Case E	Case F
a_{OLTC}	1.020	0.990	1.030	1.030	1.015	1.025
a_{SVR}	1.005	0.990	1.005	1.010	1.000	1.005
CB_1	ON	ON	ON	ON	ON	ON
CB_2	OFF	OFF	ON	ON	ON	OFF
CB_3	OFF	OFF	ON	ON	OFF	OFF
CB_4	OFF	OFF	ON	ON	OFF	OFF

PVSs use reactive power capability for grid support.

In the following the performance of the proposed approach is analyzed in terms of voltage profile. Fig. 4.20 shows such voltage profile, which is referred in the following to as two-levels VOP (it includes the 123-bus feeder and the nodal voltage at the slack bus). For the sake of comparison, other two voltage profiles are considered: the first one is obtained by solving the PF equations without carrying out any optimization (it is referred to as no VOP); the second one is obtained in absence of the second level VOP (it is referred to as first level VOP). The results evidence that, in absence of any voltage control action, the nodal voltages get close to the lower limit of the acceptable operational range. The two-levels VOP improves the voltage profile, thank to the second level VOP that move further up the nodal voltages in comparison to the adoption of the first level VOP only. In fact, adopting the two-levels VOP the voltage profile is more close to 1.0 p.u. .

The performance of the second level VOP is further analysed by comparing the voltage profile with the one obtained by adopting a centralized approach which minimizes the distance of the voltages of all the nodes of the feeder with respect to the rated value (1.0 p.u.) with a classical voltage optimal power flow; results are shown in Fig. 4.21. In spite of the reduced number of nodal voltages that are measured and considered (only 4) and of the linearization of the PF equations, the proposed ADMM gives results, in terms of voltage profiles, that are very near to the ones obtained by the classical centralized method, which requires a state-estimation of the entire

Table 4.9: Optimal set-points of unconventional VCDs for different cases (Two-Levels)

	Case A		Case B		Case C		Case D		Case E		Case F	
Set-points	P_{EESS} (kW)	Q_{PVS} (kVAr)	P_{EESS} (kW)	Q_{PVS} (kVAr)	P_{EESS} (kW)	Q_{PVS} (kVAr)	P_{EESS} (kW)	Q_{PVS} (kVAr)	P_{EESS} (kW)	Q_{PVS} (kVAr)	P_{EESS} (kW)	Q_{PVS} (kVAr)
DER_1	-50	-100	50	100	-50	-100	-50	-100	-50	-100	-50	-100
DER_2	–	-100	–	100	–	-100	–	-100	–	-100	–	–
DER_3	-50	-100	50	100	-50	-100	-50	-100	-50	-100	-50	-100
DER_4	-50	-100	50	100	-50	-100	-50	-100	-50	-100	–	–
DER_5	50	100	-50	-100	50	100	50	70	-50	-100	50	100
DER_6	–	21	–	-45	–	100	–	-22	–	-65	–	82
DER_7	–	-100	–	100	–	-100	–	-100	–	-100	–	-100
DER_8	50	51	-50	52	50	61	50	-100	50	100	–	–
DER_9	–	-100	–	100	–	-100	–	-100	–	89	–	-100
DER_{10}	50	-49	-50	-68	50	-6	50	100	50	-75	–	-5
DER_{11}	50	100	-50	-100	50	100	50	100	50	100	–	–
DER_{12}	–	100	–	-100	–	100	–	100	–	100	–	100
DER_{13}	50	100	-50	-100	50	100	50	100	50	100	50	100
DER_{14}	–	32	–	80	–	-83	–	100	–	-87	—	99
DER_{15}	–	100	–	-100	–	100	–	100	–	100	–	–

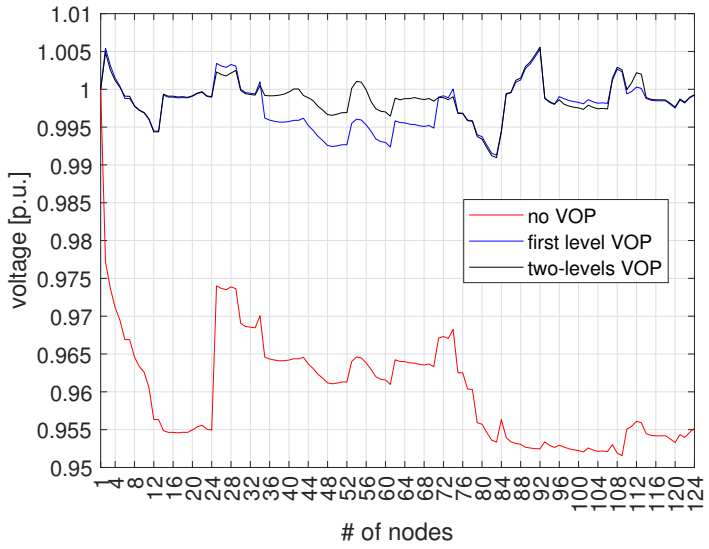

Figure 4.20: Voltage profiles in the Case A: no VOP (red), with only the first level VOP (blue), with the two-levels VOP (black) (Two-Levels)

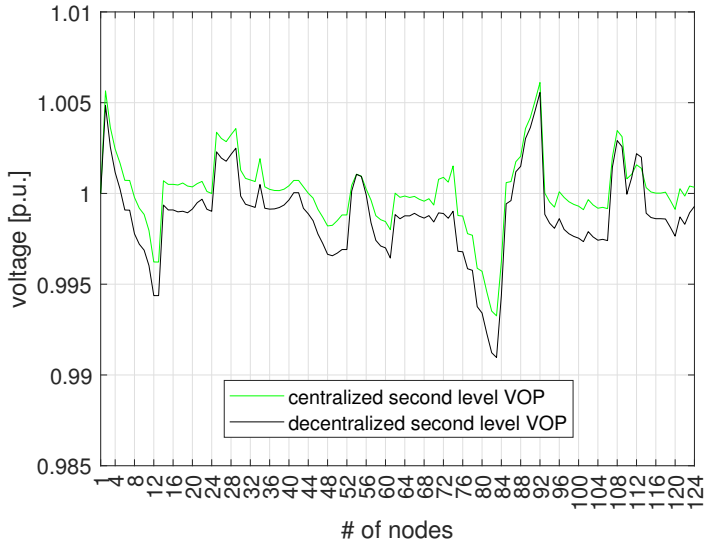

Figure 4.21: Voltage profiles in the Case A: centralized second-level VOP (green) and decentralized second-level VOP (black) (Two-Levels)

distribution system and uses the non-linear PF equations. For this reason, in the continuation of this analysis, only the second level optimization obtained by the proposed ADMM will be considered.

The performance of the two-levels VOP is evaluated in the following operating conditions:

- Case B: operating conditions equal to the Case A except for the loads, which are equal to 30 % of the rated values;
- Case C: operating conditions equal to the Case A except for the loads, which are equal to 100 % of the rated values;
- Case D: operating conditions equal to the Case A except for the total generation, which is equal to 0.9 MW with unity power factor;
- Case E: operating conditions equal to the Case A except for the total generation, which is equal to 3.75 MW with unity power factor;
- Case F: operating conditions equal to the Case A except for the generation; in this case a different distribution of PVSs and EESSs is considered in the VCZs (i.e. 2 PVSs and 2 EESSs in VCZ_1; 1 SVR, 4 CBs, 4 PVSs and 1 EESSs in VCZ_2; 1 PVS in VCZ_3; 3 PVSs and

1 EESSs in VCZ_4) for a total generation equal to 2 MW with unity power factor.

The optimal set-points of conventional and unconventional VCDs are reported in Table 4.8 and Table 4.9, respectively, for all the considered cases. Furthermore, Fig.s 4.22-4.26 report the voltage profiles without optimization, with the only first level VOP and with the complete two-levels VOP for the Case B, Case C, Case D, Case E, Case F, respectively.

Both load variations (Fig.s 4.22- 4.23) and generation variations (Figures 4.24- 4.26) have a great impact on the voltage profiles with respect to the Case A, especially in the absence of optimization in which some nodal voltages go below the lower limit (Case C, Case D and Case F). From the analysis of the set-points and of the voltage profiles, it is apparent that the proposed second level VOP significantly improves the voltage profiles with respect to the ones obtained in absence of any action on the DERs.

The Case F refers to a lower penetration of DERs in the network. In particular, only 10 PVSs and 4 EESSs are installed into the grid. Comparing Case F with Case A (that are characterized by the same load), it is possible to see how a lower penetration of DERs implies that in the Case F the voltage profile significantly decreases towards values of lower voltage in absence of any type of optimization. Considering the voltage profiles resulting from the first level and the second level of optimization, while in the Case A they are almost overlapped, in the Case F they are more distant and the second optimization level is the one that makes the voltage profile closest to the reference voltage of 1 p.u.. This result shows that also in presence of lower penetration of DERs, the two levels optimization is still very effective.

The test network is simulated for 8 hours of operation by a sequence of steady-state operating conditions. During the simulation the total load of the network and the total active power generated by the PVSs vary every 1-minute according to the time evolution depicted in Fig. 4.27.

For the sake of simplicity, hereafter the time evolutions of the voltages at the four PNs are analyzed, assuming them as representatives of the voltage profiles of the system.

First of all, the test network has been simulated in absence of any conventional VCDs and of any PV system or DERs. The results are reported in Fig. 4.28, evidencing that, in absence of any voltage control action, the

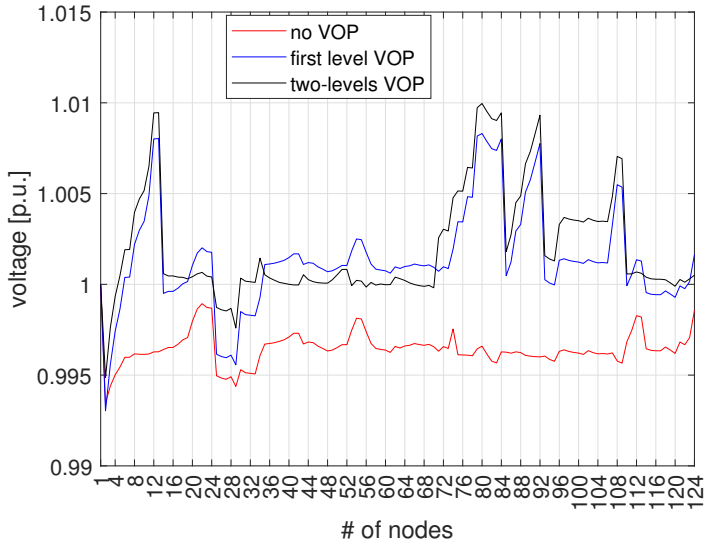

Figure 4.22: Voltage profiles in the Case B: no VOP (red), with only the first level VOP (blue), with the two-levels VOP (black) (Two-Levels)

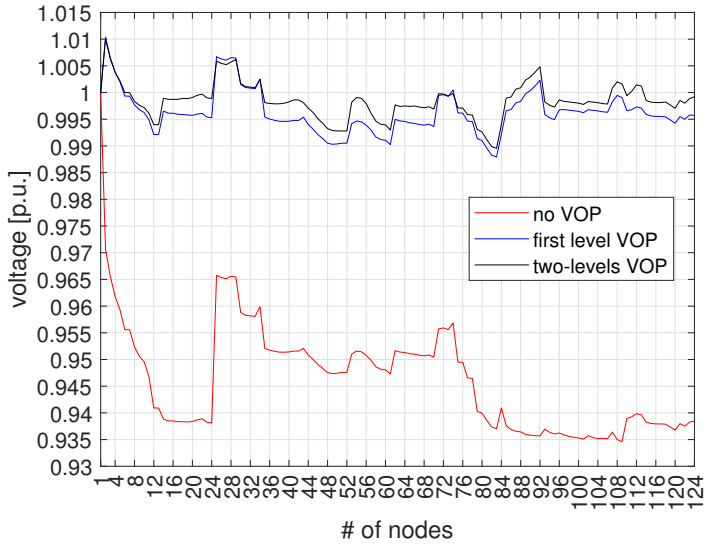

Figure 4.23: Voltage profiles in the Case C: no VOP (red), with only the first level VOP (blue), with the two-levels VOP (black) (Two-Levels)

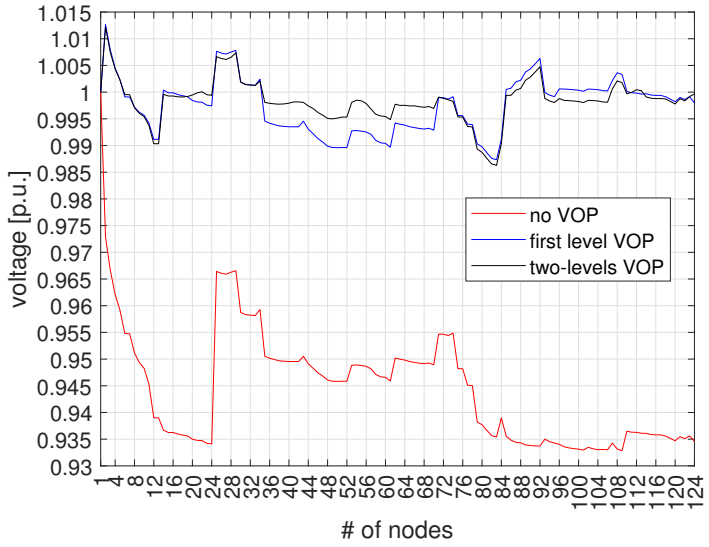

Figure 4.24: Voltage profiles in the Case D: no VOP (red), with only the first level VOP (blue), with the two-levels VOP (black) (Two-Levels)

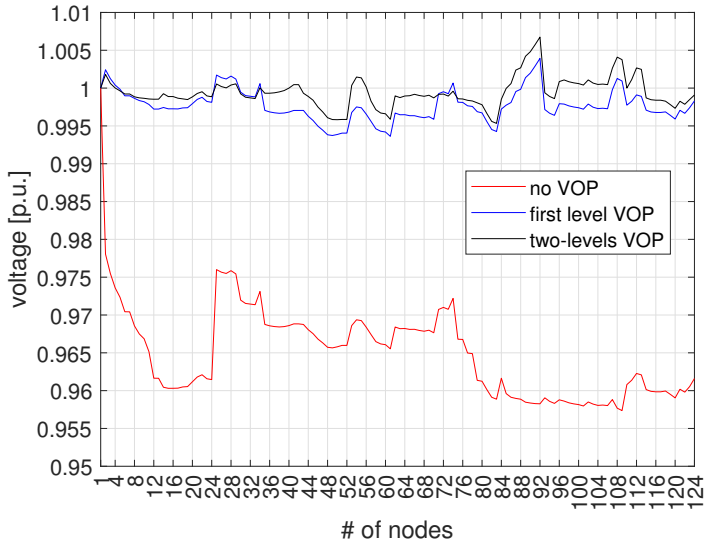

Figure 4.25: Voltage profiles in the Case E: no VOP (red), with only the first level VOP (blue), with the two-levels VOP (black)(Two-Levels)

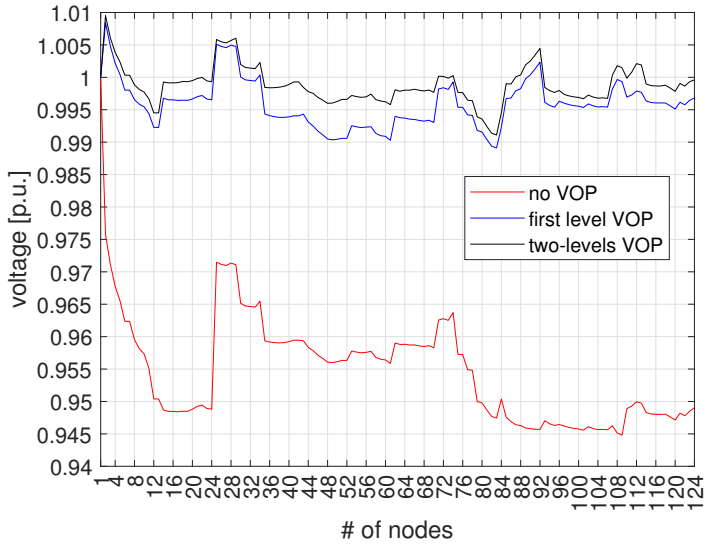

Figure 4.26: Voltage profiles in the Case F: no VOP (red), with only the first level VOP (blue), with the two-levels VOP (black) (Two-Levels)

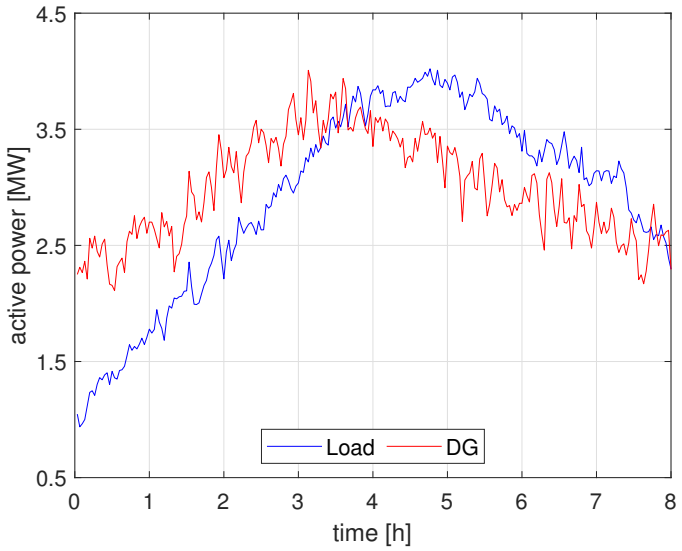

Figure 4.27: Time evolution of the total load (blue) and total active power generated by the PVSs (red) (Two-Levels)

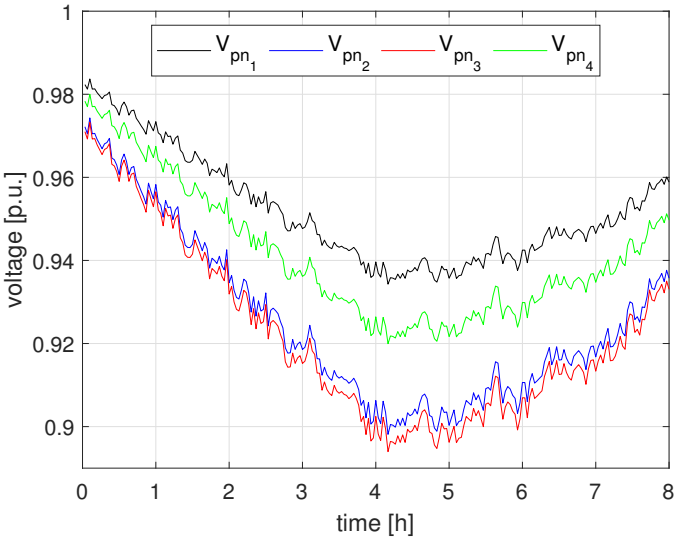

Figure 4.28: Time evolution of voltages at the PNs in absence of conventional VCDs and of DERs (Two-Levels)

passive network cannot supply the full load without causing undervoltages out the acceptable operational range.

To overcome this problem, the conventional VCDs are installed and the first level VOP is solved by the centralized control system every hour on the basis of the load level (passive network). The results are reported in Fig. 4.29 in which the step voltage variations caused by the first level VOP are clearly evident every full hour. The conventional VCDs, if adequately optimized, significantly improve the nodal voltages, keeping them in the range 0.98–1.02 p.u. during the whole simulation.

When the 15 PVSs are connected to the network, they inject the active power generated according to Fig. 4.27, thus causing an increase in the nodal voltage amplitudes. The results are reported in Fig. 4.30 and, in comparison with Fig. 4.29, clearly show the overvoltages that are caused by the DGs.

To overcome this problem the PVSs are equipped with a reactive power capability and enriched by EESSs. A second level VOP is solved every 10 minutes according to the decentralized approach and the proposed ADMM algorithm. The results are reported in Fig. 4.31 and give evidence of the benefits introduced by the DER optimization. In particular the voltage amplitudes at the PNs are brought back within the range 0.98–1.02 p.u. during the whole simulation. Fig. 4.32 reports the time evolution of the total reac-

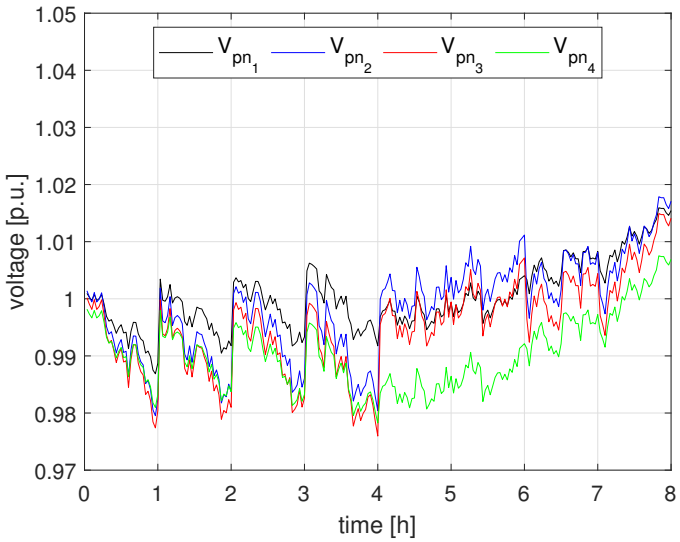

Figure 4.29: Time evolution of voltages at the PNs with the first level VOP and without DERs (Two-Levels)

tive power injected by the PVSs and of the total active power injected by EESSs. It is evident that the variations of these quantities take place every 10 minutes when the second level VOP is solved and the total powers are generally negative, as expected to reduce the voltages. It is worth noticing that it does not imply that all the DERs absorb powers, because they are individually dispatched to optimize the voltage profile of the feeder.

4.3.5 Final considerations about the two-levels algorithm

The problem of optimizing the voltage profiles in power distribution networks has been tackled by a two-steps procedure. Firstly, the network has been partitioned into VCZs with PNs; then, a twolevels time-scale based coordinated approach has been applied to VOP. The first level evaluates the set-points of conventional VCDs by centralized optimization of the PN voltages [41]. The second level adopts a decentralized approach which optimizes in each VCZ the PN voltage by acting on the DERs present in the same VCZ; the VCZ solutions are driven to the global optimum by a data exchange between PNs. The application of the proposed VOP to the IEEE 123- bus test system with DERs has been presented and results have evidenced the negative impact of uncontrolled DGs in presence of conventional VCDs and the benefits introduced by DER optimization. The proposed method reduces

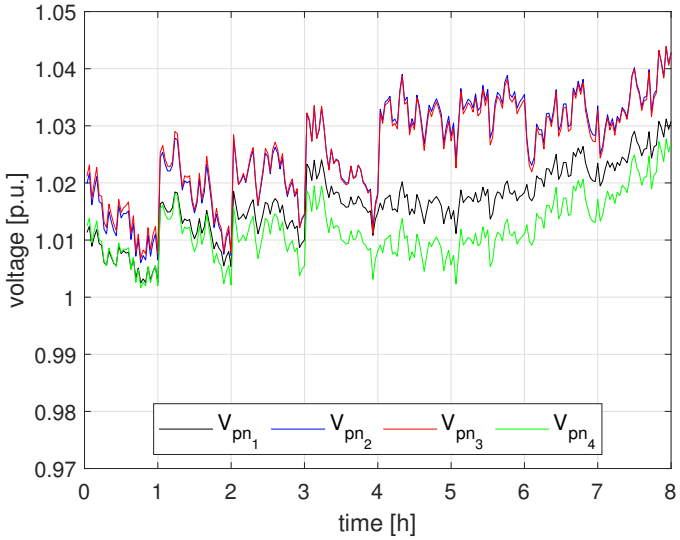

Figure 4.30: Time evolution of voltages at the PNs with the first level VOP and with uncontrolled PVSs (Two-Levels)

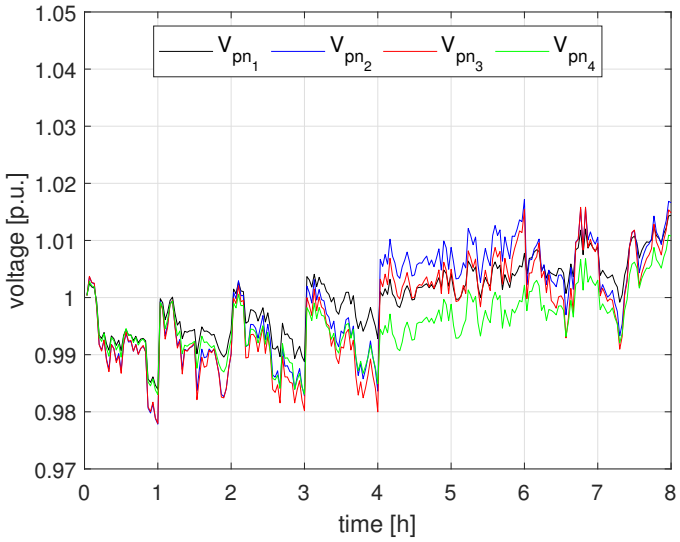

Figure 4.31: Time evolution of voltages at the PNs with the VOP (Two-Levels)

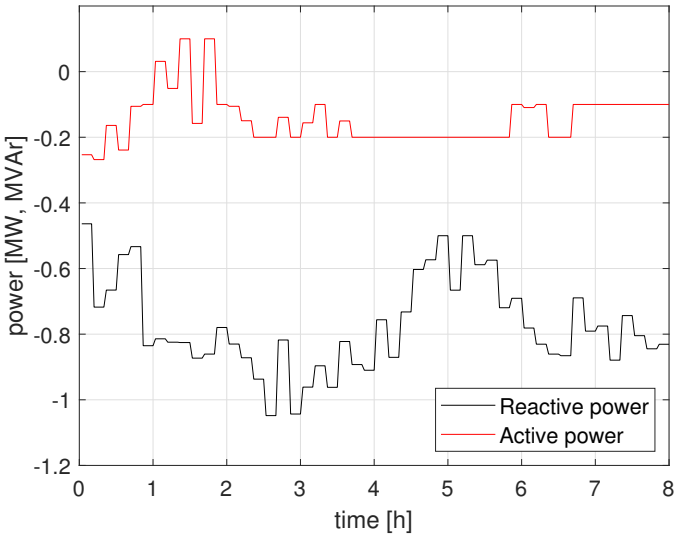

Figure 4.32: Time evolution of total reactive power (black) injected by the PVSs and of the total active power (red) injected by the EESSs (Two-Levels)

the need for adding DERs as additional variables in the first level VOP, thus reducing the complexity and dimensionality of the VOP in large distribution systems, and provides additional flexibility to the distribution system operator by the zone control of DERs for voltage regulation. Added to this, the proposed technique has economic benefits, due to limited communication requirements, without significant loss of accuracy with respect to centralized approaches.

Appendix

The following definitions apply to (4.41) and (4.43).

$$\mathbf{H}_i = \begin{pmatrix} 1 & \mathbf{0}_{x_i}^{\mathrm{T}} \\ \mathbf{0}_{x_i} & \mathbf{0}_{x_i}^{\mathrm{T}}\mathbf{0}_{x_i} \end{pmatrix} + c \begin{pmatrix} 1 & -\Gamma_{u_{ii}} \\ -\Gamma_{u_{ii}}^{\mathrm{T}} & \Gamma_{u_{ii}}^{\mathrm{T}}\Gamma_{u_{ii}} \end{pmatrix} + c \sum_{\substack{j=1 \\ j\neq i}}^{N_{vcz}} \begin{pmatrix} 0 & 0 \\ 0 & \Gamma_{u_{ji}}^{\mathrm{T}}\Gamma_{u_{ji}} \end{pmatrix}$$

$$\mathbf{h}_i^{\mathrm{T}} = \left(y_{i\mathrm{ref}} \;\; \mathbf{0}_{x_i}^{\mathrm{T}}\right) + \lambda_i \mathbf{e}_{ii}^{\mathrm{T}} + c\,\mathbf{e}_{ii}^{\mathrm{T}}(w_i - \mathbf{e}_{ii}^{\mathrm{T}}\mathbf{u}_i^*) + \sum_{\substack{j=1 \\ j\neq i}}^{N_{vcz}} \lambda_j \mathbf{e}_{ji}^{\mathrm{T}} + c\,\mathbf{e}_{ji}^{\mathrm{T}}(w_j - \mathbf{e}_{ji}^{\mathrm{T}}\mathbf{u}_i^*)$$

$$\mathbf{e}_{ii}^{\mathrm{T}} = (1 \; -\boldsymbol{\Gamma}_{u_{ii}}) \;\; \mathbf{e}_{ij}^{\mathrm{T}} = (0 \; -\boldsymbol{\Gamma}_{u_{ij}}) \;\; j = 1, ..., N_{vcz} \;\; j \neq i$$

where $\mathbf{0}_{x_i}$ is a vector of zeros with dimension $dim(\mathbf{x}_i)$.

Conclusions

The national electric power system was conceived with a hierarchical structure in which a limited number of large-scale production plants supplied the loads through the transmission and distribution networks.

Nowadays, the grid is undergoing a deep transformation linked to the constantly-increasing use of RESs for "zero impact" energy production. There have been many international climate agreements promoting the reduction of the emissions of greenhouse gases by a massive penetration of the DERs exploiting RESs. Consequently, the traditional distribution grid must completely change its operation, transforming itself from a "passive" network, in which energy flows from the supplying substation to the customers, to an "active" network in which the consumer also becomes a producer. This transition is known as the evolution towards smart grids. To this aim, it is necessary to develop new strategies that are sustainable from an economic and financial point of view and which, at the same time, overcome the technical limits of the existing networks.

This research has focused on the specific problem of voltage regulation in the new scenario of the smart distribution grids. In fact, it is necessary to rethink the traditional management techniques, because the conventional control devices (transformers with under-load tap changers, capacitor banks and step voltage regulators) are no longer sufficient and innovative control devices must be added. As evidenced also by this research, a new significant contribution to voltage regulation comes from innovative control strategies of the active and reactive power injections by DERs.

In the first part of the research activity, the characteristics of the different control structures were studied, starting from the centralized approach. The

voltage optimization problem (VOP) is formulated similarly to an optimal power flow addressing the problem of optimizing the voltage profile in an active distribution network by exploiting the powers supplied by the DERs.

The objective function to be minimized is the distance of the nodal voltages with respect to the reference values. The equality constraints are the non linear power flow equations of the network while the inequality constraints are the acceptable ranges of the nodal voltages and of the powers injected by the DERs. The problem considered is therefore a non convex large problem. Surely it provides the optimal voltage control solution but it presents possible convergence problems and significant computational burden.

To overcome such problems, a linear modeling of the distribution system was studied in the second part of the research activity.

To model the distribution system, in the presence of DER, after representing it through the equivalent circuits of the components, linearization has been adopted. Starting from the branch, three different types of models have been considered. The constrained-Jacobian exact one (previously proposed in literature), the structural one (*LinDistFlow*) and the structural one with losses. By combining the branches, the feeder modeling is obtained, with and without losses, and the modeling of the lateral is outlined. Eventually, the model of the substation in combined with the feeders to obtain the distribution system model.

A simple straight-forward algorithm has also been presented to evaluate the sensitivity matrices for the structural linear model of the distribution system. The algorithm can be extended to to the linear model with losses.

In the third part of the research activity, starting from the centralized formulation of the VOP, the study concerned solving the problem adopting the decentralized approach.

To this aim, a partition of the network into VCZs was carried out. The steps taken to achieve this result are:

- definition of an electrical distance between the nodes of the network;
- grouping of VCZ nodes;
- identification of the PN in each VCZ;

- determination of the optimal number of VCZ.

Then, the centralized optimization problem has been rewritten specializing it for the two zones. The decomposition of the problem was carried out through the application of the alternating direction method of multipliers (ADMM), a methodology widely used in the field of management and control problems of smart grids according to the decentralized approach. First, the augmented Lagrangian (LA) method and the Method of Multipliers (MMs) have been applied. More specifically, the LA method is used to solve constrained optimization problems. The constraints are introduced in the objective function and weighted with multipliers that must be updated at each iteration. Through MMs, on the other hand, successive minimizations of the problem are carried out. In order to arrive at the final decomposition, further manipulations are necessary due to the presence of the quadratic terms introduced by LA which do not allow the splitting into two subproblems. ADMM was used to overcome this problem. This is a cyclical method. At each cycle, LA is optimized with respect to a set of variables and only subsequently the minimization is performed with respect to the remaining variables.

The proposed approach guarantees the convergence of the optimization problem with a limited number of iterations and an accuracy of the solutions very close to that obtained with the centralized approach. Finally, from numerical simulations the improvements on the voltage profiles compared to the absence of regulation are evident.

The decentralized approach was further investigated adopting another decomposition approach. In this case, after dividing the network into two VCZs and reformulating the centralized problem using the LA method and the MMs method, the decomposition was performed using the APP. This method, to our knowledge, has never been used for voltage regulation in active distribution networks. APP modifies the initial problem by adding an auxiliary function to the objective function and performs a substitution of the quadratic terms (related to LA) with a linear approximation around the solution of the previous step. It is therefore possible to carry out the decomposition between the two areas and the optimization that each VCZ has to solve is a small quadratic programming problem with limited data exchange.

To verify the effectiveness of the method, several numerical simulations were carried out on a distribution network of twenty-four nodes with six DGs. The precision of the solutions obtained with the proposed decentralized approach was evaluated and it was found to be very close to that obtained with the centralized method. It has also been verified that the decentralized approach with the APP method guarantees an improvement in terms of voltage profile.

Finally, the problem of optimizing voltage profiles in energy distribution networks has been tackled with a two-levels argorithm. After dividing the network into VCZs with PNs, a coordinated approach on two levels with different time scales was applied to the VOP. The first level evaluates the setpoints of conventional VCDs by centralized optimization of PN voltages. The second level adopts a decentralized approach which optimizes the PN voltage in each VCZ by acting on the DER present in the same VCZ; VCZ solutions are driven to the global optimum by a data exchange between PNs.

The application of the proposed VOP to the IEEE 123 bus test system with DER was presented and the results highlighted the negative impact of uncontrolled DGs in the presence of conventional VCDs and the benefits introduced by DER optimization. The proposed method reduces the need to add DERs as additional variables in the first level VOP, thus reducing the complexity and dimensionality of the VOP in large distribution systems and provides further flexibility to the distribution system operator by zone control of the DERs for voltage regulation. In addition to that, the proposed technique has economic advantages, due to the limited communication requirements, without a significant loss of accuracy compared to centralized approaches. From the analysis of the set-points and the voltage profiles it can be seen that the proposed second level VOP significantly improves the voltage profiles compared to those obtained in the absence of any action on the DERs.

Glossary

n_h is the number of branches that compos the $h-th$ feeder
R_{tr} is the resistance of the MV/LV transformer
X_{eq} is the equivalent impedance
X_{tr} is the reactance of the MV/LV transformer
X_{sc} is the short-circuit impedance of the MV node
V_{MV} is the amplitude of the no-load voltage which is assumed to be fixed
P_{MV} is the input active power
Q_{MV} is the input reactive power
V_{tr} is the voltage amplitude
P_{tr} is the outgoing active power
Q_{tr} is the outgoing reactive power
R_j is the resistance of the equivalent circuit of a j-th branch of a LV distribution system
X_j is the reactance of the equivalent circuit of a j-th branch of a LV distribution system
V_{j-1} is the voltage amplitude that characterize the branch at the node $j-1$
P_{j-1} is the input active power that characterize the branch at the node $j-1$
Q_{j-1} is the input reactive power that characterize the branch at the node $j-1$
V_j is the voltage amplitude at the receiving node j
P_j is the outgoing active power at the receiving node j
Q_j is the reactive power at the receiving node j
$P_{S,j}$ is the active shunt power, variable external to the receiving node j
$Q_{S,j}$ is the shunt reactive power, variable external to the receiving node j
$P_{DER,j}$ is the active power injected by the DER connected to the $j-th$ node
$Q_{DER,j}$ is the reactive power injected by the DER connected to the $j-th$ node
$P_{L,j}$ is the active power absorbed by the uncontrolled load connected to the

$j-th$ node, which are assumed to be constant
$Q_{L,j}$ is the reactive power absorbed by the uncontrolled load connected to the $j-th$ node, which are assumed to be constant
x_j is the vector $(P_j, Q_j, V_j^2)^T$
J_j is the Jacobian matrix evaluated in the initial operating point
$V^2_{pn_i}$ the squared voltage amplitude at the PNs
$V^2_{pn_{i,\text{ref}}}$ reference values
a_{oltc} tap position of the OLTC
a_{svr_j} tap positions of the SVRs
Q_{cb_t} reactive powers of the CBs
Γ_i^{oltc}, Γ_{ij}^{svr}, Γ_{it}^{cb} are the sensitivities of the bus voltage at the i-th PN to, respectively, the squared voltage at the terminal bus of the OLTC
ΔV^2_{oltc} is the squared voltage at the terminal bus of the j-th SVR
$\Delta V^2_{svr_j}$ is the squared voltage to the reactive power injected by the t-th CB
Δa^2_{oltc} is the sensitivities of s^{oltc}
$\Delta a^2_{svr_j}$ is the sensitivities of s_j^{svr}
$\mathbf{y}$ is the vector of the PN voltages
$\mathbf{x}_c$ is the vector of set-points of the conventional voltage control devices
$\mathbf{u}_i$ is the vector including all the variables, namely the PN nodal voltage and the set-points of the unconventional voltage devices connected to the VCZ
c is the penalty parameter
λ_i are the Lagrange multipliers

Acronyms

DG Distributed Generation
RES Renewable Energy Sources
DER Distributed Energy Risources
ICT Information and Communication Technologies
VCD Voltage Control Device
OLTC On-Load Tap Changer
SVR Step Voltage Regulator
CB Capacitor Bank
PV Photovoltaic System
EESS Electric Energy Storage System
PCC Point of Common Coupling
VCZ Voltage Control Zone
PN Pilot Node
C.C. Control Center
ZCC Zone Control Center
LV Low Voltage
MV Medium Voltage
HV High Voltage
VOP Voltage Optimization Problem
PF Power Flow
ORPF Optimal Linear Power Flow
MMs Lagrange Multipliers
LA Augmented Lagrangian
ADMM Alternate Direction Multiplier Method
APP Auxiliary Problem Principle

List of Figures

1.1 The subdivision of the Italian electrical system 2
1.2 The Renewable Sources 3
1.3 The New Components 4
1.4 The Traditional Electrical System 5
1.5 The New Electrical System 6

2.1 Local Control 9
2.2 Centralized control architecture 10
2.3 Distributed control architecture 10
2.4 Decentralized Control 11

3.1 Low Voltage Distribution System with DERs 14
3.2 Electric equivalent circuit of the MV/LV Substation 14
3.3 Electric equivalent circuit of the $j-th$ branch 15
3.4 Electric Equivalent Circuit of the h-th Feeder 20
3.5 Flow Chart Algorithm 35
3.6 Highlighted Network Division 36
3.7 Path for the branch $3-4$ 37
3.8 Graphic Example n. 1 for the Calculation of Matrix $\mathbf{T}_P^{Pder}$ . . 38
3.9 Graphic Example n. 2 for the Calculation of Matrix $\mathbf{T}_V^{Pder}$ and $\mathbf{T}_V^{Qder}$ 39
3.10 Graphic Example for the Calculation of Matrix $\mathbf{T}_V^{V_{RT}}$ 40

4.1 Decentralized Algorithm (ADMM) 48
4.2 Distribution system 49
4.3 Case 1: voltage profile in VCZ_1 (ADMM) 52
4.4 Case 1: voltage profile in VCZ_2 (ADMM) 52
4.5 Case 2: voltage profile in VCZ_1 (ADMM) 52

4.6 Case 2: voltage profile in VCZ_2 (ADMM) 53
4.7 Case 3: voltage profile in VCZ_1 (ADMM) 53
4.8 Case 3: voltage profile in VCZ_2 (ADMM) 53
4.9 Decentralized Algorithm (APP) 62
4.10 Error vs. n° of iterations: *Case 2* (right), *Case 4* (left) (APP) 66
4.11 Voltage profile in *Case 1*: VCZ_1 (top) VCZ_2 (bottom) (APP) 67
4.12 Voltage profile in *Case 2*: VCZ_1 (top) VCZ_2 (bottom) (APP) 67
4.13 Voltage profile in *Case 3*: VCZ_1 (top) VCZ_2 (bottom) (APP) 68
4.14 Voltage profile in *Case 4*: VCZ_1 (top) VCZ_2 (bottom) (APP) 68
4.15 Representation of the VOP Formulation (Two-Levels) 71
4.16 Information Exchange in the First Level VOP. 73
4.17 Information Exchange in the Second Level VOP. 74
4.18 Distributed Algorithm (Two-Levels) 79
4.19 The 123-bus test feeder with DERs, VCZs and PNs (Two-Levels) 80
4.20 Voltage profiles in the Case A: no VOP (red), with only the first level VOP (blue), with the two-levels VOP (black) (Two-Levels) 83
4.21 Voltage profiles in the Case A: centralized second-level VOP (green) and decentralized second-level VOP (black) (Two-Levels) 84
4.22 Voltage profiles in the Case B: no VOP (red), with only the first level VOP (blue), with the two-levels VOP (black) (Two-Levels) 86
4.23 Voltage profiles in the Case C: no VOP (red), with only the first level VOP (blue), with the two-levels VOP (black) (Two-Levels) 86
4.24 Voltage profiles in the Case D: no VOP (red), with only the first level VOP (blue), with the two-levels VOP (black) (Two-Levels) 87
4.25 Voltage profiles in the Case E: no VOP (red), with only the first level VOP (blue), with the two-levels VOP (black)(Two-Levels) 87
4.26 Voltage profiles in the Case F: no VOP (red), with only the first level VOP (blue), with the two-levels VOP (black) (Two-Levels) 88
4.27 Time evolution of the total load (blue) and total active power generated by the PVSs (red) (Two-Levels) 88

4.28 Time evolution of voltages at the PNs in absence of conventional VCDs and of DERs (Two-Levels) 89
4.29 Time evolution of voltages at the PNs with the first level VOP and without DERs (Two-Levels) 90
4.30 Time evolution of voltages at the PNs with the first level VOP and with uncontrolled PVSs (Two-Levels) 91
4.31 Time evolution of voltages at the PNs with the VOP (Two-Levels) 91
4.32 Time evolution of total reactive power (black) injected by the PVSs and of the total active power (red) injected by the EESSs (Two-Levels) 92

List of Tables

4.1 Active Power Injections and Reactive Power Ranges for DGs (ADMM) 50
4.2 Voltage Profile Index [$10^{-}3$ $p.u.$] (ADMM) 54
4.3 Number of iterations and Voltage Profile Index (ADMM) . . . 54
4.4 Active Power Injections and Reactive Power Ranges for DGs (APP) 64
4.5 Comparison of the objective functions [$p.u.$] (APP) 64
4.6 Number of iterations to reach convergence (APP) 66
4.7 Values of the Silhouette index for various network partioning (Two-Levels) 81
4.8 Optimal set-points of conventional VCDs for different cases (Two-Levels) 82
4.9 Optimal set-points of unconventional VCDs for different cases (Two-Levels) 83

Bibliography

[1] G. M. Casolino, A. R. Di Fazio, A. Losi, and M. Russo, "Smart modeling and tools for distribution system management and operation," in *2012 IEEE International Energy Conference and Exhibition (ENERGYCON)*, 2012, pp. 635–640.

[2] M. Ahmed, R. Bhattarai, S. J. Hossain, S. Abdelrazek, and S. Kamalasadan, "Coordinated voltage control strategy for voltage regulators and voltage source converters integrated distribution system," *IEEE Transactions on Industry Applications*, vol. 55, no. 4, pp. 4235–4246, 2019.

[3] B. Zhang, A. Y. S. Lam, A. D. Domínguez-García, and D. Tse, "An optimal and distributed method for voltage regulation in power distribution systems," *IEEE Transactions on Power Systems*, vol. 30, no. 4, pp. 1714–1726, 2015.

[4] S. C. Dhulipala, R. V. A. Monteiro, R. F. d. Silva Teixeira, C. Ruben, A. S. Bretas, and G. C. Guimarães, "Distributed model-predictive control strategy for distribution network volt/var control: A smart-building-based approach," *IEEE Transactions on Industry Applications*, vol. 55, no. 6, pp. 7041–7051, 2019.

[5] N. Efkarpidis, T. D. Rybel, and J. Driesen, "Technical assessment of centralized and localized voltage control strategies in low voltage networks," *Elsevier Sustainable Energy, Grids and Networks*, vol. 8, pp. 85–97, 2016.

[6] A. R. Di Fazio, M. Russo, and M. De Santis, "Decentralized voltage optimization based on network partitioning in distribution systems with

dgs," in 1^{st} *IEEE International Conference on Energy Transition in the Mediterranean Area, SyNERGY MED 2019*, May 2019, pp. 1–6.

[7] P. D. F. Ferreira, P. M. S. Carvalho, L. A. F. M. Ferreira, and M. D. Ilic, "Distributed energy resources integration challenges in low-voltage networks: Voltage control limitations and risk of cascading," *IEEE Transactions on Sustainable Energy*, vol. 4, no. 1, pp. 82–88, 2013.

[8] K. K. Mehmood, S. U. Khan, S.-J. Lee, Z. M. Haider, M. K. Rafique, and C.-H. Kim, "A real-time optimal coordination scheme for the voltage regulation of a distribution network including an oltc, capacitor banks, and multiple distributed energy resources," *International Journal of Electrical Power & Energy Systems*, vol. 94, pp. 1–14, 2018.

[9] T. Tewari, A. Mohapatra, and S. Anand, "Coordinated control of oltc and energy storage for voltage regulation in distribution network with high pv penetration," *IEEE Transactions on Sustainable Energy*, vol. 12, no. 1, pp. 262–272, 2021.

[10] A. R. Di Fazio, M. Russo, and M. De Santis, "Zoning evaluation for voltage optimization in distribution networks with distributed energy resources," *Energies*, vol. 12, no. 3, 2019.

[11] V. B. Pamshetti, S. Singh, A. K. Thakur, and S. P. Singh, "Multistage coordination volt/var control with cvr in active distribution network in presence of inverter-based dg units and soft open points," *IEEE Transactions on Industry Applications*, vol. 57, no. 3, pp. 2035–2047, 2021.

[12] I. Džafić, R. Jabr, E. Halilovic, and B. Pal, "A sensitivity approach to model local voltage controllers in distribution networks," *IEEE Trans. on Power Systems*, vol. 29, no. 3, pp. 1419–1428, May 2014.

[13] A. R. Di Fazio, M. Russo, and M. De Santis, "Zoning evaluation for voltage control in smart distribution networks," in 18^{th} *IEEE International Conference on Environment and Electrical Engineering, EEEIC 2018*, jun 2018, pp. 1–6.

[14] S. Mahdavi, H. Panamtash, A. Dimitrovski, and Q. Zhou, "Predictive coordinated and cooperative voltage control for systems with high penetration of pv," *IEEE Transactions on Industry Applications*, vol. 57, no. 3, pp. 2212–2222, 2021.

[15] P. N. Vovos, A. E. Kiprakis, A. R. Wallace, and G. P. Harrison, "Centralized and distributed voltage control: Impact on distributed generation penetration," *IEEE Transactions on Power Systems*, vol. 22, no. 1, pp. 476–483, Feb 2007.

[16] *IEEE Standard for Interconnection and Interoperability of Distributed Energy Resources with Associated Electric Power Systems Interfaces*, IEEE Std 1547-2018 (Revision of IEEE Std 1547-2003) Std., 2018.

[17] A. Madureira and J. A. Lopes, "Coordinated voltage support in distribution networks with distributed generation and microgrids," *Renewable Power Generation, IET*, vol. 3, pp. 439 – 454, 01 2010.

[18] K. E. Antoniadou-Plytaria, I. N. Kouveliotis-Lysikatos, P. S. Georgilakis, and N. D. Hatziargyriou, "Distributed and decentralized voltage control of smart distribution networks: Models, methds, and future research," *IEEE Trans. on Smart Grid*, vol. 8, no. 6, pp. 2999–3008, 2017.

[19] A. Abessi, V. Vahidinasab, and M. S. Ghazizadeh, "Centralized support distributed voltage control by using end-users as reactive power support," *IEEE Transactions on Smart Grid*, vol. 7, no. 1, pp. 178–188, 2016.

[20] V. Alimisis and P. C. Taylor, "Zoning evaluation for improved coordinated automatic voltage control," *IEEE Transactions on Power Systems*, vol. 30, no. 5, pp. 2736–2746, Sept 2015.

[21] A. R. Di Fazio, M. Russo, S. Valeri, and M. De Santis, "Sensitivity-based model of low voltage distribution systems with distributed energy resources," *Energies*, vol. 9, no. 10, 2016, http://www.mdpi.com/1996-1073/9/10/801.

[22] M. Baran and F. Wu, "Optimal sizing of capacitors placed on a radial distribution system," *IEEE Trans. on Power Delivery*, vol. 4, no. 1, pp. 735–743, Jan. 1989.

[23] J. Martí, H. Ahmadi, and L. Bashualdo, "Linear power-flow formulation based on a voltage-dependent load model," *IEEE Trans. on Power Delivery*, vol. 28, no. 3, pp. 1682–1690, Jul. 2013.

[24] S. Bolognani and S. Zampieri, "On the existence and linear approximation of the power flow solution in power distribution networks," *IEEE Transactions on Power Systems*, vol. 31, no. 1, pp. 163–172, 2016.

[25] A. R. Di Fazio, M. Russo, S. Valeri, and M. De Santis, "Linear method for steady-state analysis of radial distribution systems," *International Journal of Electrical Power & Energy Systems*, vol. 99, pp. 744–755, 2018.

[26] Y. Chai, L. G. C. Wang, Z. Zhao, X. Du, and J. Pan, "Network partitioning and voltage coordination control for distribution networks with high penetration of distributed pv units," *IEEE Trans. on Power Systems*, vol. 33, no. 3, pp. 3396–3407, 2018.

[27] P. Lagonotte, J. C. Sabonnadiere, J. Y. Leost, and J. P. Paul, "Structural analysis of the electrical system: application to secondary voltage control in france," *IEEE Trans. on Power Systems*, vol. 4, no. 2, pp. 479–486, 1989.

[28] P. J. Rousseeuw, "Silhouettes: A graphical aid to the interpretation and validation of cluster analysis," *Journal of Computational and Applied Mathematics*, vol. 20, pp. 53–65, 1987. [Online]. Available: https://www.sciencedirect.com/science/article/pii/0377042787901257

[29] M. Nayeripour, H. Fallahzadeh-Abarghouei, E. Waffenschmidt, and S. Hasanvand, "Coordinated online voltage management of distributed generation using network partitioning," *Electric Power Systems Research*, vol. 141, pp. 202–209, Dec 2016.

[30] D. P. Bertsekas and J. N. Tsitsiklis, *Parallel and Distributed Computation - Numerical Methods*. Prentice-Hall, 1989.

[31] G. Cohen, "Auxiliary problem principle and decomposition of optimization problems," *Journal of Optimization Theory and Application*, vol. 32, no. 3, pp. 277–305, 1980.

[32] G. Cohen and D. Zhu, "Decomposition coordination methods in large scale optimization problems: the nondifferentiable case and the use of augumented lagrangians," *Advances in Large Scale Systems*, vol. 1, pp. 203–266, 1984.

[33] A. Losi and M. Russo, "On the application of the auxiliary problem principle," *Springer Journal of Optimization Theory and Application*, vol. 117, no. 2, pp. 377–396, May 2003.

[34] A. Thakallapelli and S. Kamalasadan, "Alternating direction method of multipliers (admms) based distributed approach for wide-area control," *IEEE Transactions on Industry Applications*, vol. 55, no. 3, pp. 3215–3227, 2019.

[35] Y. Liu, L. Guo, C. Lu, Y. Chai, S. Gao, and B. Xu, "A fully distributed voltage optimization method for distribution networks considering integer constraints of step voltage regulators," *IEEE Access*, vol. 7, pp. 60 055–60 066, 2019.

[36] A. R. Di Fazio, C. Risi, M. Russo, and M. De Santis, "Zone-based voltage optimization in distribution grids with dgs," in 20^{th} *IEEE International Conference on Environment and Electrical Engineering, EEEIC 2020*, jun 2020, pp. 1–8.

[37] Z. Shen, M. Liu, W. Lu, and S. Lin, "Coordinated decentralized reactive power optimization of multi-area power systems with discrete variables based on the alternating direction method of multipliers and ward equivalence," *International Journal of Electrical Power and Energy Systems*, vol. 7, pp. 266–273, Mar 2019.

[38] A. R. Di Fazio, C. Risi, M. Russo, and M. De Santis, "Decentralized voltage optimization based on the auxiliary problem principle in active distribution systems," in 55^{th} *IEEE International Universities Power Engineering Conference, UPEC 2020*, sept. 2020, pp. 1–6.

[39] J. Zhong, E. Nobile, A. Bose, and K. Bhattacharya, "Localized reactive power markets using the concept of voltage control areas," *IEEE Transactions on Power Systems*, vol. 19, no. 3, pp. 1555–1561, Aug 2004.

[40] A. R. D. Fazio, C. Risi, M. Russo, and M. D. Santis, "Coordinated optimization for zone-based voltage control in distribution grids," *IEEE Transactions on Industry Applications*, vol. 58, no. 1, pp. 173–184, 2022.

[41] P. Jahangiri and D. C. Aliprantis, "Distributed volt/var control by pv inverters," *IEEE Transactions on Power Systems*, vol. 28, no. 3, pp. 3429–3439, 2013.